MAXIMIZING USE OF AIR-SIDE ECONOMIZATION, DIRECT AND INDIRECT EVAPORATIVE COOLING FOR ENERGY EFFICIENT DATA CENTERS

by

BETSEGAW KEBEDE GEBREHIWOT

Presented to the Faculty of the Graduate School of

The University of Texas at Arlington in Partial Fulfillment

of the Requirements

for the Degree of

DOCTOR OF PHILOSOPHY

THE UNIVERSITY OF TEXAS AT ARLINGTON

May 2016

Acknowledgements

I would like to thank my research advisor, Prof. Dereje Agonafer, for encouraging me to join graduate school and providing me opportunities to work on many project and with many students. I am greatly indebted to his mentorship and support. I would also like to thank my committee members Dr. Abdolhossein Haji-Sheikh, Dr. Miguel Amaya, Dr. Veerendra Mulay, and Dr. Fahad Mirza for their valuable input to this work.

This material is based upon work supported by the National Science Foundation Center for Energy Smart Electronic Systems (ES2) under Grant No. IIP- 1134821. Many NSF I/UCRC ES2 industry mentors have provided inputs to this research at different stages of its life. I would like to especially thank the following people for their contribution: Mike Kaler, Naveen Kannan and James Hoverson of Mestex, Tom Craft and Mark Hendrix of CommScope, Dr. Veerendra Mulay of Facebook, Bharathkrishnan Muralidharan and Dr. Saurabh Shrivastava of Panduit, Mark Seymour of Future Facilities, David Quirk (previously at Verizon Wireless), and Richard Werner (previously at Comcast). I would also like to thank Dr. P. J. Singh of IBM for taking his time to discuss with me impact of contaminants on IT equipment.

Many students who have graduated and those who are still in school have contributed to the development of this work. I am grateful to have many of them as friends and would like to especially thank Vishnu Sreeram and Suhas Sathyanarayan for their support. I would also like to thank Sally Thompson for being there whenever I needed assistance and for her warm smiles that makes tough times bearable.

Last, but not least, I would like to thank my family for their encouragement to pursue my dream and for their love and kindness. I don’t think I would have made it this far without their support.

February 29, 2016

Abstract

MAXIMIZING USE OF AIR-SIDE ECONOMIZATION, DIRECT AND INDIRECT EVAPORATIVE COOLING FOR ENERGY EFFICIENT DATA CENTERS

Betsegaw Gebrehiwot, PhD

The University of Texas at Arlington, 2016

Supervising Professor: Dereje Agonafer

Data centers house information technology (IT) equipment such as servers and network switches which are vital for our networked modern society by providing digital data storage, data processing and connectivity. Data centers house few hundreds to tens of thousands of IT equipment that consume few kilowatt-hours to multi-megawatt-hours of electrical energy that gets dissipated as heat. IT equipment need to be properly cooled so that they operate reliably for their expected lifetime.

For air cooled IT equipment, manufacturers provide heat sinks, cold plates, fans, et cetera to remove heat from the vicinity of heat dissipating components and data centers need to continuously supply cold air to the IT equipment and remove hot from the vicinity of the IT equipment. Type of cooling system used in a data center is an important factor in the overall efficiency and reliability of the data center. This dissertation focuses on use of air-side economization (ASE), direct evaporative cooling (DEC), indirect evaporative cooling (IEC), and indirect/direct evaporative cooling (I/DEC) as a way to reduce cooling cost of data centers.

A test bed modular data center, which has a cooling unit that operates in ASE or two-stage I/DEC modes, and located in Dallas, TX, is primarily used for this study. Included in the study are analysis of weather data to determine what percentage of a

year these cooling systems can be used, modeling of the test bed modular data center using computational fluid dynamics (CFD) tool, discussion on improvements that can be made to the cooling system and factors that limit use of ASE and I/DEC, method for improving the DEC control system, et cetera. In addition, CFD modeling of another modular data center is used to show importance of proper airflow management within cold aisle of data centers and impact of hot aisle pressurization on operating point of server fans.

This material is based upon work supported by the National Science Foundation Center for Energy Smart Electronic Systems (ES2) under Grant No. IIP-1134821. Any opinions, findings, and conclusions or recommendations expressed in this material are those of the author(s) and do not necessarily reflect the views of the National Science Foundation.

Table of Contents

List of Illustrations

List of Tables

Chapter 1

Introduction

Data Centers and Their Increasing Importance

Data centers are digital data storage, processing, and connectivity centers that have become backbone of modern society. Services that involve emails, online purchases, audio and video streaming, digital medical records, et cetera all rely on presence of data centers for saving, accessing, protecting, and sharing data. Environmental Protection Agency (EPA) [1] defines data centers as "Data Center applies to spaces specifically designed and equipped to meet the needs of high density computing equipment such as server racks used for data storage and processing. … The Data Center space is intended for sophisticated computing and server functions; it should not be used to represent a server closet or computer training."

Within the last two decades the amount of digital data generated, stored and transmitted has greatly increased. In 2011, IDC [2] reported that the zettabyte barrier was surpassed in 2010 and estimated that the amount of information created and replicated will surpass 1.8 zettabytes in 2011 – a 9 fold increase in just five years. The increasing amount of digital data is fueled by widespread availability of internet and use of devices that are connected to the internet. This trend is expected to increase as more and more people and devices get connected to the internet, especially with the expected increase in Internet of Things (IoT) [3].

Data Centers: Energy Consumption

Data centers house equipment such as servers, network switches, power distribution units (PDUs), uninterruptable power supply units (UPSs), switch gears, cooling units, et cetera. All of these equipment consume energy during their operation.

Electricity used in 2010 by global data centers was estimated to be between 1.1% and 1.5% of total electricity use and for the US this number was between 1.7% and 2.2% [4]. Delforge [5] reported that U.S. data centers consumed an estimated 91 billion kWh of electricity in 2013 and are on-track to reach 140 billion kWh by 2020. The high electric consumption of data centers and the forecast that this is an increasing trend has drawn data center industries', US government's and other's attention to the need to grow data centers efficiently and sustainably.

Data Centers: Breakdown of Energy Consumption and Importance of Cooling

Total power consumption of a given data center is mainly derived from electric consumption of information technology (IT), power and cooling equipment, and lighting. Essentially all power consumed by the IT equipment is converted to heat [6, 7]. Unless heat is continuously removed from heat dissipating devices, the devices may fail to operate reliably resulting in possible IT equipment shut down. Air cooled IT equipment typically have built in cooling system consisting of heat sinks, heat pipes, vapor chambers, baffle plates, and fans that draw cold air in and push hot air out of the IT equipment. Since data centers house thousands of IT equipment, data center level cooling system is needed to provide cold air to all IT equipment and to remove hot air exhausted from all IT equipment out of the data center space. There are many data center level cooling solutions available in the market and the choice of one versus the other can have significant effect on the overall efficiency of a given data center.

Figure 1-1 shows electric consumption of two large data centers which are adjacent to each other, operated by same company, and have approximately equivalent data center equipment load [8]. The main difference between the two data centers is that the facility on the left uses multiple distributed unit system, which is based on air-cooled computer room air conditioning (CRAC) units, while the facility on the right uses central air handler system. In both systems, the computer loads (IT equipment), UPS losses (power equipment), heating, ventilating, and air conditioning (HVAC) (cooling equipment), and lighting contribute to the total power consumption of the data centers. As can be seen in these two data centers and consistently supported by benchmarking data [8], the electric consumptions of the cooling and the power equipment account for a significant portion of the overall data center electric consumption. In addition, the higher computer loads when using central air handler unit versus using multiple distributed CRAC units shows that the type of cooling system in a given data center can have significant impact on the overall energy efficiency of the data center.

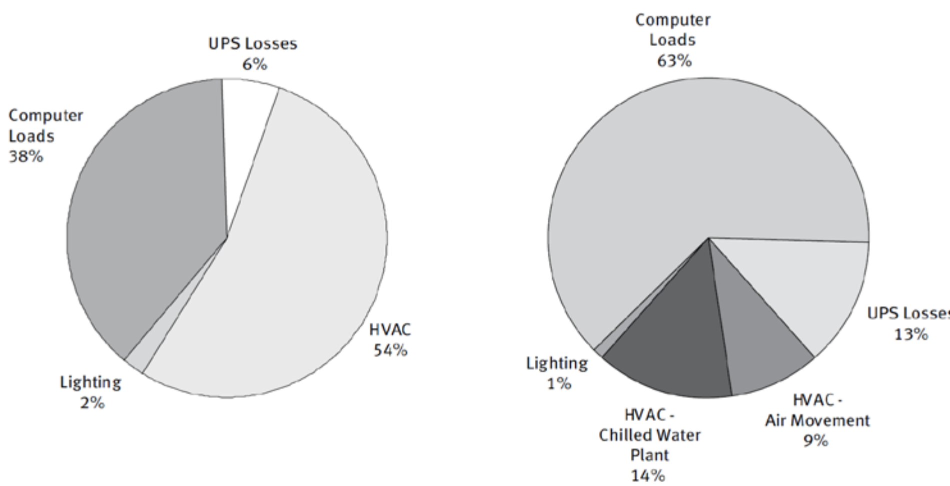

Figure 1-1 Electricity consumption distribution in two datacenters [8]

ASHRAE Thermal Guidelines, Metrics, and Efficiency Recommendations

Data center energy efficiency improvement efforts put forth by data center companies, associations, government agencies, private and public research institutions, and others have resulted in IT equipment inlet air guidelines, metrics, efficiency recommendations, et cetera.

Manufacturers of different IT equipment define different ambient conditions, such as air temperature and relative humidity ranges, for operation of their equipment. Since data centers house IT equipment from different vendors, a common IT equipment environmental condition that allows all equipment housed in the data center to reliably operate is needed. In 2004, ASHRAE provided Thermal Guidelines for environmental specification of IT equipment with emphasis on performance and availability, instead of compute efficiency, of the IT equipment [9]. Since then the Thermal Guidelines has been updated twice: first in 2008 and second in 2011. The 2008 update focused on maintaining high reliability of the IT equipment and also operating data centers in the most energy efficient manner. The 2011 update widened the temperature and humidity envelopes compared to the 2004 or 2008 Thermal Guidelines. This update also defined additional two data center classes increasing the number of data center classes to four. Table 1-1 and Figure 1-2 show the 2011 Thermal Guidelines for Data Processing Environments – Expanded Data Center Classes and Usage. The Thermal Guidelines apply to the inlet air conditions to the IT equipment.

Table 1-1 ASHRAE 2011 Thermal Guideline Classes [9]

Classes (a)	Equipment Environmental Specifications							
	Product Operations (b)(c)					Product Power Off (c) (d)		
	Dry-Bulb Temperature (˚C) (e) (g)	Humidity Range, non-Condensing (h) (i)	Maximum Dew Point (˚C)	Maximum Elevation (m)	Maximum Rate of Change(˚C/hr) (f)	Dry-Bulb Temperature (˚C)	Relative Humidity (%)	Maximum Dew Point (˚C)
Recommended (Applies to all A classes; individual data centers can choose to expand this range based upon the analysis described in this document)								
A1 to A4	18 to 27	5.5ºC DP to 60% RH and 15ºC DP						
Allowable								
A1	15 to 32	20% to 80% RH	17	3050	5/20	5 to 45	8 to 80	27
A2	10 to 35	20% to 80% RH	21	3050	5/20	5 to 45	8 to 80	27
A3	5 to 40	-12˚C DP & 8% RH to 85% RH	24	3050	5/20	5 to 45	8 to 85	27
A4	5 to 45	-12˚C DP & 8% RH to 90% RH	24	3050	5/20	5 to 45	8 to 90	27
B	5 to 35	8% RH to 80% RH	28	3050	NA	5 to 45	8 to 80	29
C	5 to 40	8% RH to 80% RH	28	3050	NA	5 to 45	8 to 80	29

Metrics developed to measure various aspects of data centers include data center energy productivity (DCeP) [10], power usage effectiveness (PUE) [10, 11], water usage effectiveness (WUE™) [12], and carbon usage effectiveness (CUE™) [10, 13]. DCeP quantifies useful work produced by a data center based on the amount of energy it consumes. This metric allows each user to define "useful work" as applicable to the user's business and is calculated by dividing useful work produced by the total energy consumed by the data center [10]. PUE is used to measure infrastructure energy efficiency and is probably the most used of the above four metrics. It is calculated by dividing the total data center source energy by IT source energy [10]. WUE™ addresses water usage in data centers and is calculated by dividing annual water usage by IT equipment energy [12]. CUE™ is used to quantify the carbon dioxide emission equivalents (CO_2eq) from energy associated with a data center [10]. It is calculated by dividing total carbon dioxide emission equivalents from the energy consumption of the facility by the total IT energy consumption.

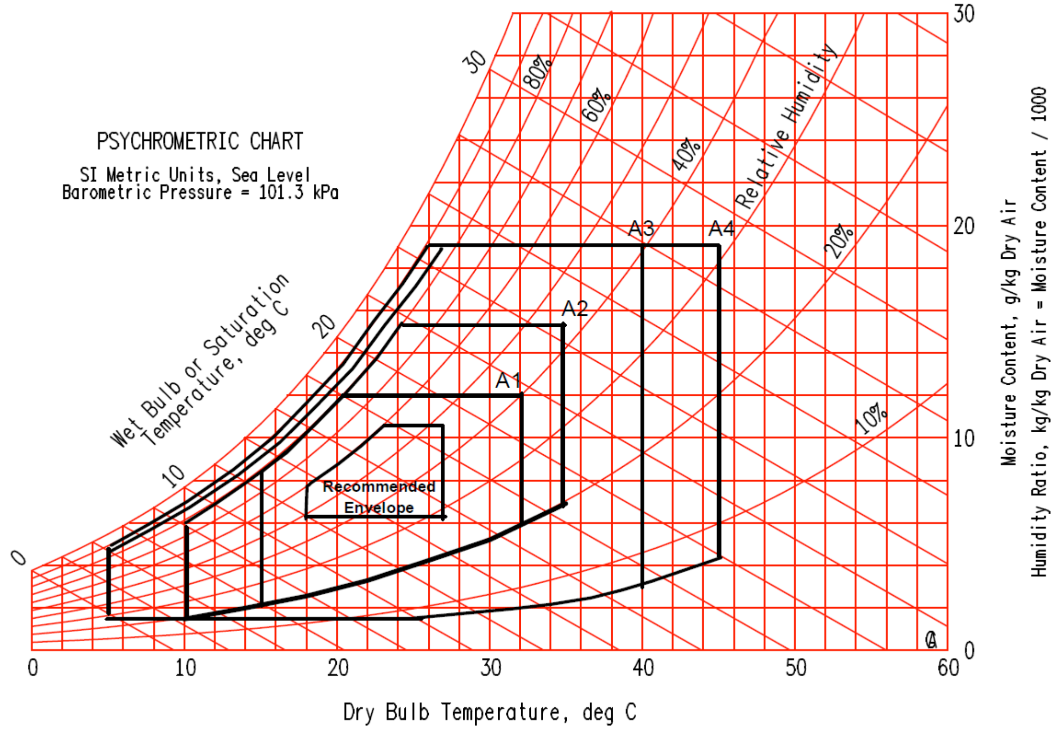

Figure 1-2 ASHRAE Environmental Classes for Data Centers [9]

Best practice recommendations and research findings on construction and operation of data centers have been published by American Society of Heating, Refrigerating, and Air-Conditioning Engineers (ASHRAE), Pacific Gas and Electric Company (PG&E), The Green Grid (TGG), United States Environmental Protection Agency (US EPA), Natural Resources Defense Council (NRDC), and others. Some of their recommendations include using hot aisle and cold aisle containment (see Figure 1-3) to separate cold air going into the IT equipment form hot air exhausted from the IT equipment [8, 14], placing blanking panels in place of empty server slots in racks and cabinets to prevent hot air from returning back into the cold aisle [15], properly selecting and placing perforated tiles in front of servers [16, 17] using computational fluid dynamics

(CFD) tools to better understand flow patterns, and using free cooling when ambient air conditions are favorable [8]. ASHRAE's Datacom Series [18] provide a comprehensive discussion on various aspects of data center cooling, power, contamination, PUE™ calculations, et cetera.

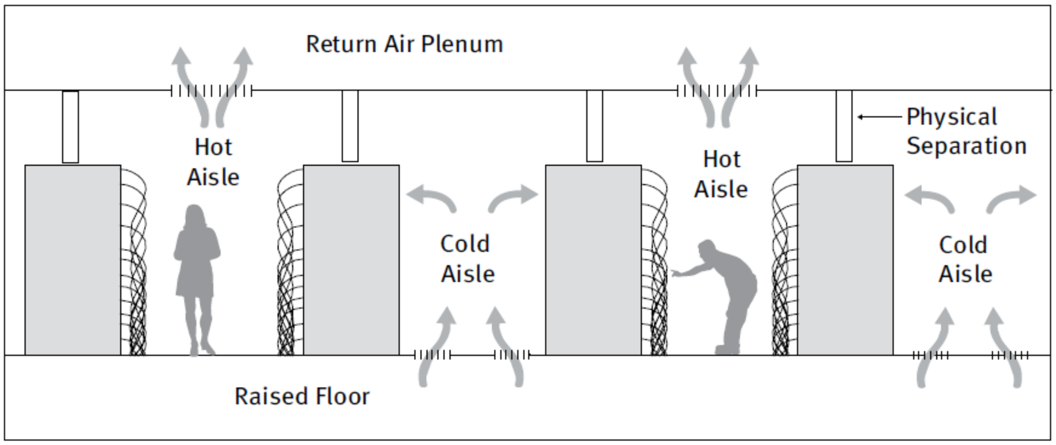

Figure 1-3 Hot Aisle/Cold Aisle Configuration [8]

Air-Side Economization

One of the recommendations provided by various sources on how to reduce data center energy consumption is to use air-side economization (ASE) partially or completely when ambient air conditions are favorable. ASHRAE [19] defines air economizer as "a duct and damper arrangement and automatic control system that together allow a cooling system to supply outdoor air to reduce or eliminate the need for mechanical cooling during mild or cold weather." In this method of cooling, outside air is drawn from the ambient air using fans or blowers and filtered for particulate (and sometimes for gaseous) contaminants as it passes through air filters before being introduced into cold aisle of a data center.

Use of ASE can significantly reduce overall energy consumption of data center cooling system when compared to compressor based cooling systems. ASE is commonly referred to as free cooling, although, technically, there is cost associated with running fans and blowers of ASE systems. The main limitations of using this method of cooling for cooling data centers are that outside air needs to be within a specified temperature and humidity range and air contaminants, both particulate and gaseous, should be within manageable and acceptable ranges. These limitations result in ASE to be used for only few number of hours in a year. To increase the number of hours outside air can be used to cool data centers using compressor-less cooling system, direct evaporative cooling (DEC), indirect evaporative cooling (IEC), or two-stage indirect/direct evaporative cooling (I/DEC) system could be used.

This dissertation discusses use of ASE and I/DEC as a way to reduce cooling cost of data centers. It presents benefits, challenges, and limitations of using these cooling methods. In addition, testing of an IT equipment and DEC media and modeling of a testbed modular data center which is cooled by an ASE and I/DEC unit are discussed.

Chapter 2

Literature Review

Moist Air and Psychrometric Chart

Atmospheric air is a mixture or dry air, water vapor, and contaminants. Dry air is composed of approximately 78.1% nitrogen, 20.9% oxygen, 0.9% argon, and the remaining percentage of other gases [20]. The mixture of water vapor and dry air is referred to as moist air. The thermodynamic properties of moist air and analysis of moist air processes are commonly described using psychrometrics charts. All thermodynamic properties of moist air can be defined using three independent thermodynamic properties of air according to Gibbs phase rule (Equation 2-1) [21]. Since moist air is a two-component mixture (C = 2) and it exists in only gaseous phase (ϕ = 1), its degree of freedom or the minimum number of thermodynamic properties that must be specified in order to define all other thermodynamic properties of moist air equals 3 (f = 2 - 1 + 2 = 3).

$$f = C - \phi + 2 \qquad \text{2-1}$$

where C = number of components

ϕ = number of phases

f = degree of freedom

Pressure is commonly used as one of the three thermodynamic properties since it can be related to altitude. Equation 2-2 [20] gives the standard atmospheric pressure as a function of altitude.

$$p = 29.92(1 - 6.8753 \text{ x } 10^{-6}\text{Z})^{5.2559} \qquad \text{for -16,500 ft < Z < 36,000 ft} \qquad \text{2-2}$$

where p = barometric pressure, in. Hg.

Z = altitude, ft

Psychrometric charts are typically published for a specified barometric pressure and show the relationship between dry-bulb temperature, thermodynamic wet-bulb temperatures, dew-point temperature, enthalpy, relative humidity, specific humidity, and specific volume of moist air.

Equations that can be used to determine thermodynamic properties of moist air from its three independent thermodynamic properties are provided in [20]. [20] also provides equations can be used to calculate moist air properties after moist air goes through processes such as sensible heating and cooling, cooling and humidification, adiabatic mixing of moist airstreams, and adiabatic mixing of water injected into moist air.

Direct Evaporative Cooling

DEC is a method of cooling warm air through direct contact of air and water. As warm air comes in contact with water, the warm air gives up its energy to evaporate the water in the form of latent heat of vaporization thereby decreasing the air temperature and increasing its humidity content. This method of cooling is also referred to as adiabatic cooling since the total energy content of the cooling system remains constant. Two of the most common methods of implementing this cooling system are using water sprays, including misting and fogging systems, and using DEC media. In the first method, incoming warm air is sprayed with water originating from water diffusers. In the latter method, water is poured or sprayed on top surface of a DEC media and as water flows down the media, a fan or a blower draws warm air across the media thereby creating direct contact between water and air.

There are many different types of DEC media available in the market made from cellulose, fiber glass, water retaining finned type aluminum sheets, aspen fiber, plastic, et cetera. Example for each type of these media is given in Figure 2-1, Figure 2-2, Figure 2-3, Figure 2-4, and Figure 2-5 respectively. DEC media can be classified as rigid and non-rigid media [22]. Aspen fiber is the only non-rigid media out of the above examples.

Since data center require clean air for IT equipment cooling and aspen fiber media may have loose particles that can blow off of it, this media may not be suitable for data center cooling use. Plastic rigid media, unlike other media listed above, does not absorb water and become wet. As a result, it requires higher water flow rate than other media. However, it has lower pressure drop than comparable cellulose pads [23]. The author is not aware of a data center that uses aspen or plastic rigid media for data center applications. Cellulose and glass fiber based rigid media which have similar flute angle, thickness, and number of sheets per length may also have similar saturation efficiency and system resistance curves. The main advantage of fiber glass media over cellulose media is that the fiber glass is more fire retardant than cellulose material. Performance of rigid DEC media made from corrugated sheets of cellulose or fiberglass material depend on many factors including thickness of the media, flute angles, number of sheets per foot, and material of the media. Airflow resistance and saturation efficiency of the media are two important performance factors. Koca et al. [22] discusses test procedure for evaluating DEC media and compares various cellulose rigid media based on their flute angles. Standard procedure for laboratory testing of DEC devices is given in [25].

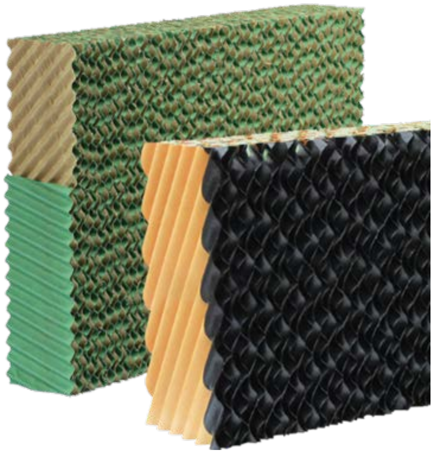

Figure 2-1 CELdek® rigid media [26]

Figure 2-2 GLASdek® rigid media [27]

Figure 2-3 Aspen fiber media [28]

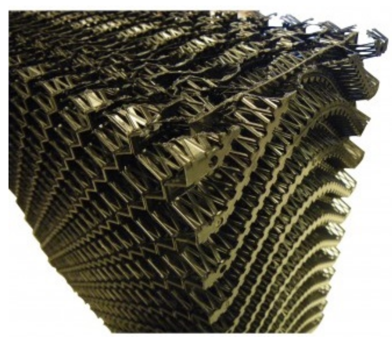

Figure 2-4 Big Dutchman® Plastic Evaporative Cooling Pad [29]

Figure 2-5 OXYVAP® water retaining finned type aluminum sheets [30]

Saturation effectiveness is used to determine evaporative cooler performance. For, both, direct and indirect evaporative cooling units, this factor measures how much the leaving air temperature from DEC and IEC units approaches the thermodynamic wet-bulb temperature of the entering air or how much the leaving air is close to complete saturation. The saturation effectiveness is expressed as:

$$\epsilon_e = 100\,\frac{t_1 - t_2}{t_1 - t'} \qquad \text{2-3}$$

where

ϵ_e = saturation effectiveness,%

t_1 = dry-bulb temperature of entering air, °F

t_2 = dry-bulb temperature of leaving air, °F

t' = thermodynamic wet-bulb temperature of entering air, °F

Both spray and rigid media types DEC systems have been used in data centers. For example, [24] reports that Facebook used spray type DEC at its Prineville, OR, location before replacing this system with rigid media type DEC. Schematic of the data center's cooling system is shown in Figure 2-1. Array of spray nozzles used for in the misting system are shown in Figure 2-2. What prompted the change was that Facebook's staff smelled smoke coming from fire that spread across an area near Facebook's data center. The company's data center team was then interested to find a way to treat and scrub outside air as it makes its way into the data center. The company also used misting and rigid media DEC system primarily for humidification purposes at its Luleå, Sweden, data center [31]. The rigid media DEC used at this data center is shown in Figure 2-3.

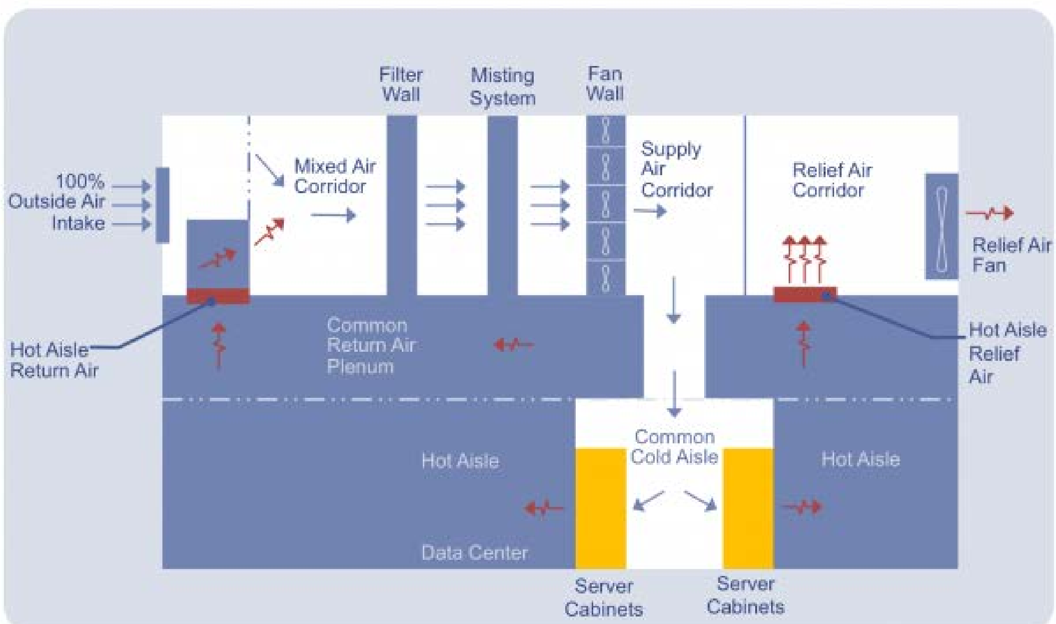

Figure 2-6 Facebook's penthouse data center cooling system schematic that uses misting type DEC system [32]

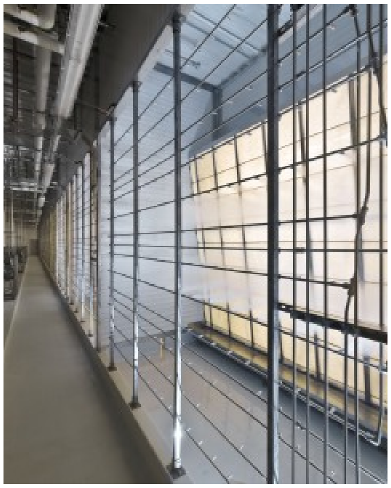

Figure 2-7 Misting DEC system at Facebook’s datacenter [32]

Figure 2-8 DEC media used at Facebook's data center at Luleå, Sweden [31]

Indirect Evaporative Cooling

In IEC, there is no direct contact between data center supply air and water. There are many configurations of IEC possible. Probably the most common configuration is to pass supply air (primary air) through channels and disperse water on the outer surface of the channels to wet the outer surfaces of the channels. A secondary air (scavenger air) would then blow bottom-to-top or side-to-side evaporating the water on the outer surfaces of the channels which in turn cools the primary air flowing through the channels - see the schematic in Figure 2-4.

Another way to achieve IEC is to blow data center supply air across a water-to-air cooling coil that has cold water flowing through it. The water leaving the coil, which is warmer than the inlet water temperature, is ducted to a cooling tower and dispersed on top of a DEC media. Cooling tower fan draws outside air across the DEC media thereby cooling the water flowing down the media. The cold water is collected at the bottom of the cooling tower and is pumped back into the cooling coil. Since there is no addition of water into the supply air, the specific humidity of the inlet air remains constant while the dry-bulb temperature decreases and the relative humidity increases. Palmer [33] refers to this specific configuration as waterside economizer.

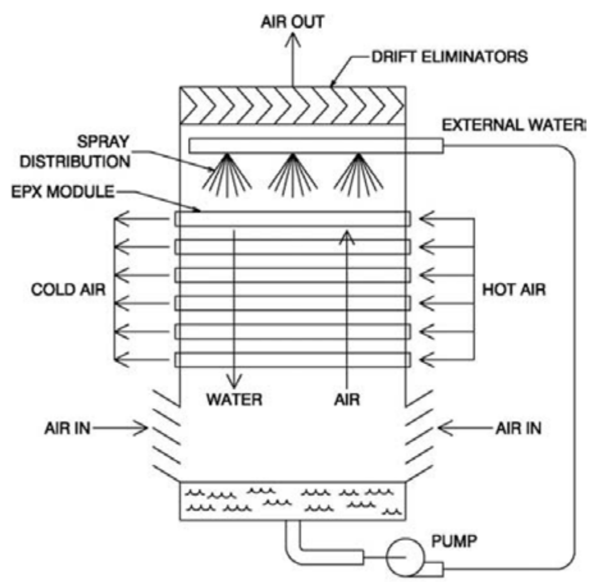

Figure 2-9 Indirect evaporative cooling [34]

The equation to find saturation effectiveness of IEC units is same as equation 2-3. The limit for these systems is the web-bulb temperature of the scavenger air. However, a special type of IEC which uses multi-stage IEC has the dew-point temperature as its limit. This cooling system operates on Maisotsenko Cycle (a.k.a. M-cycle). Figure 2-5 shows a simplified representation of the Maisotsenko cycle. In this cycle product air is cooled indirectly with working air which is initially cooled by an IEC process. A data center that used this cooling system in addition to ASE in Boulder, CO, reported saving of 70% for summer and 90% for winter months [35]. Further discussion on this cooling cycle can be found in [36].

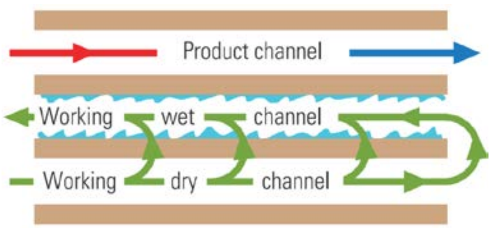

Figure 2-10 Simplified representation of the M Cycle [36]

Indirect / Direct Evaporative Cooling

Use of two-stage I/DEC unit allows for a wider range of ambient air conditions to be used for cooling data centers. This cooling system commonly uses IEC as the first stage cooling followed by DEC as the second stage. For climates that require DX cooling, I/DEC systems may be able to add a DX cooling system as a third stage.

Metzger et al. [37] used Figure 2-6 to show energy saving potential of using ASE, DEC, and multi-stage indirect evaporative cooling. The seven regions shown in this figure are divided based on type of cooling technology that can be implemented to bring outside air into the recommended envelope of the 2011 ASHRAE Thermal Guideline for Data Processing Environments. The authors analyzed energy saving potentials of using these cooling technologies and graphically mapped their findings on United States map using a geographical information system (GIS) software. They reported that a combination of bins 6 and 7 have an average of 30%-40% energy saving potential, a combination of bins 4, 5, 6, and 7 have an average of 80%-90% energy saving, and a combination of all bins except bin 1 has an average of greater than 90% energy savings potential.

Water quality for rigid media DEC units

Dissolved minerals are commonly found in water. Concentration of dissolved minerals in water is commonly measured using conductivity measuring instruments. The unit of conductivity is Siemens (S), formerly called mho. Table 2-1 shows conductivity of different solutions [38]. Another terminology industry uses to describe amount of concentration is total dissolved solids (TDS). “The total TDS is a mass estimate and is dependent on the mix of chemical species as well as the concentration while conductivity is only dependent on the concentration of chemical species. [38]” Once conductivity value is measured, it can be multiplied by an empirically determined factor to find the TDS concentration. Munters [39] recommends maintaining water at Puckorius Scaling Index of 6.5 $\pm$ 0.5 for its CELdek and GLASdek products. This index is calculated from the sump water’s conductivity, temperature, calcium hardness, total alkalinity (ppm as $CaCo_3$) and pH_{eq} of total alkalinity.

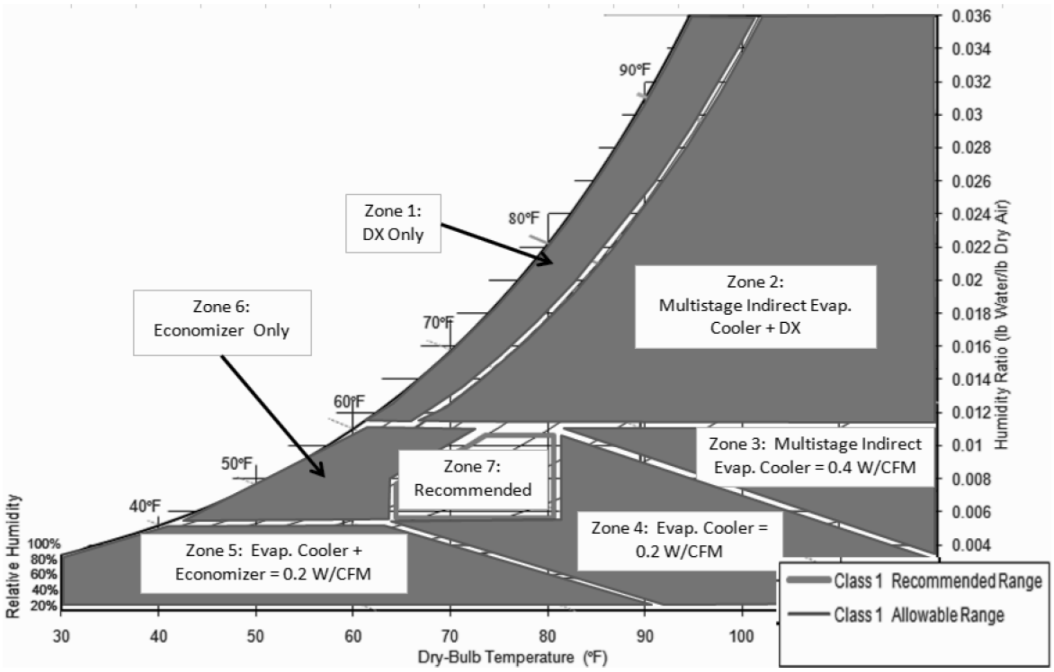

Figure 2-11 Psychrometric Bin Analysis [37]

Table 2-1 Water conductivity of solutions

Solution	Conductivity
Absolute pure water	0.055 µS/cm
Power plant boiler water	1.0 µS/cm
Good city water	50 µS/cm
Ocean water	53 mS/cm
Distilled water	0.5 µS/cm
Deionised water	0.1 - 10 µS/cm
Demineralised water	0 - 80 µS/cm
Drinking water	0.5 - 1 mS/cm
Wastewater	0.9 - 9 mS/cm
Seawater	53 mS/cm
10 % NaOH	355 mS/cm
10 % H_2SO_4	432 mS/cm
31 % HNO_3	865 mS/cm

Since DEC works by evaporating water off of wet surfaces of DEC media, minerals left behind in the water flowing down the media increase total concentration of minerals in the sump. If the sump water is recirculated, without proper bleed-off and addition of makeup water, the mineral concentration further increases in the sump and, over time, minerals start to deposit on the rigid DEC media. In addition, if sufficient water flow over the media is not maintained, severe deposition occurs. Heavy deposition of scale can result in reduced airflow through the media, reduced surface area for evaporation, and deterioration of the media due to high pH levels which leach stiffening agents and degrade the media [39]. Thus mineral concentration in the sump of DEC needs to be monitored and proper level of mineral concentration maintained to increase life of DEC media and gain the full benefit of this cooling method. The following are few of the good practices provided in [39] that minimize water related problems with DEC media:

1. "Provide good, even water distribution, (1 .5 GPM per square foot of top surface area) from one end of the pad, to the other."
2. "Adequate bleed off is the simplest form of scale control."
3. "Clean and flush distribution headers on a regular basis."
4. "Consider constructing shorter pad walls if scaling is a problem (i.e., two banks five foot high instead of one bank ten feet high)."
5. "When media experiences extreme evaporation, a flush cycle should be provided every 24 hours - with the air flow off."

To control the amount of moisture added to a system the water supply to the media can be turned on/off frequently. However, this method of controlling moisture addition results in mineral build up on the media. To work around this problem, staged systems can be used. These systems allow some section of the media to be wetted while other sections remain dry. Figure 2-7, Figure 2-8, and Figure 2-9 show three ways to have staged DEC system [40]. The horizontally split distribution, Figure 2-7, is better than having tall-pad systems since in tall-pad systems the water may evaporate before it reaches the bottom. If this happens, high scale build up can happen. The vertically split configuration, Figure 2-8, is used for systems that require precise control of temperature and humidity. “Commonly, water is supplied to every other pad along a bank of media using separate distribution headers. [40]” If more moisture needs to be added to the system, the remaining systems are also supplied with water. In the multiple banks in series, Figure 2-9, two to three stages of DEC are placed in the airflow direction. Four or six inch deep media are used depending on the required evaporative efficiencies of the media. Vertically splitting the media is not needed.

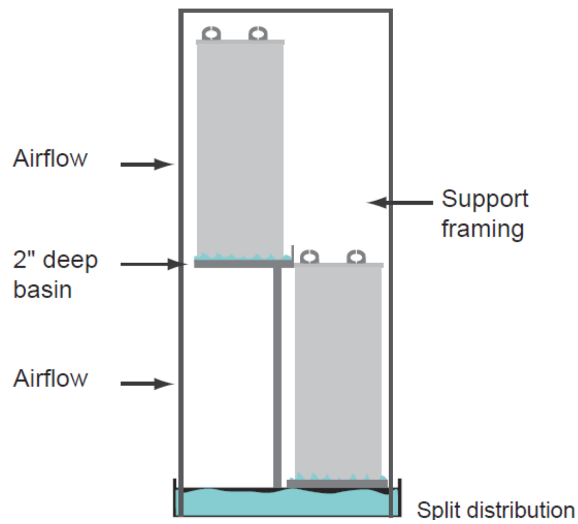

Figure 2-12 Horizontally split distribution [40]

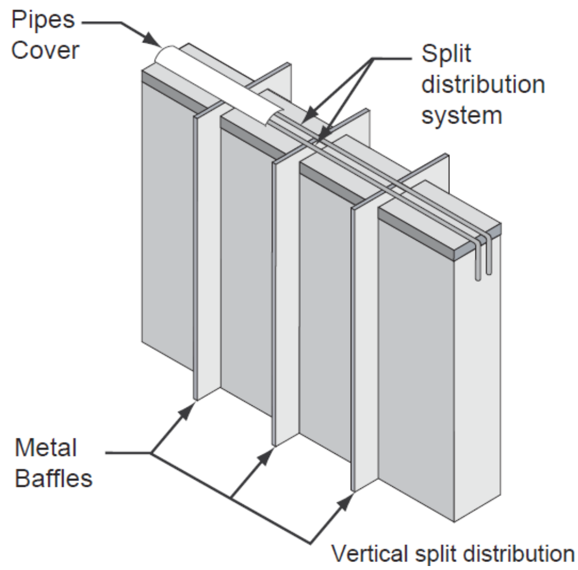

Figure 2-13 Vertically split distribution [40]

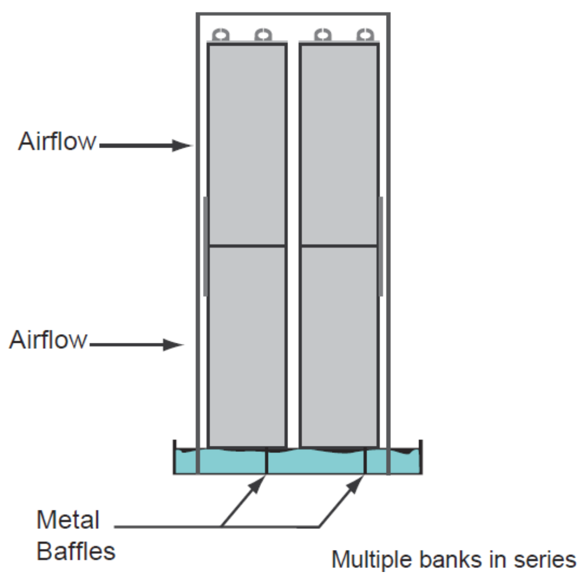

Figure 2-14 Multiple banks in series [40]

Contamination of Air with Particulate and Gaseous Matter

One of the factors that limit use of outside air for cooling IT equipment is type and level of particulate (dust) and gaseous contaminant in outside air. Both, particulate and gaseous, contaminants negatively affect reliability of IT equipment. Below are few examples on how particulate matter affect reliability of IT equipment. Particulate matter:

1. may get lodged between server heat sink fins and block or reduce air flow between the heat sink fins. This results in reduced cooling performance of the heat sink.
2. may contain electrically conductive material, such as zinc whiskers, which can short circuit IT equipment components
3. may contain materials that have low deliquescent relative humidity and if these get deposited on IT equipment, they can become conductive when the relative humidity in the data center reaches the deliquescent relative humidity of the particulate matter. Deliquescent relative humidity is "the relative humidity at which the dust absorbs enough water to become wet and promote corrosion and/or ion migration. [41]"

Thus supply air used for cooling IT equipment needs to be filtered. Filtration is especially needed if outside air is brought into data center space since factors outside the data center can affect quality of air entering the data center. ASHRAE recommends using Minimum Efficiency Reporting Value (MERV) 8 filters for continuously filtering room air and MERV 11 or MERV 13 filters for air entering the data center. This method of filtration achieves ISO Class 8 cleanliness which ASHRAE recommends for data centers [41]. For ASE systems, MERV 13 is preferred since it has higher filtration efficient than MERV 11 filters.

Gaseous contaminants such as sulfur dioxide (SO_2) and Hydrogen Sulfide (H_2S) affect reliability of IT equipment differently than that of particulate contaminants. Figure 2-10 and Figure 2-11 show two common ways sulfur containing gases corrode circuit board components: copper creep corrosion and corrosion of silver metallization [41]. ASHRAE recommends using gas-phase filtration if data centers have severity level higher than G1 according to ISA-71.04 (ISA 1985) [41].

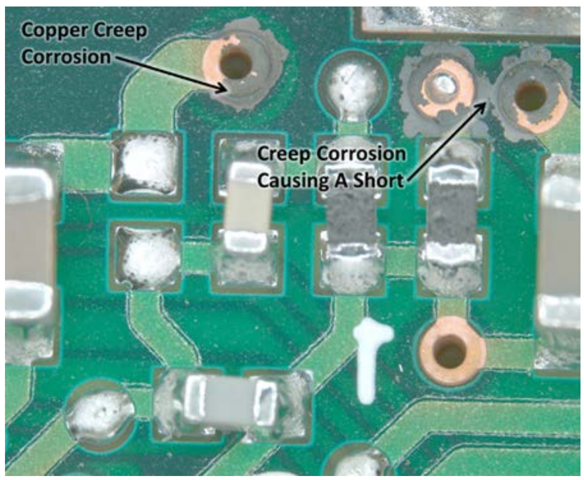

Figure 2-15 Example of copper creep corrosion [41]

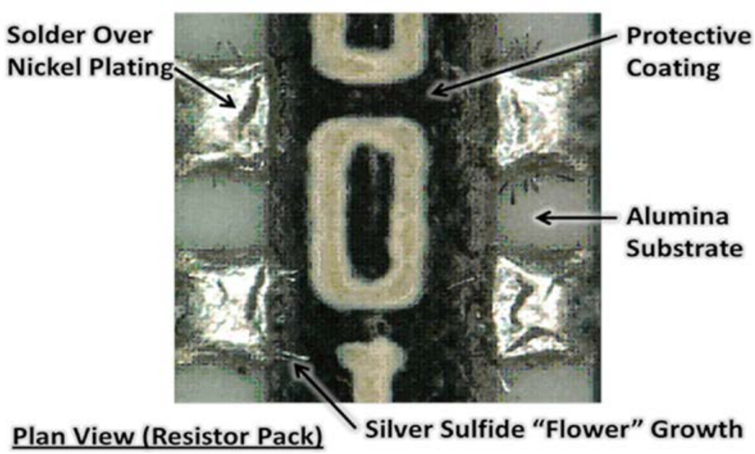

Figure 2-16 Example of corrosion of silver metallization [41]

Computational Fluid Dynamics (CFD)

To design data centers and gain better understanding of fluid flow patterns and temperature and pressure distributions in data centers, use of CFD tools has become instrumental. These CFD tools solve complex governing equations of conservation of mass, momentum, and energy. The governing equations for incompressible Newtonian fluid with constant thermal conductivity, *k*, are provided below. Derivation of the governing equations is available in many fluid mechanics books such as [42].

Conservation of mass:

$$\boldsymbol{\nabla} \bullet \mathbf{u} = 0 \qquad \text{2-4}$$

Conservation of momentum:

$$\rho \frac{D\mathbf{V}}{Dt} = \rho \mathbf{f} + \boldsymbol{\nabla} p + \mu \nabla^2 \mathbf{V} \qquad \text{2-5}$$

Conservation of energy:

$$\rho \frac{De}{Dt} = \frac{\partial Q}{\partial t} + k\nabla^2 T + \phi$$

where

$$\phi = \boldsymbol{\nabla} \bullet \left(\tau_{ij} \bullet \mathbf{V}\right) - (\boldsymbol{\nabla} \bullet \tau_{ij}) \bullet \mathbf{V} \qquad \text{2-6}$$

$$\tau_{ij} = \mu \left[\left(\frac{\partial u_i}{\partial x_j} + \frac{\partial u_j}{\partial x_i}\right) - \frac{2}{3}\delta_{ij}\frac{\partial u_k}{\partial x_k}\right] \qquad i, j, k = 1, 2, 3 \text{ and}$$

δ_{ij} is the Kronecker delta function

CFD tools have been used to study different aspects of data centers. For example, CFD is used to study modeling strategies for perforated tiles in raised floor data center [43, 44], impact of pressure distribution in underfloor plenums on airflow through perforated tiles, underfloor air blockage due to cables and pipes, gap between racks, et cetera [45], importance of hot/cold aisle containment to increase inlet air temperature to

IT equipment [46]. Seger and Solberg [47] discuss importance of using CFD tool to model contaminant carryover from outside data centers when ASE is used.

Chapter 3

Testing, Modeling, and Analysis

Test Bed Modular Data Center

To study use of ASE, DEC, and IEC for data center cooling applications, a modular data center has been built in Dallas, Texas. This data center is shown in Figure 3-1 and Figure 3-2. The IT pod, the schematic of which is shown in Figure 3-3, has two sections. Section 1 contains a workstation computer that is used for accessing servers stored in Section 2. Section 2 of the IT pod is configured in a hot/cold aisle configuration and contains four 42U Panduit P/N S6212BP cabinets. The cabinets contain a total of 120 HP SE1102 servers. Supply air from a cooling unit, Aztec Sensible Cooling Model ASC-15-2A11-00, is delivered to the cold aisle through a supply duct. Hot air from the hot aisle is ducted to be returned to the cooling unit or to be exhausted to the ambient. The return duct has pressure relief dampers for pressure control. Description of the cooling unit's construction can be found in its technical guide [48].

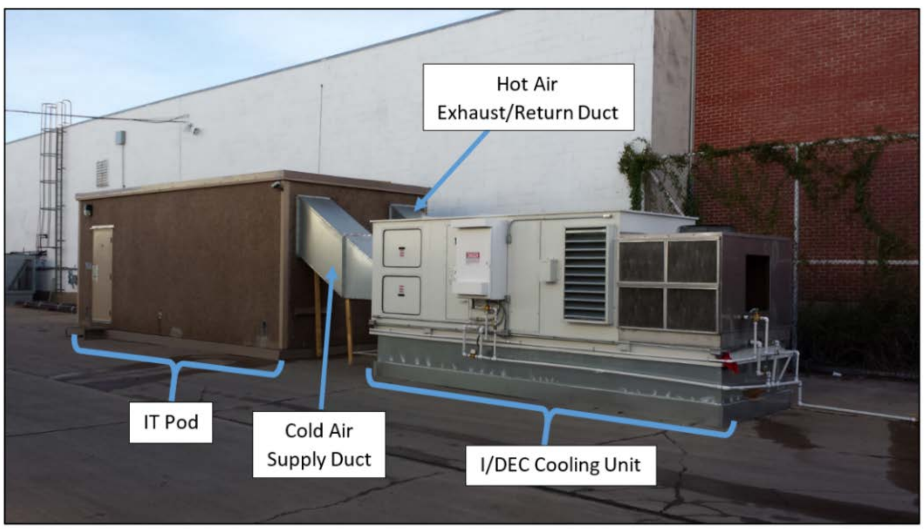

Figure 3-1 Modular Data Center: Shows Cold Air Supply Duct

(Figure adapted, with permission, [49] © 2015 IEEE)

Figure 3-2 Modular Data Center: Shows Hot Data Center Return Duct

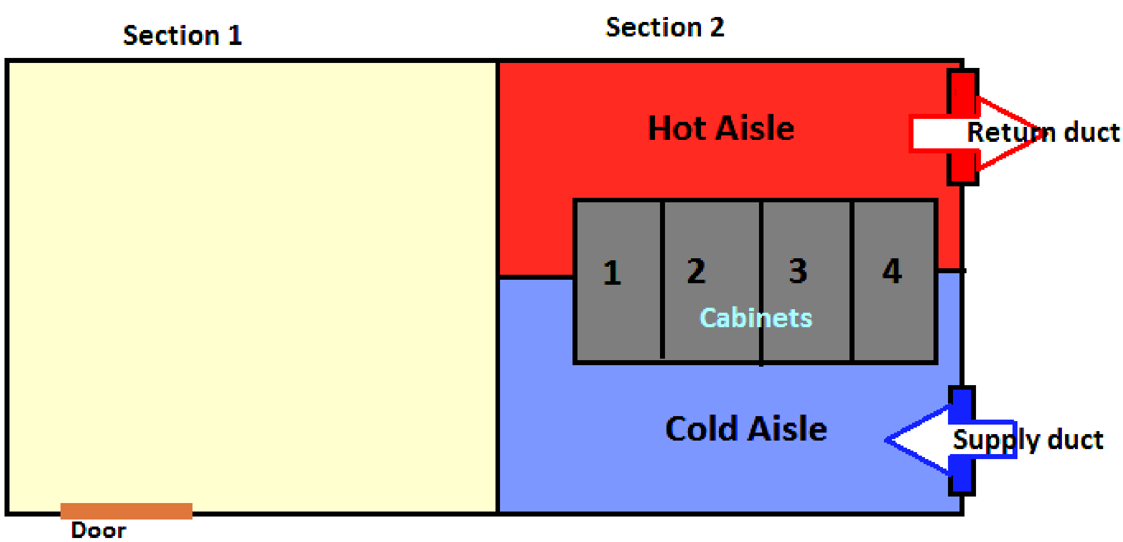

Figure 3-3 Schematic of IT Pod - Top View [49] © 2015 IEEE

Figure 3-4 shows pictures taken inside the IT pod. The picture in the middle shows two doors: one on the left and the other on the right leading to the hot and the cold aisles, respectively.

Hot Aisle   Hot Aisle   Cold Aisle   Cold Aisle

Figure 3-4 Hot/Cold aisle configuration inside the IT pod

Model of the cooling unit is shown in Figure 3-5. At the inlet of the mixing chamber, positions of the return air damper and the ambient air damper determine the proportion of return air to ambient air that gets mixed in the mixing chamber. The cooling unit's control system determines the angle at which the dampers are open. Once air enters the mixing chamber from the ambient and/or from the return duct, it passes through a set of MERV 11 filters, IEC coils and DEC media before a blower or two blowers pulls the air in and supplies it to the cold air supply duct. The supply duct then delivers cold air to the cold aisle.

Leaving water from the IEC coils is ducted to the cooling tower section and distributed on top of 12 inch thick cellulose DEC media (Munters 6065/15). The cooling tower fan draws air across the DEC media resulting in evaporation and cooling of the water flowing down the media. Cold water from the bottom of the DEC media is collected and pumped back into the cooling coil. The IEC coil then sensibly cools the conditioned air.

The DEC media that comes in contact with the conditioned air is also a 12 inch thick Munters 6065/15. This section has its own water reservoir and water pump. The quality of air that flows through this media is relatively better than that of the DEC media in the cooling tower. This is because the conditioned air is filtered with MERV 11 filter before it comes in contact with the DEC media while ambient air is filtered with MV EZ Kleen filters before it comes in contact with DEC media in the cooling tower.

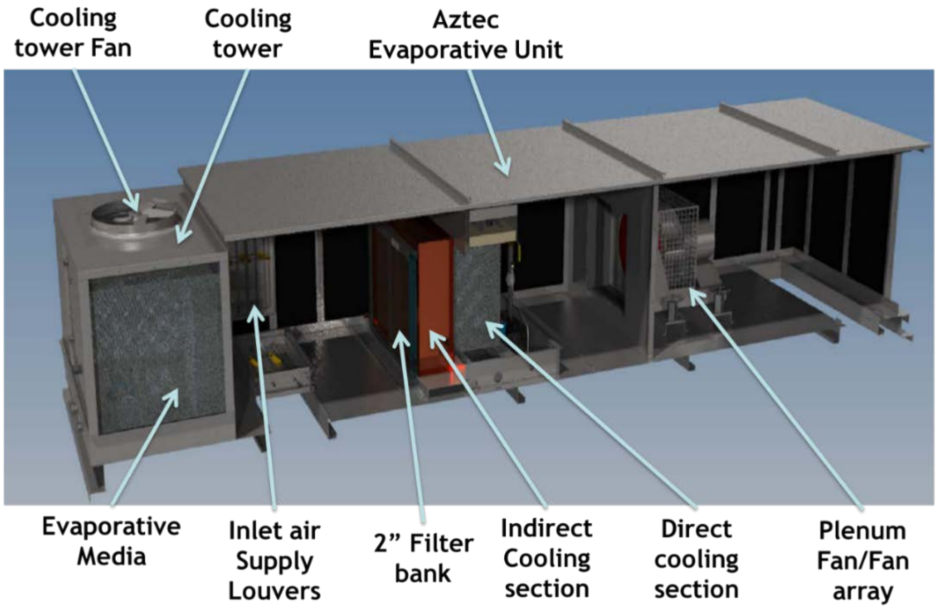

Figure 3-5 Internal details of the cooling unit

The amount of Total Dissolved Solids (TDS) needs to be monitored in the reservoirs of the cooling tower and the DEC media which comes in direct contact with the conditioned air. If the TDS level reaches a preset maximum level in either of the sumps, the water in the sump that has high concentration of TDS is dumped and the sump is refilled with make-up water. Alternatively, continuous bleed-off can be maintained to keep the level of TDS low. To make up for water that has evaporated, water is added into both sumps such that the water level in the sumps remains constant.

The test bed modular data center is equipped with various sensors such as temperature, humidity, static pressure, et cetera which are used for controlling the cooling unit’s blower speed, DEC water pump on/off state, et cetera. Most of the sensor data is available through a webpage dedicated to this test bed modular data center. Figure 3-6 shows a sample of the data that can be obtained from the webpage.

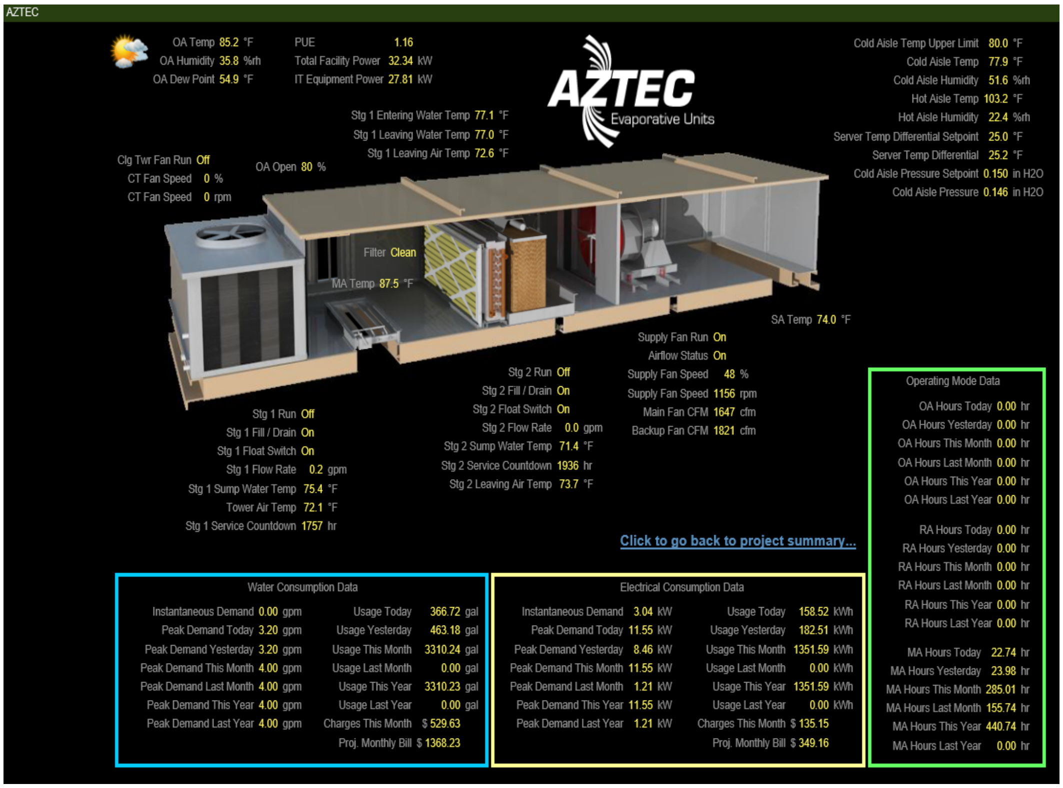

Figure 3-6 Screenshot of webpage showing data about the research modular data center

Estimation of IT Pod Power Requirement

To estimate the electric power required to power all servers inside the IT pod and the amount of air needed to cool them, two sets of tests were conducted on a HP SE1102 server. All 120 servers inside the IT pod are same as this server. Internal details of this server with its top cover removed are shown in Figure 3-7.

The first set of tests are aimed at estimating the power consumption of the server. In these tests the server is stressed using stress tools lookbusy [50] and Prime95 [51]. To use lookbusy, CentOS, a Linux distribution, is first installed on the server whereas to use Prime95, Windows Server 2008 R2 operating system is first installed on the server. All power measurements are made using a Yokogawa CW121 Clamp-On power meter and all tests are conducted at room temperature.

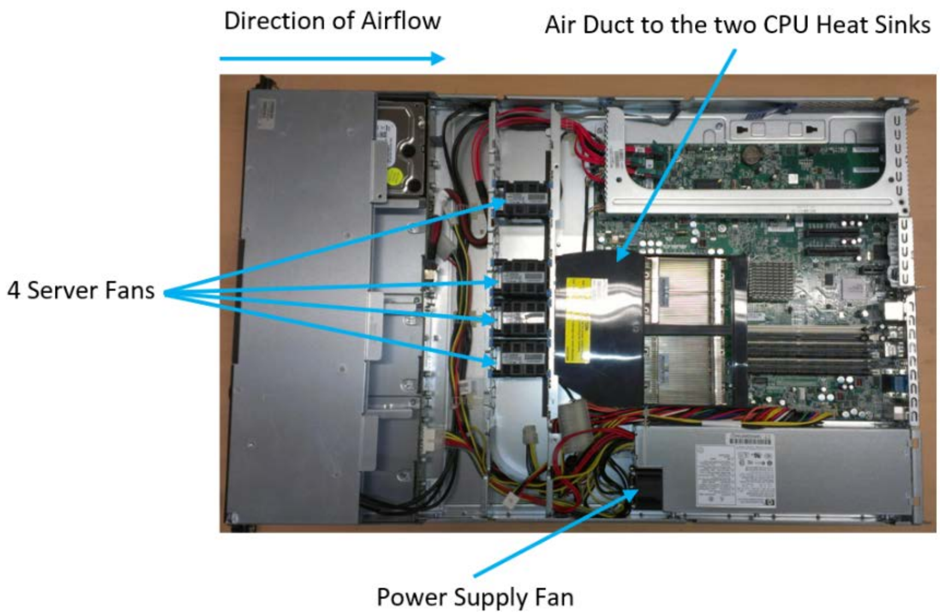

Figure 3-7 HP SE1102 Server with its top cover removed.

Lookbusy Test

Using lookbusy program the server is tested two times: first with the server plugged into a 120V AC power outlet and the second into a 208V AC power outlets. In each case, the server is tested with the lookbusy program set to 98% CPU utilization. Results of these two tests are shown in Figure 3-8.

From start to about 170 s the server is booting up. In this time period the server power consumption fluctuates from about 10 W to 182 W. Idle state is reached around 170 s. From 170 s to the time lookbusy program is commanded to run at 98% CPU utilization, power fluctuation is observed ranging from 90 W to 120 W. When the server is running at 98% CPU utilization, it consumes about 150 W in, both, the 120V AC and the 208V AC cases.

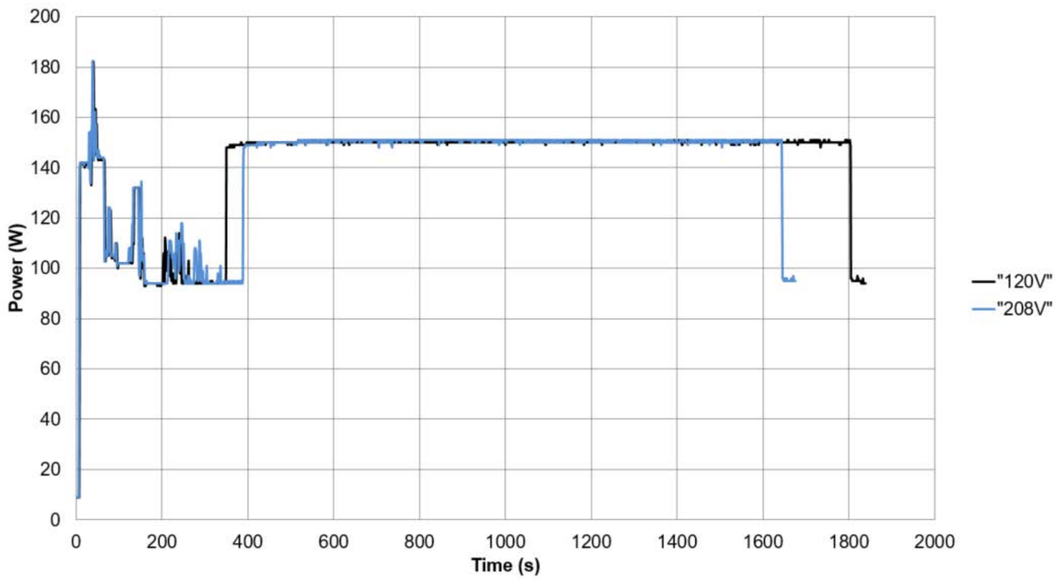

Figure 3-8 Power Consumption of HP SE1102 - lookbusy at 98% CPU utilization

Prime95 Test

The server is tested two times with two different stress (torture) test settings of Prime95 version 27.9. These two settings are the Small FFT and the In-place large FFTs. In both tests all 8 threads of the CPU are tested and the server is powered by 123 V AC. During the test, two T Type thermocouples were placed at the front side of the server to measure inlet air temperature and four T Type thermocouples were placed around the rear side of the server to measure exhaust air temperature. Agilent 34972A is used to acquire temperature data. The test setup, including the location of the thermocouples, is shown in Figure 3-9.

Results from the tests are shown in Figure 3-10, Figure 3-11, Figure 3-12, and Figure 3-13. Figure 3-10 and Figure 3-12 show power consumption of the server when

Small FFTs and In-place large FFTs settings are used to stress the server, respectively. In Figure 3-10, two power spikes during booting up of the server are shown. The recorded maximum power draw during booting up is 181 W. Since Prime95 program is not running at idle state, the power draw at idle states shown in Figure 3-10 and Figure 3-12 is same, 93 W. When the server is stressed using the Small FFTs setting, it draws about 180 W as shown in Figure 3-10 whereas when it's stressed using In-place large FFTs setting, it draws about 195 W as shown in Figure 3-12.

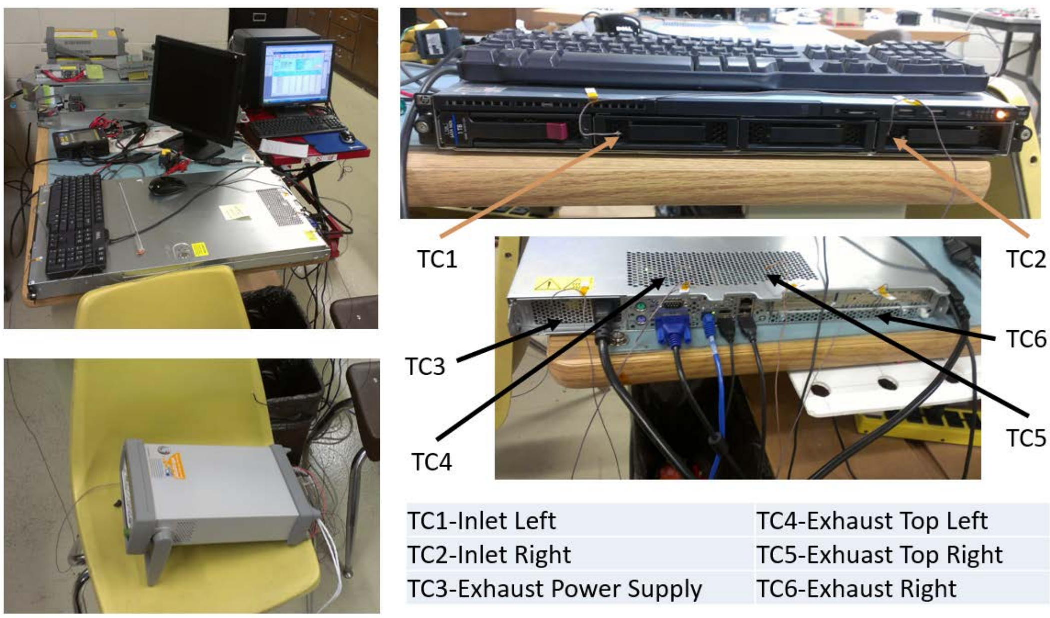

Figure 3-9 HP SE1102 stress test setup (Figure adapted, with permission, [52])

Inlet air and exhaust air temperature readings of the thermocouples when the server was tested using Small FFTs and In-place large FFTs settings are shown in Figure 3-11and Figure 3-13, respectively. As can be seen in both cases, increase in exhaust air temperature is observed when the power consumption of the server increases. Inlet air temperature remained more or less constant at 23˚C throughout the tests. The exhaust air temperature depends on the location of the thermocouples. When the server is stress tested for an extended period of time, the highest exhaust temperature is measured behind the power supply in both tests.

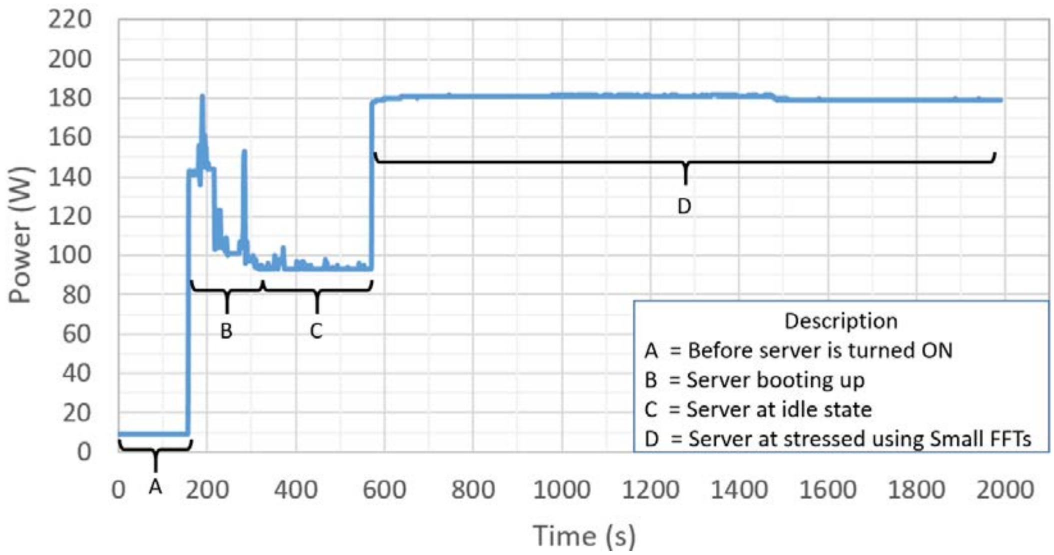

Figure 3-10 HP SE1102 power consumption test result: Prime95 (Small FFTs)

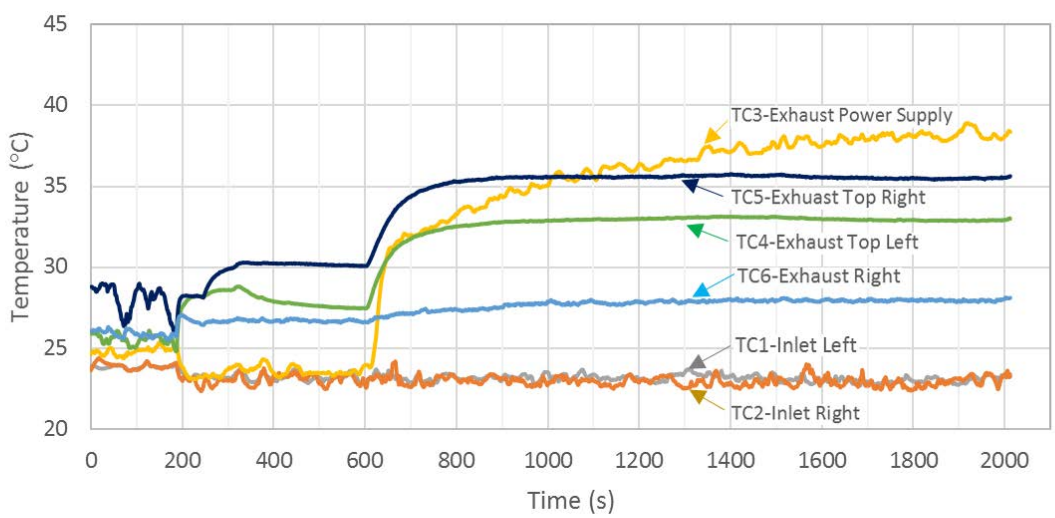

Figure 3-11 Server inlet and exhaust air temperatures: Prime95 (small FFTs) stress test

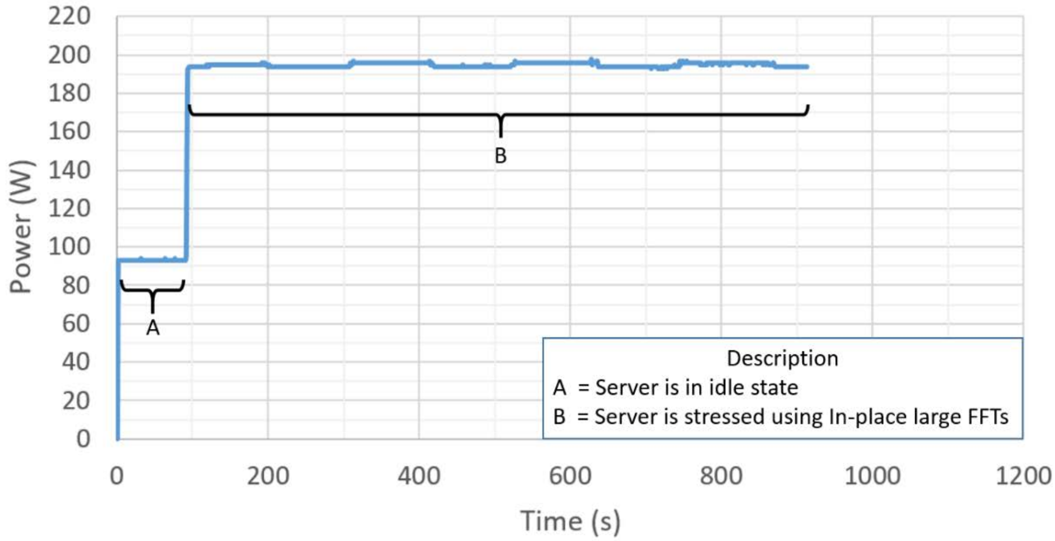

Figure 3-12 HP SE1102 power consumption test result: Prime95 (In-place large FFTs)

(Figure adapted from [52])

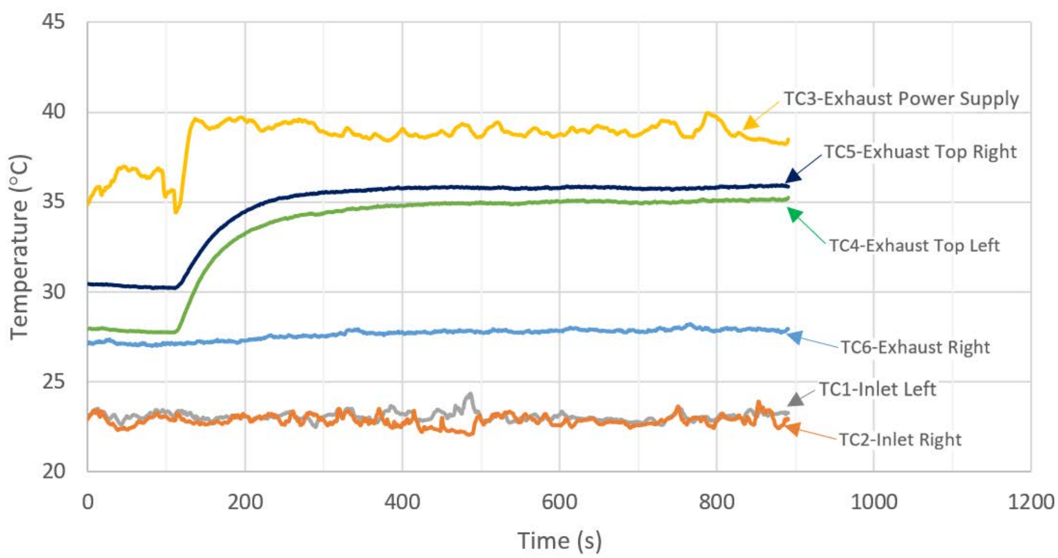

Figure 3-13 Server inlet and exhaust air temperatures: Prime95 (In-place large FFTs)

stress test

IT Pod Airflow Requirement

To estimate the amount of airflow the cooling unit, ASC-15-2A11-00, should be able supply the IT pod, a HP SE1102 server is first tested on a 30 inch diameter airflow bench to find out how much airflow is required for its operation. The server is mounted on the airflow bench as shown in Figure 3-14. General guidelines for setting up the airflow bench and the device under test are followed as provided in [53].

Three tests were conducted to find out how much airflow the fans in the server draw from their surrounding at different periods of the server's operation: booting up, idle state, and 98% CPU utilization. For stressing the server to 98% CPU utilization lookbusy program is used.

Figure 3-14 HP SE1102 mounted on an airflow bench

The server is turned on first and the speed of the airflow bench blower is adjusted until the static pressure across the server is 0 psi. At this point, differential pressure across the airflow bench nozzle plate is recorded. This procedure is repeated for all three test. The test for airflow rate during booting up required restarting the server many times to sync the time the maximum flow rate through the server happens and when the differential pressure across the server is 0 Pa (0 psi). In all tests, room barometric pressure, room dry-bulb and wet-bulb temperatures, equivalent diameter of the open nozzles, and differential pressure across the nozzle plate are used to calculate airflow rate through the server.

Test results are shown in Table 3-1. The airflow rate during idle state is more or less same as 98% CPU utilization state. In both cases, the server draws about 0.01321 m^3/s to 0.01369 m^3/s (28 to 29 CFM). During startup the server is much noisier as a result of the server fans running at higher speed than the server at idle state. During this time the server draws about 0.02265 m^3/s (49 CFM). All of these tests were conducted with the server inlet air at room temperature. The flow rate through the server is expected to be higher if inlet air temperature is higher than room temperature.

For the 120 servers inside the IT pod, a minimum of 49 CFM x 120 server = 5880 CFM is needed. This calculation did not take into account the air flow requirement of additional IT equipment, such as switches, expected increase in airflow rate if inlet air temperature is at higher temperature, or possible increase in the number of servers in the future. To have a conservative estimate that considers the above cases, two variable frequency drive (VFD) blowers are installed in the cooling unit that can each deliver up to 6000 CFM.

Table 3-1 Airflow through HP SE1102 at three operating states

	During Boot UP	**CPU at Idle State**	**CPU at 98% Utilization**
	Flow Rate (CFM)	Flow Rate (CFM)	Flow Rate (CFM)
Test 1	48.6 ± 1.8	28.2 ± 0.5	28.3 ± 0.6
Test 2	48.6 ± 1.1	28.2 ± 0.7	29.0 ± 0.5
Test 3	48.6 ± 1.2	28.2 ± 0.7	29.0 ± 0.6
Average	48.6 ± 1.4	28.2 ± 0.6	28.7 ± 0.6

System Resistance Curve of HP SE1102

To create a computational fluid dynamics (CFD) model of the HP SE1102 server the system resistance of the server is measured on an airflow bench. To make this measurement, all four of the server fans shown in Figure 3-7 are first removed. Then the server is mounted on to an airflow bench similar to how the server is mounted in Figure 3-14. The server is not powered on in this test. Difference in static pressure across the server is measured at different flow rates. Figure 3-15 shows the system resistance curve obtained from the test.

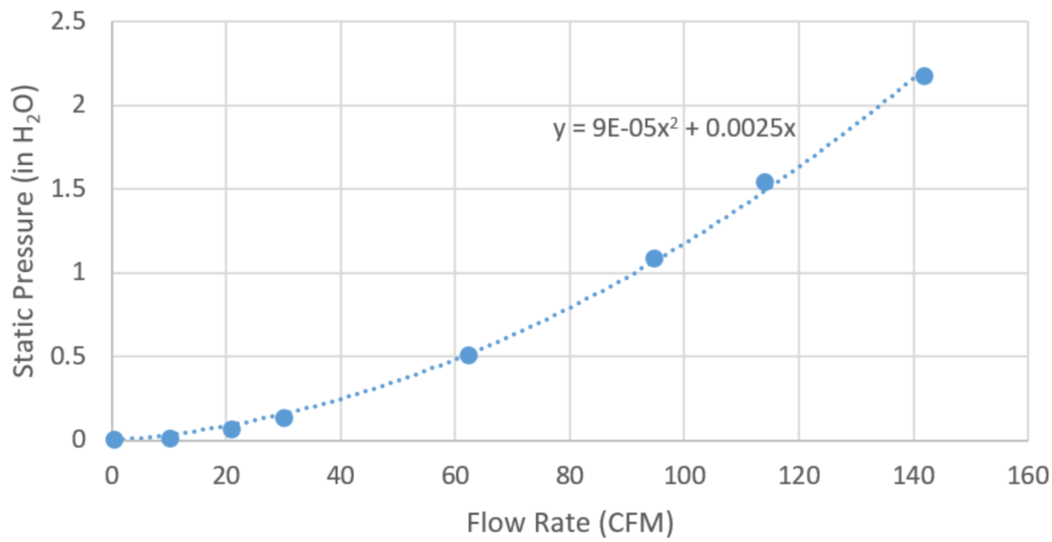

Figure 3-15 System resistance curve of HP SE1102

Direct Evaporative Cooling Media

In this section, DEC media test setup and test results are presented. The DEC media have been tested in lab to find their system resistance and saturation efficiency curves. The test results are used to develop DEC media models. In addition, this section discusses a method for wetting rigid DEC media that could improve life of the media, reduce water consumption, and provide more granular control on amount of water added to the system.

Description of Test Setup

Figure 3-16 shows a three section 0.61 m x 0.61 m x 1.83 m (24 in x 24 in x 72 in) rectangular duct attached to an airflow bench. The section attached to the airflow bench (the upstream duct) and the end section (the downstream duct) each has one Dwyer A-302F-A static pressure sensor mounted on each side of the duct. A plastic egg crate light diffuser, which covers the cross sectional area of the duct, is placed at the air inlet of the upstream duct and another one is placed at the middle of the downstream duct. On each of these plastic egg crate light diffusers, RF Code R155 humidity-temperature tags are mounted such that one tag covers one-ninth of the cross sectional area of the duct (see Figure 3-17). The middle section of the duct is where the DEC media is placed. This section has water reservoir, water pump, water distribution header, and water level regulator. Figure 3-18 shows the middle section of the duct, placement of the DEC media, the reservoir (sump), the pad for water distribution and the water supply. Figure 3-19 shows the location of the water supply and the water pump from downstream side of the duct.

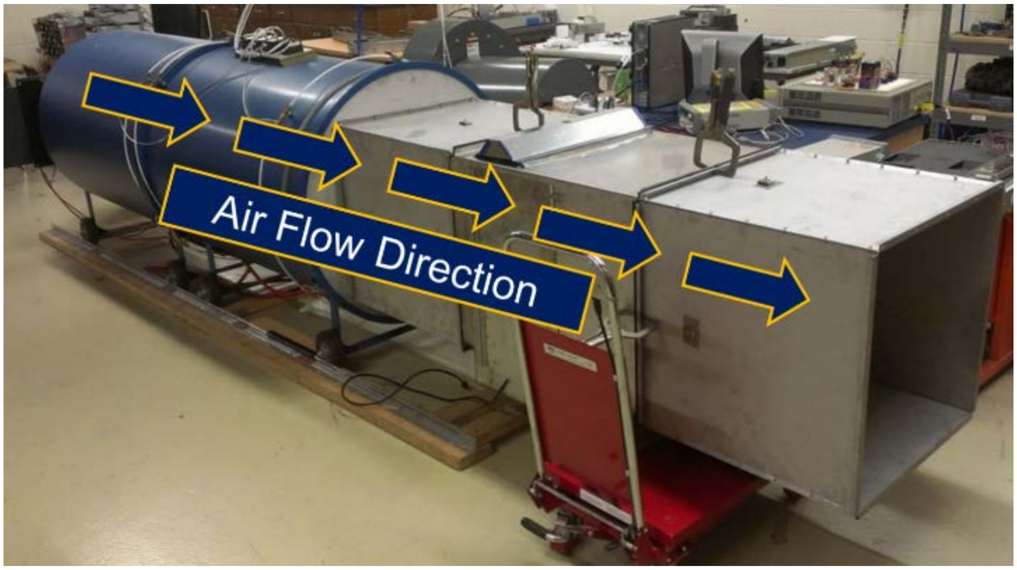

Figure 3-16 A three section rectangular duct attached to an airflow bench

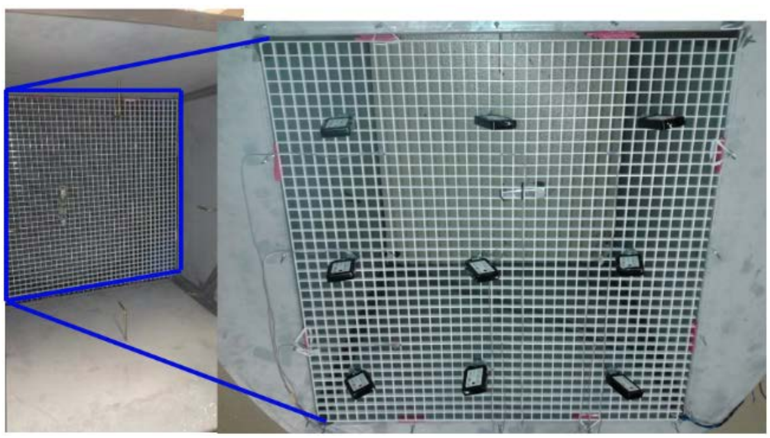

Figure 3-17 Humidity-temperature sensors mounted on a plastic egg crate light diffuser in the upstream duct (Figure adapted, with permission, [54] © 2015 IEEE)

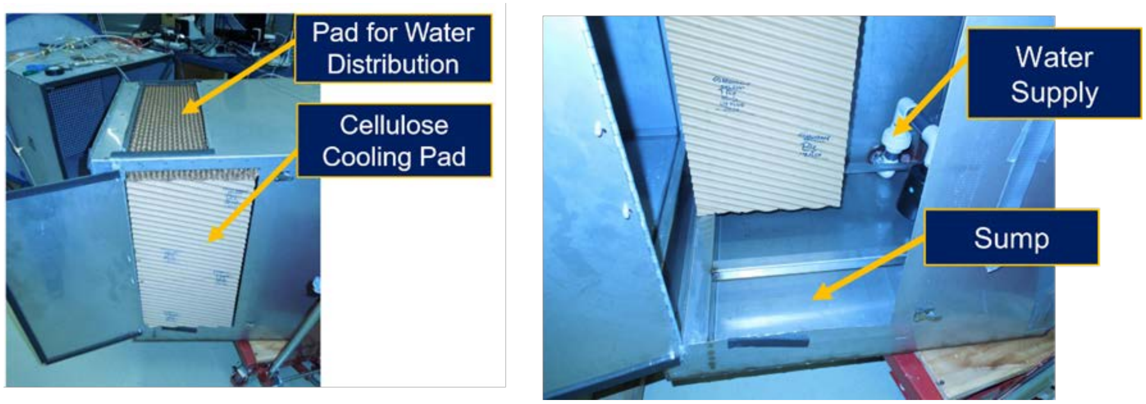

Figure 3-18 Middle section of the rectangular duct contains the DEC media and the sump

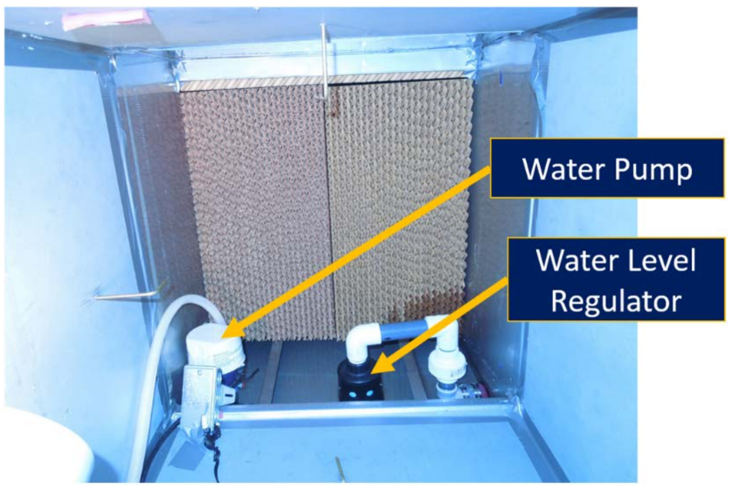

Figure 3-19 Water level regulator, water pump, and pressure taps downstream of the duct

Manufacturer of the DEC media recommends distributing 1.5 gpm per square foot of top surface area of the media [55]. Since the top surface area of the media is 1 ft x 2 ft, the water flow rate from the water pump is adjusted to about 1.893 x 10^{-4} m^3/s (3 gpm). Water flow rate from the water distribution header was measured by collecting the water discharged from the header into a graduated bucket and observing how long it took to fill 0.0038 m^3 (1 gal) or 0.0076 m^3 (2 gal).

To create a more representative operational environment for the DEC media test in laboratory room, air upstream of the DEC media needs to have higher temperature than typical room temperature. To achieve the high upstream air temperature, two ProFusion Heat Industrial Fan-Forced Heaters (Model HA22-48M) were placed at the inlet of the airflow bench blower. The heaters are powered by 208V AC supply and each heater can dissipate as much as 3600 W at this voltage.

Since the heaters add sensible heat the upstream air temperature increases and its humidity decreases. This allows testing the media in a condition where DEC use is most beneficial: dry and hot ambient conditions. Humidity of upstream air is further reduced by dehumidifying the room air with five dehumidifiers which were placed spread out in the room. All dehumidifiers were run before the wet DEC media test began so that by this began the humidity level in the room is at its lowest point possible given the limitations of the dehumidifiers' capacity and the continuous operation of the room's air conditioning system. During the wet media test the humidity of the room increased as a result of water evaporation from the DEC media; however, the continuous dehumidification and heat addition by the heaters kept the upstream air relative humidity less than 45%.

The room's dry-bulb temperature, humidity, and dew-point temperature were recorded using OM-EL-USB-2-LCD data logger. The room's barometric pressure is measured using Princo Fortin type mercurial barometer.

DEC Media Test Results

Of the various DEC media tests conducted in lab, test results for a 304 mm (12 in) thick Munters 6065/15 cellulose media are discussed below. Additional lab DEC media test discussions and results can be found in [54].

System resistance curve of dry Munters 6065/15 is obtained my measuring static pressure difference across the media at specific face velocities. Figure 3-20 shows system resistance of the media. Saturation effectiveness curve (see Figure 3-21) of the media is obtained by applying Equation 2-3.

Figure 3-22 and Figure 3-23 show dry-bulb temperature and relative humidity of air upstream and downstream of the media versus time, respectively. The rectangular box on the left hand side of both figures highlights a test condition when the face velocity is kept at 2.54 m/s (500 FPM). From this box, it can be seen that to fully wet the media it takes about 15 minutes. In Figure 3-24, saturation effectiveness change during wetting of the media is shown. The region enclosed by the box on the right hand side highlights the sensor readings when face velocity is gradually reduced to 0 m/s (0 FPM).

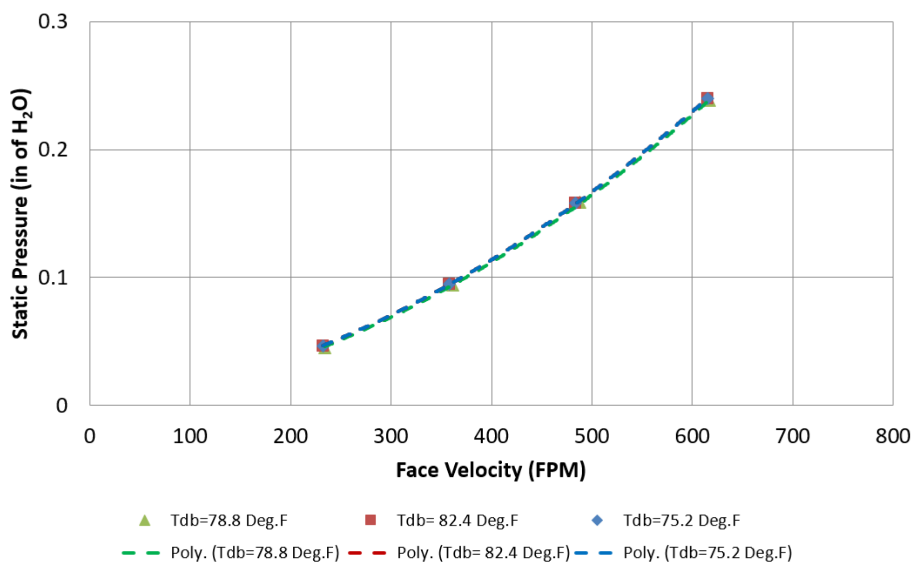

Figure 3-20 System resistance curve of a 305 mm (12 in) thick dry Munters 6560/15 media at different upstream air temperatures

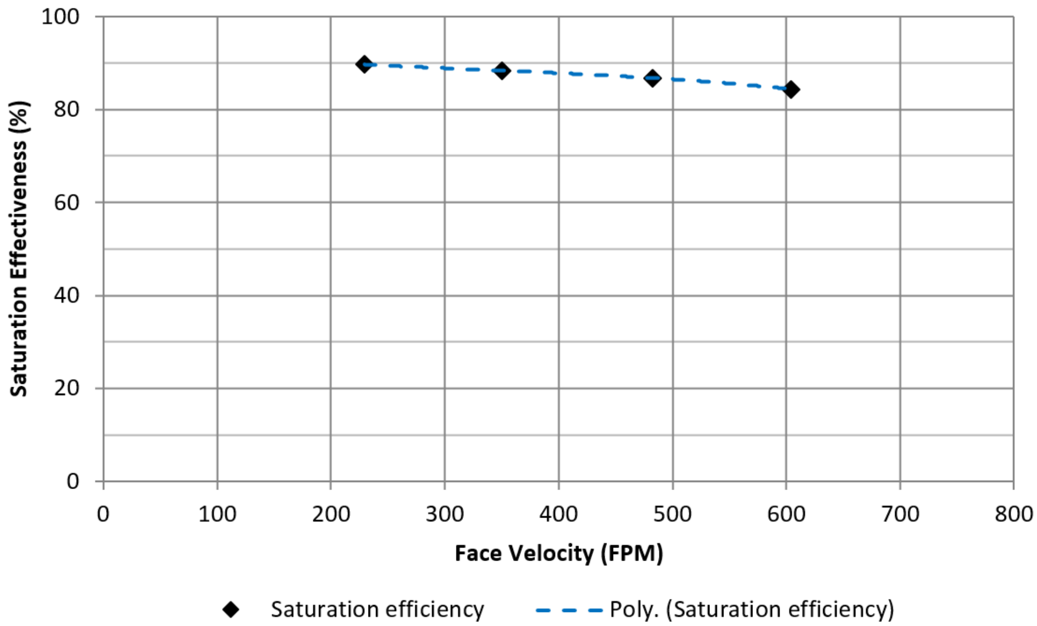

Figure 3-21 Saturation effectiveness of a 305 mm (12 in) thick Munters 6560/15 media

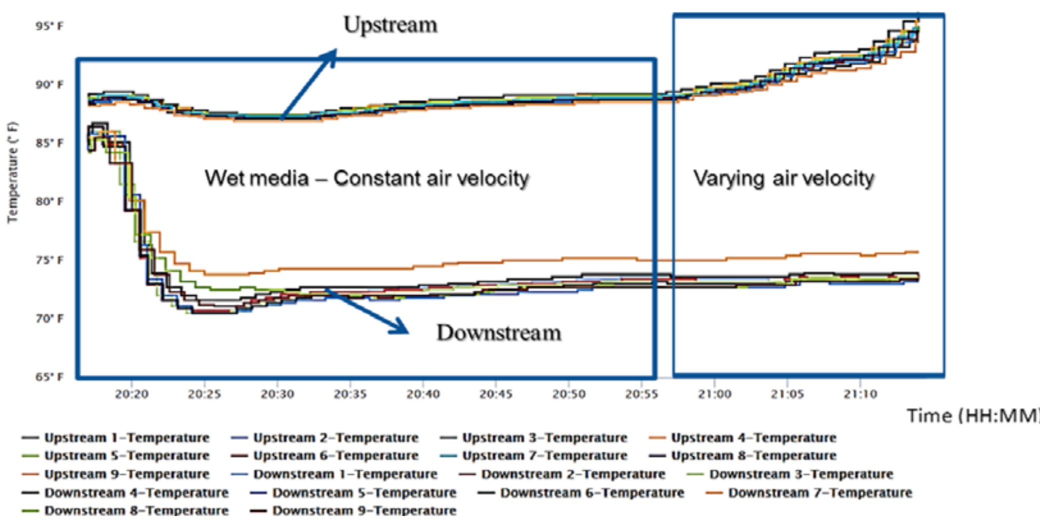

Figure 3-22 Temperature readings upstream and downstream of Munters 6560/15 media over time. (Figure adapted, with permission, [54] © 2015 IEEE)

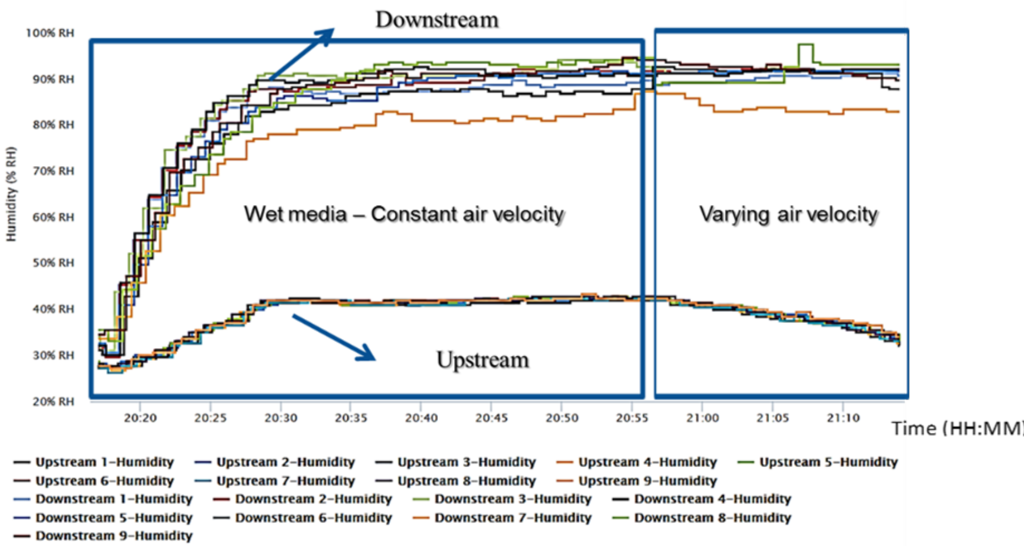

Figure 3-23 Relative humidity readings upstream and downstream of Munters 6560/15 media over time. (Figure adapted, with permission, [54] © 2015 IEEE)

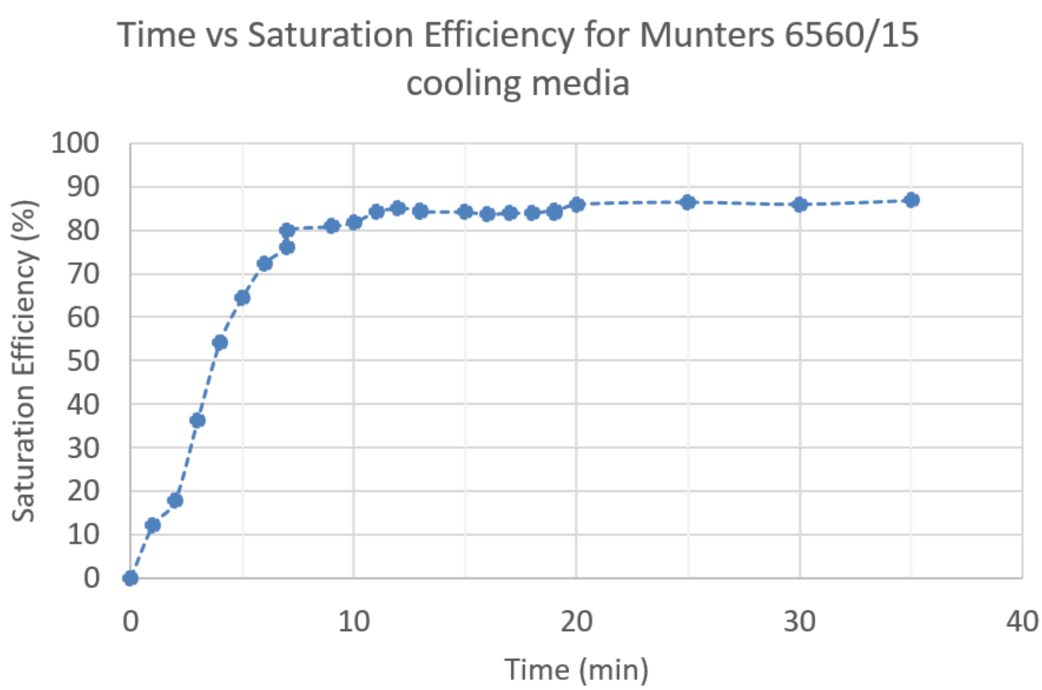

Figure 3-24 Saturation effectiveness change during wetting of the media (Figure adapted, with permission, [31] © 2015 IEEE)

Staging rigid DEC media

When using vertical staging of DEC media, [40] described that “commonly, water is supplied to every other pad along a bank of media using separate distribution headers. As the demand for humidification increases, the rest of the pads are supplied with water as well.” This method of controlling the water stages suggests that the media is either 0%, 50% or 100% wet at any given period of time (i.e. 3 stages). Another configuration of vertically staged media may be achieved by dividing the full width of the media into two, three, four or more number of equal sections and providing individually controlled water distribution headers. In this way, if the media is divided into two equal sections, the media is either 0%, 50% or 100% wet at any given time (i.e. 3 stages). Similarly, for three equal sections, the stages are 0%, 33.3%, 66.7%, and 100% (i.e. 4 stages). For four equal sections, the stages are 0%, 25%, 50%, 75%, and 100% (i.e. 5 stages). An alternative way of dividing and supplying water to the media which results in more number of stages is discussed below.

Increasing the number of stages while maintaining same number of sections allows more precise control of humidity and temperature. In addition, it reduces total water consumption of the system. In equally divided media, wetting one section is same as wetting any other section. Similarly, for a media which is divided into three or more equal sections, the sum of any two wet sections is same as any other two wet section of the media. On the other hand, if each section of an unequally divided media is used, each section by itself counts as one stage. In addition, the sum of wet areas of two sections can be different from sum of wet areas of other two sections. Thus to increase the number of stages but also provide smooth transition from one stage to the other, a MATLAB code is written to find width of DEC media sections for known total width of the media and number of sections. For the MATLAB code, see Appendix A MATLAB Code to Calculate Width of Unequal Sections for Vertically Split DEC Media Distribution. Assuming a media with a total width of 100 in is given, Table 3-2 and Table 3-3 show available stages if equal and unequal 2, 3, and 4 sections, respectively, are used to divide the media. Table 3-4 shows all stages for a four section medium obtained using the MATLAB code. Some of the stages, such as 3 and 5, 4 and 6, 7 and 8, have same percentage of wetted media. However, within each pair, the media is wetted using different combination of pumps.

Table 3-2 Available stages in equal split wall sections

	Equal Sections		
Number of Sections	Stages in %	Total number of stages	Width of sections (in)
2	0, 50, 100	3	50
3	0, 33.3, 66.7, 100	4	33.3
4	0, 25, 50, 75, 100	5	25

Table 3-3 Available stages in unequal split wall sections

	Unequal Sections		
Number of Sections	Stages in %	Total number of stages	Width of sections (in)
2	0, 33.3, 66.7, 100	4	33.3 and 66.7
3	0, 16.7, 33.3, 50, 66.7, 83.3, 100	7	16.6, 33.3, and 50
4	0, 10, 20, 30, 40, 50, 60, 70, 80, 90, 100	11	10, 20, 30, and 40

Table 3-4 Four section media showing pump on/off state

Stage #	Section width (1 = ON & 0 = OFF)				% of media that's wet
	10 in	20 in	30 in	40 in	
1	1	0	0	0	10
2	0	1	0	0	20
3	0	0	1	0	30
4	0	0	0	1	40
5	1	1	0	0	30
6	1	0	1	0	40
7	1	0	0	1	50
8	0	1	1	0	50
9	0	1	0	1	60
10	0	0	1	1	70
11	1	1	1	0	60
12	1	1	0	1	70
13	1	0	1	1	80
14	0	1	1	1	90
15	1	1	1	1	100

Overview of the CFD Models in the following Sections

In the following few pages CFD model of an I/DEC unit, ASC-20-2A11-00 is presented as published in [56]. This cooling unit has same configuration as ASC-15-2A11-00 except that it is designed to for higher cooling capacity. For example, ASC-15-2A11-00 and ASC-20-2A11-00 have 15 ft^2 and 20 ft^2 of face area for the evaporative sections, respectively, and can handle as much as 7,500 CFM and 10,000 CFM with standard configurations, respectively. ASC-20-2A11-00 is referred to simply as ASC-20 in the following sections.

Another modular data center is modeled using a CFD tool, FloVENT 9.2, and included in this dissertation, in full as published in [57], starting page 87. This modular data center is designed to be cooled using ASC and fogging type DEC. The fogging system is assumed to be not in operation in this CFD model.

CFD Modeling of Indirect/Direct Evaporative Cooling Unit for Modular Data Center Applications

(Reprinted with permission © 2013 ASME) [58]

Abstract

An information technology (IT) container needs to be supplied with cold air to cool IT equipment housed in it. The type of cooling system to be used depends on many factors including geographical location of the modular data center. Data centers located in regions where the climate is cold benefit from use of air-side economization (ASE) and those located in hot and dry climate benefit from use of direct and/or indirect evaporative cooling (DIEC) systems. In terms of energy saving, ASE, direct evaporative cooling (DEC) system, and indirect evaporative (IEC) systems are better than compressor based cooling systems such as computer room air conditioning (CRAC) units and air handling units (AHU).

In this study, an existing DIEC unit which can also be operated in ASE mode is modeled in a computational fluid dynamics (CFD) tool. The cooling unit is intended to be used for supplying cold air to a containerized data center with specified volume flow rate, dry-bulb temperature and relative humidity. The CFD model is compared with published data of the cooling unit to see how well the CFD model represents the actual system and few design improvement ideas are tested by modifying the CFD model and running simulations. Results show that supplying air horizontally or as a downdraft to an IT container has negligible effect on the overall system. Results also show that orientation of dampers and placement of blanking panels inside the mixing chamber could affect the lifespan of air filters.

Introduction

Modular data centers may have their cooling system as integral part of the IT container or the cooling system could be separate from the IT container. While the former allows movement of the IT equipment and cooling system as one unit, the latter provides more space for IT equipment within the IT container and provides freedom to choose where the cooling system could be placed relative to the IT container. Figures 1-3 show three examples for placement of a cooling system with respect to the IT container. In figure 1 the cooling unit is placed on top of the IT container and in figures 2 and 3 the cooling unit is placed adjacent to the IT container.

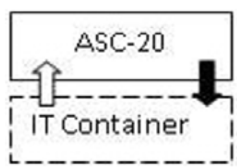

Figure 1 Side View

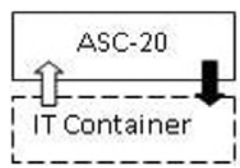

Figure 2 Top View

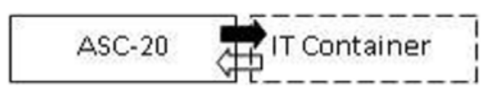

Figure 3 Top View

In this paper an existing cooling system, ASC-20 [1], which can be placed on top of an IT container or adjacent to the IT container, is modeled in a CFD tool. The unit can be operated in ASE, DEC, IEC, and DIEC modes and is intended to be used for cooling containerized data centers with a flow rate of 10,000 CFM, supply dry bulb temperature between 15°C and 32°C, and relative humidity between 20% and 80%. These temperature and humidity requirements are same as Class A1 requirements of ASHRAE TC9.9: 2011 ASHRAE Thermal Guidelines for Data Processing Environments Expanded Data Center Classes and Usage Guidance [2].

The cooling system, ASC-20, is shown in figures 4 and 5. Figure 4 shows isometric view of the actual unit. In figure 5 internal components of ASC-20 can be seen. Before cold air is supplied to the IT container, it passes through the inlet louvers, inlet dampers, air filters, IEC coils, DEC pads, and through the blowers. The IEC coils use water as the working fluid. During sensible cooling, water inside the IEC coils becomes warm and is ducted to the cooling tower (CT) where the warm water is made to flow on top of wet cooling pads inside the CT. Here ambient air blowing over the wet cooling pads cools the water flowing down the cooling pads. Cooled water is then sucked by submerged pumps inside the CT to return the cold water back to the IEC coils.

Figure 4 ASC-20: Aztec Evaporative Cooing Unit

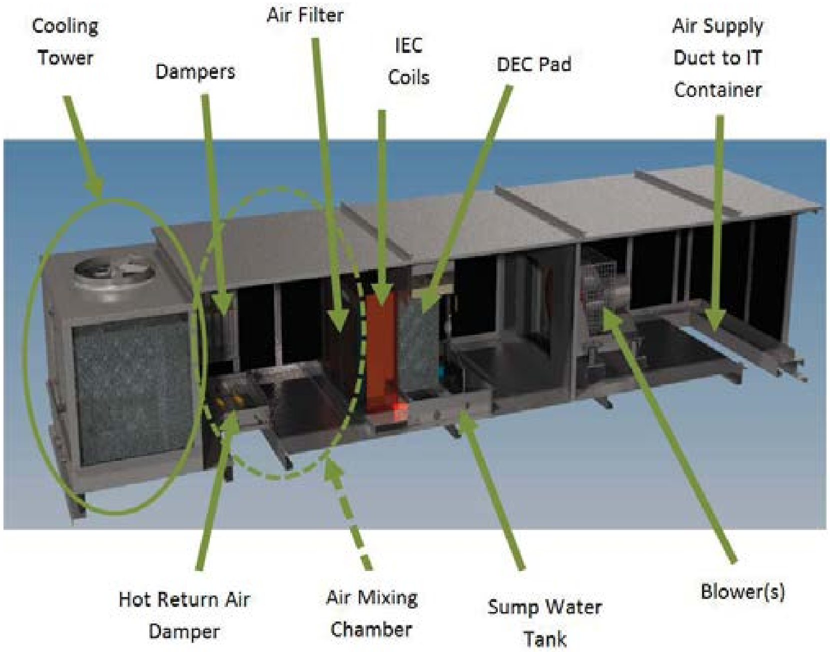

Figure 5 Internal Components of ASC-20

Components of ASC-20 used in the CFD model are shown in table 1. Using characteristics of these components, a CFD model of ASC-20 is created. The CFD model is compared with component specification provided by the manufacturer of the cooling unit to see how well the CFD model represents the actual system. Few design improvement ideas are tested by modifying the CFD model and running simulations. Results show that the CFD model is in good agreement with published data and changes made to the CFD model, such as changing orientation of inlet dampers, may significantly affect lifespan of air filters.

Table 1 ASC-20 Parts

Components	Make and Model
Air Filter	Z-LINE® Series, HV
IEC Coils	Mestex
DEC Pad	Munters HUMI-KOOL Pad
Blower	Lau SF 182-9-100
CT Air Filter	MV EZ Kleen filters
CT DEC Pad	Munters HUMI-KOOL Pad
CT Fan	Dynamaster Model FN30L6

Modeling

When CFD model of ASC-20 is created, small features that are considered to have little or no effect in the air flow and temperature distribution are removed or modified. Similarly some components are modeled as two-dimensional objects. For example, louver thickness is assumed to be negligible and is modeled as two-dimensional object.

Ambient air is assumed to be at 1 atmosphere, 100°F dry-bulb temperature, and 64.8°F wet-bulb temperature. In modeling the DEC and IEC units, 88% and 80% saturation efficiencies are assumed, respectively. K-ε turbulence model and double precision solver are used for all models. Grid sensitivity analysis was performed and it was found that a total cell count of 3.5 million and an aspect ratio of 12 would give satisfactory results. Simulation results in this paper are presented for models with at least 3.5 million cells and a maximum aspect ratio of 20.

Figure 6 and figure 7a show a model with inlet dampers on both sides of ASC-20 pointing toward the air filters; supply duct in this model delivers cold air to an IT container which is assumed to be below the cooling unit. Figures 7a through 7c show location of monitor points, size of solution domain, and relative placement of ASC-20 with respect to the solution domain. As shown in figure 8, localized, high density meshing is applied on units such as louvers and mixing chamber to capture effect of high speed flow and high turbulence in these regions.

Figure 6 will be considered a Baseline Case and a variation of this case with supply duct oriented horizontally as shown in figure 9 will be identified as Case 1. Another variation of the Baseline Case, Case 2, has all dampers on one side of ASC-20 pointing toward the cooling tower (see figure 10). A third case, Case 3, has all inlet dampers pointing toward the cooling tower (see figure 11). In addition, two variations of Case 3 are created with flow obstructions in the form of a rectangular plate and parallelepiped block inside the mixing chamber; these cases will be identified as Case 3.1 and Case 3.2, respectively (see figures 12a and 12b). The purpose of placing blanking panels inside the mixing chamber is to improve air flow distribution over the face of air filters.

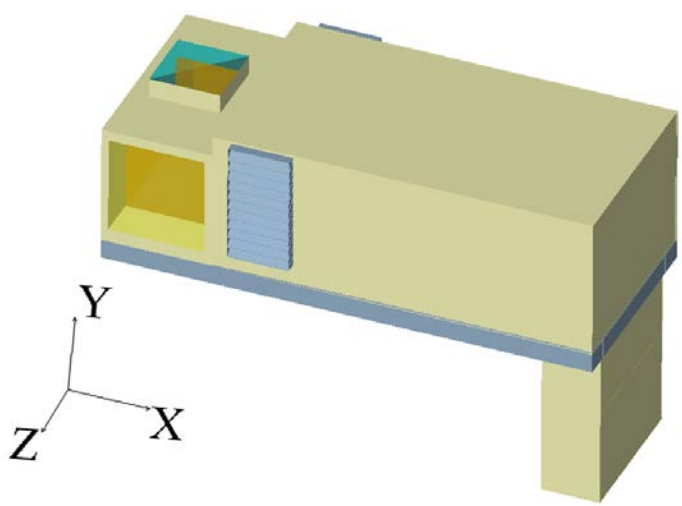

Figure 6a Baseline CFD Model of ASC-20

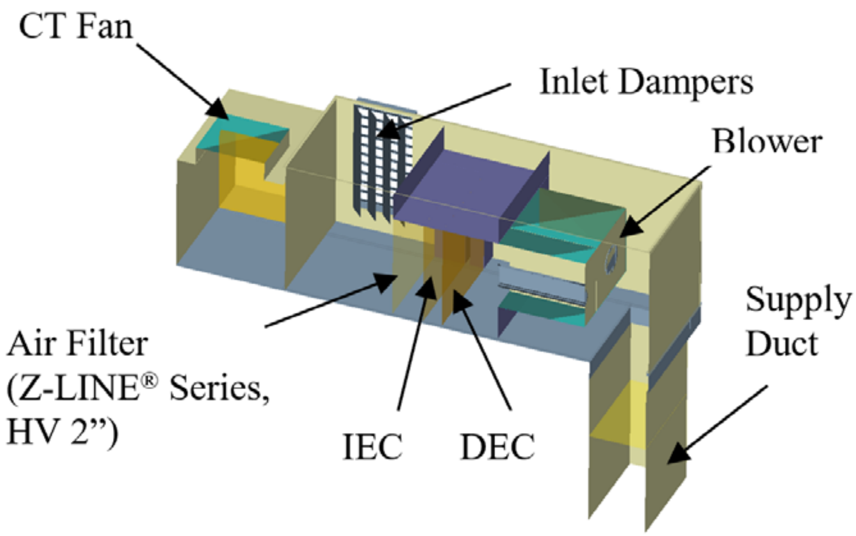

Figure 6b Baseline CFD Model of ASC-20 Internal Details

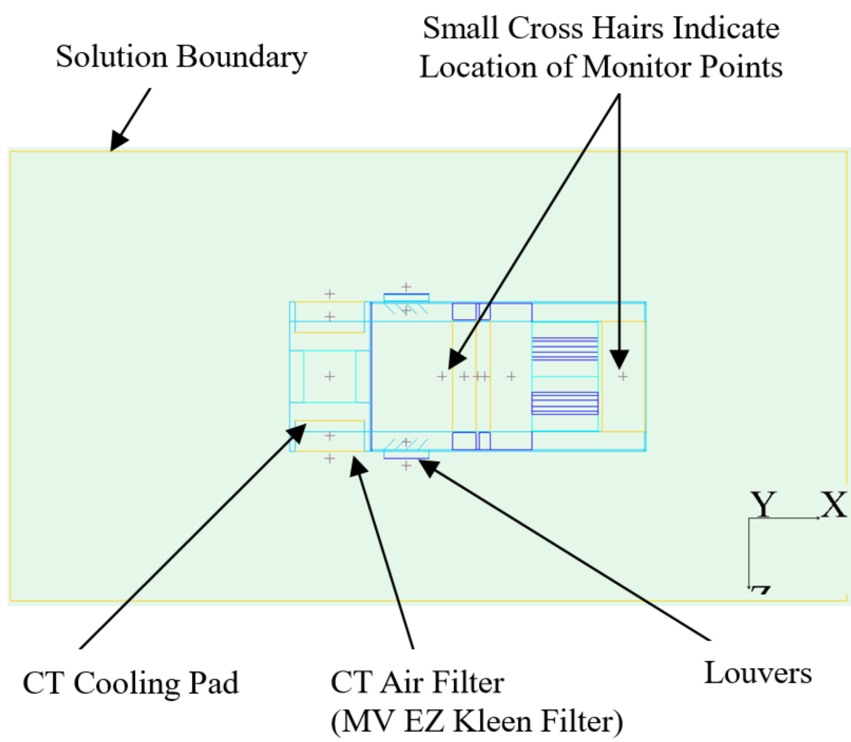

Figure 7a Top View of Baseline CFD Model: Both sets of dampers point toward the air filters.

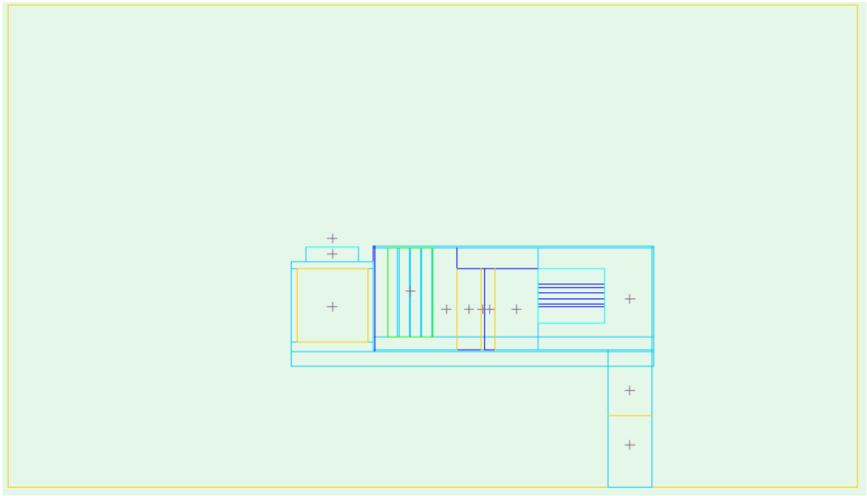

Figure 7b Side View (Negative Z View) of Baseline CFD Model

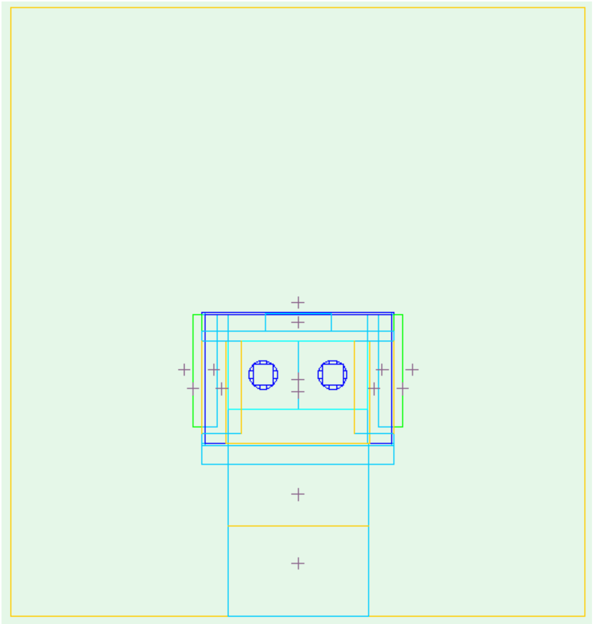

Figure 7c Side View (Negative X View) of Baseline CFD Model

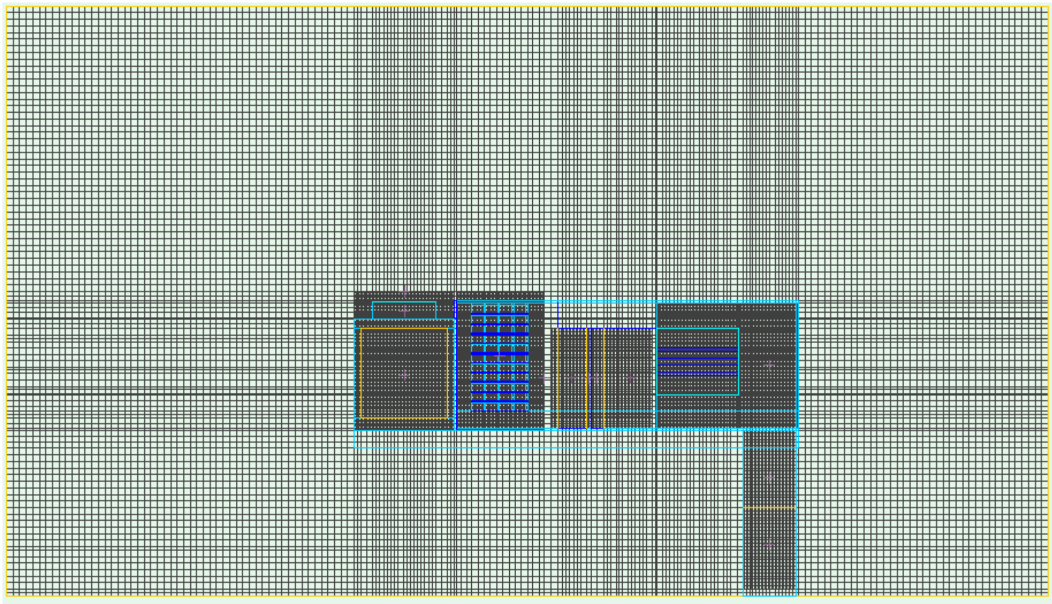

Figure 8 Side View – Meshing

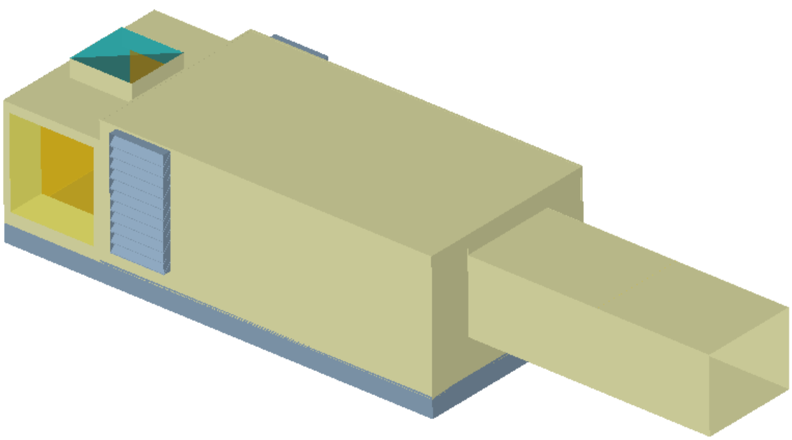

Figure 9 Case 1 Horizontal Air Supply

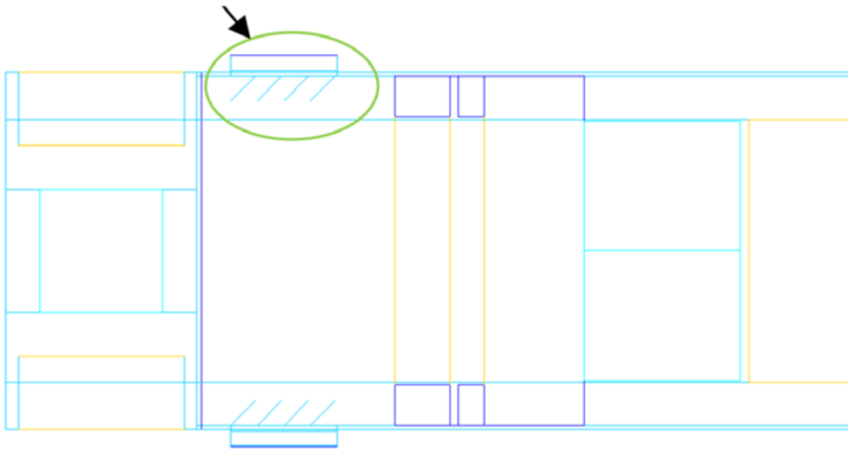

Figure 10 Case 2 One set of dampers point towards the cooling tower while the second set point towards the air filters

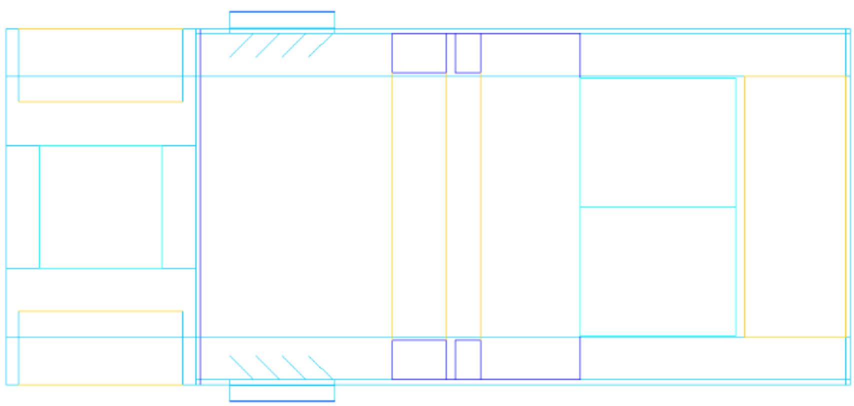

Figure 11 Case 3 Both sets of dampers point toward the cooling tower

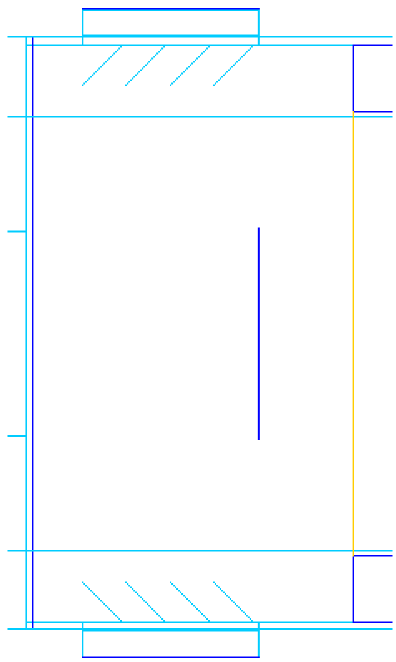

Figure 12a Case 3.1 Rectangular obstruction has width 30 inches and extends from bottom to top of ASC-20 enclosure

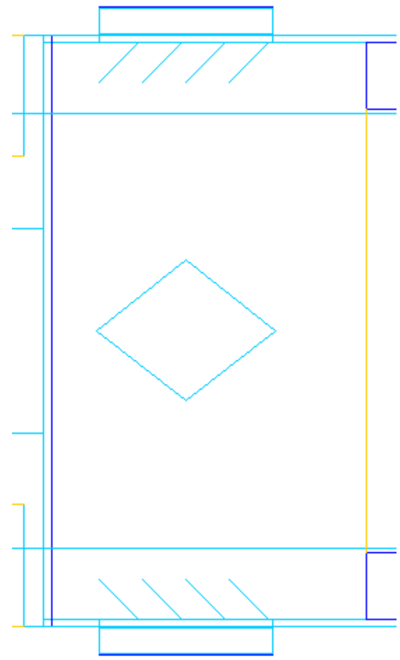

Figure 12b Case 3.2 parallelepiped extends from bottom to top of ASC-20 enclosure

Results

CFD simulation of the Baseline Case has been run and the result for speed of air through each component is provided in table 2. Static pressure for each component is calculated using the speed of air through a component and its system resistance specification. Comparison between the calculated static pressure and the results from the CFD simulation are provided in table 2.

Table 3-5 Comparison between expected and measured pressure drops for various components of ASC-20

	Air Speed (FPM)	Calculated (in H_2O)	CFD Results (in H_2O)	Difference in Pressure Drop (%)
Air Filter (Z-Line Series HV Filter 2")	535.2	0.31[2]	0.31	0.0
Indirect Evaporative Cooling Coils	535.2	0.76[3]	0.80	5.3
Munters HUMI-KOOL Pad (after the IEC Coils)	535.9	0.23[4]	0.24	4.3
Munters HUMI-KOOL Pad A in the CT Section	489.4	0.19[4]	0.19	0.0
Munters HUMI-KOOL Pad B in the CT Section	490.4	0.19[4]	0.19	0.0
MV EZ Kleen Filter A in the CT Section[1]	489.0	0.13[5]	0.13	0.0
MV EZ Kleen Filter B in the CT Section[1]	488.5	0.13[5]	0.13	0.0
Louver A + Damper A[1]	629.8	0.27[6]	0.27	0.0
Louver A + Damper B[1]	629.8	0.27[6]	0.26	3.7

[1]A or B indicate one of the two sides of ASC-20, [2]From [3], [3]From [1], [4]From [4], [5]From [5], [6]From [1]

Figure 12 shows state points on a psychrometric chart as air travels through ASC-20. Point 1 is for ambient air, Point 2 for air immediately after the IEC coils, Point 3 for air supplied to the data center, and Point 4 for air leaving the CT. Table 3 gives the theoretical values and the CFD results of dry-bulb temperature and specific humidity for the four points. The table also includes the theoretical values for relative humidity for all four points. Figures 13 and 14 show temperature and specific humidity (concentration) profiles for the Baseline Case.

Power consumption of the CT fan and the two blowers is estimated by multiplying volume flow rate by static pressure for each component. Table 4 lists the estimated power consumption for the Baseline Case and Case 1.

Figures15a through 19b show velocity profiles for all cases that supply air as downdraft. Figures with caption “X-Velocity Profile” show x-component of velocity for a cut plane located at the Z-Line Series HV 2" air filters. Looking at only the x- component of velocity, instead of air speed, may provide a better understanding of the relationship between reliability of filters and effect of air velocity on filters. Figures with velocity arrows show how air flows through ASC-20. The cut plane in this case is taken at about half the height of ASC-20 enclosure.

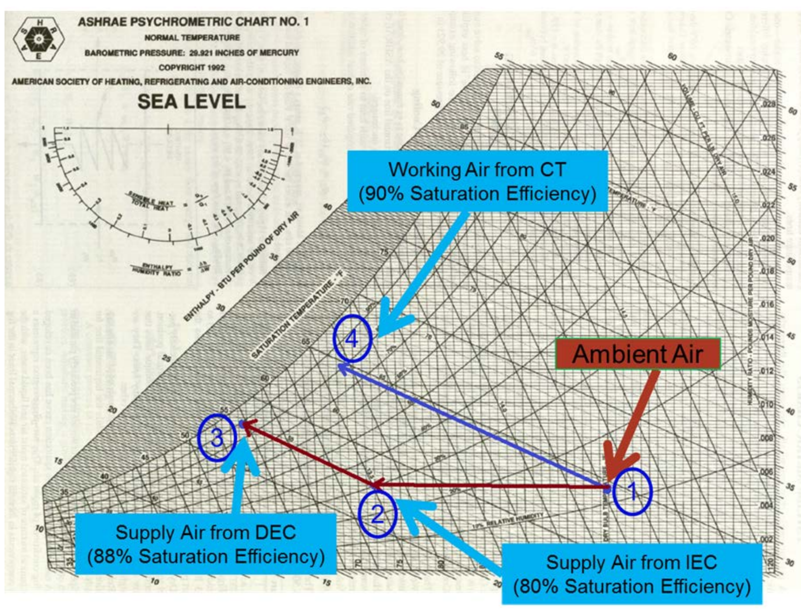

Figure 12 State Points (1) ambient air (2) air immediately after the IEC coils (3) Air supplied to data center (4) Air leaving the cooling tower

Table 3 Temperature and specific humidity values at points 1, 2, 3, and 4

	Expected Dry-Bulb Temp. (°F)	CFD Result Dry-Bulb Temp. (°F)	Expected Specific Humidity (lb/lb)	CFD Result Specific Humidity (lb/lb)	Expected Relative Humidity (%)
Point 1	100.0	100.0	0.0051	0.0051	12.5
Point 2	71.8	71.3	0.0051	0.0053	30.8
Point 3	56.6	56.1	0.0085	0.0085	87.0
Point 4	68.3	68.3	0.0123	0.0123	82.8

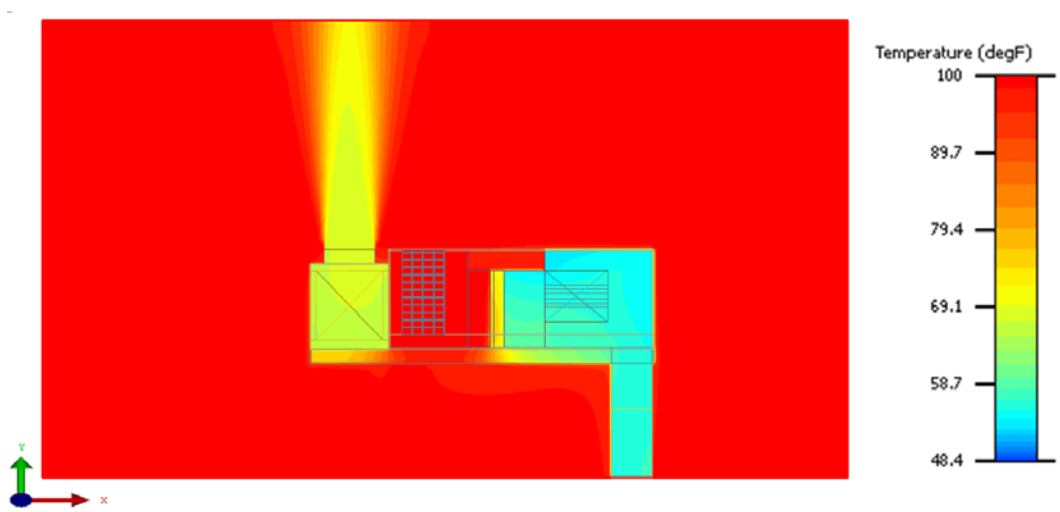

Figure 13 Dry-Bulb Temperature Profile for Baseline Case

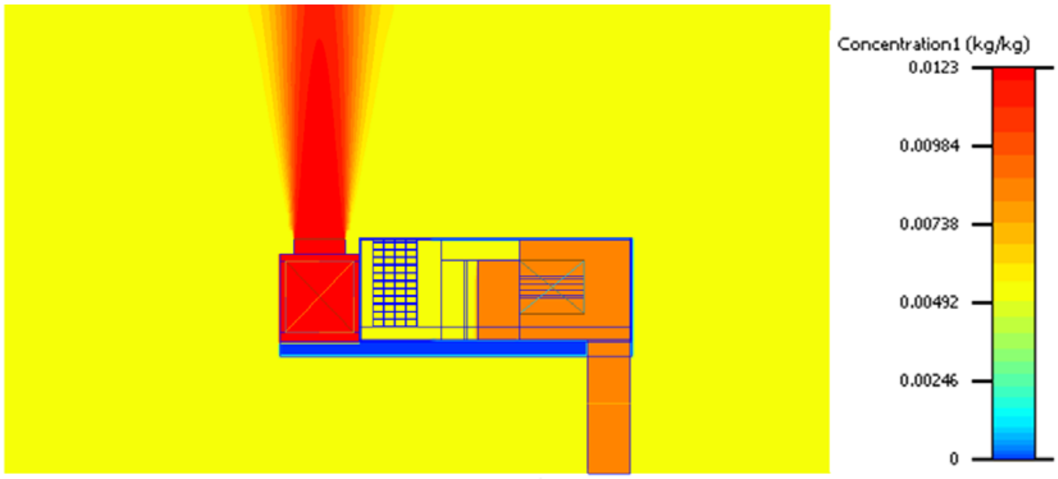

Figure 14 Specific Humidity (Concentration) Profile for Baseline Case

Table 4 Power consumption of blowers and cooling tower fan

	Baseline Case	Case 1
Blower	2531.2 W	2507.4 W
Fan	520.4 W	520.4 W
Total	3051.7 W	3027.9 W

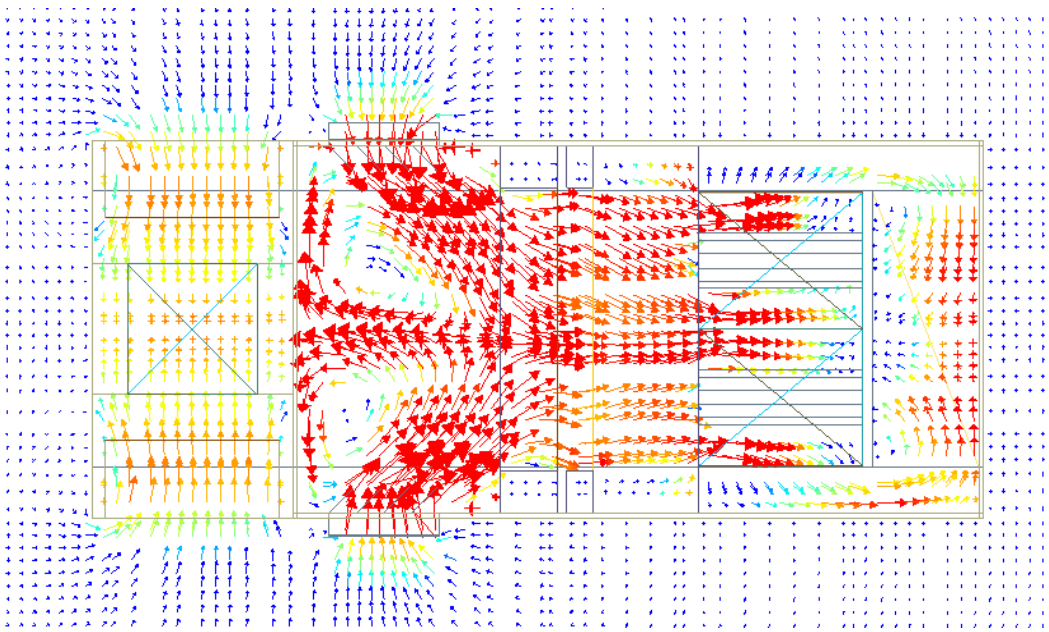

Figure 15a Baseline Case Velocity Profile - Top View

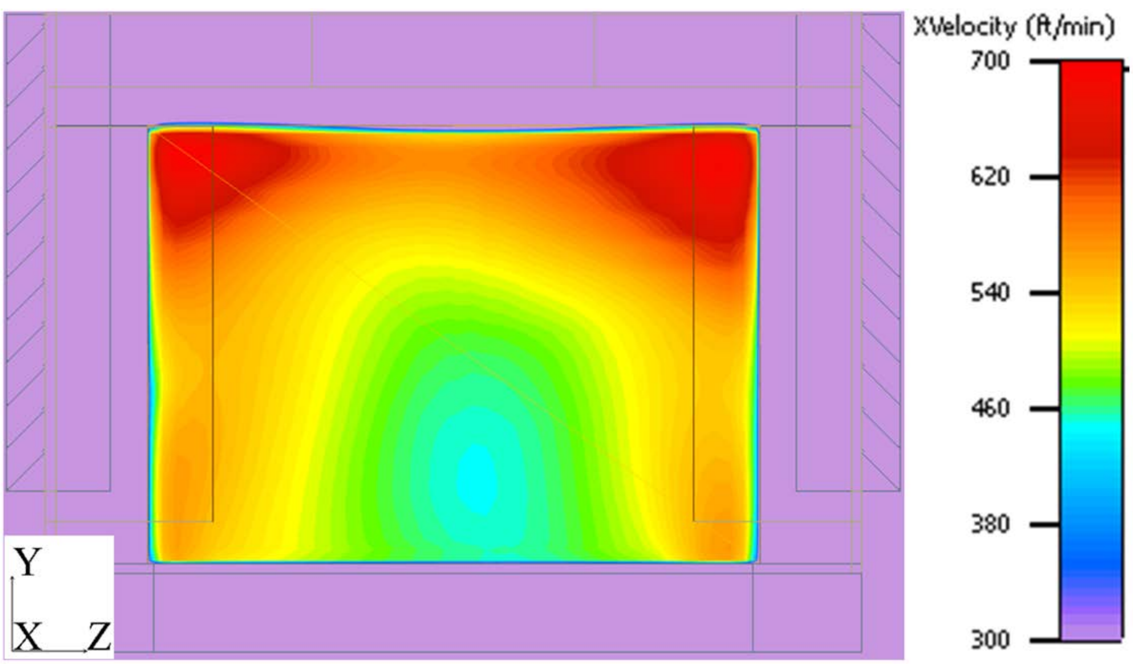

Figure 15b Baseline Case X-Velocity Profile

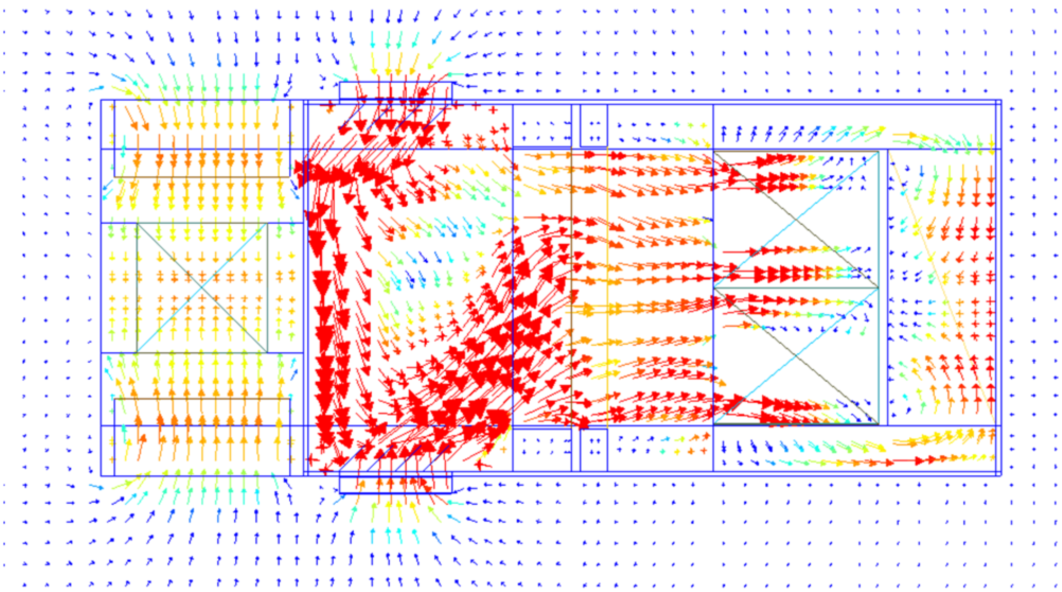

Figure 16a Case 2 Velocity Profile Top View

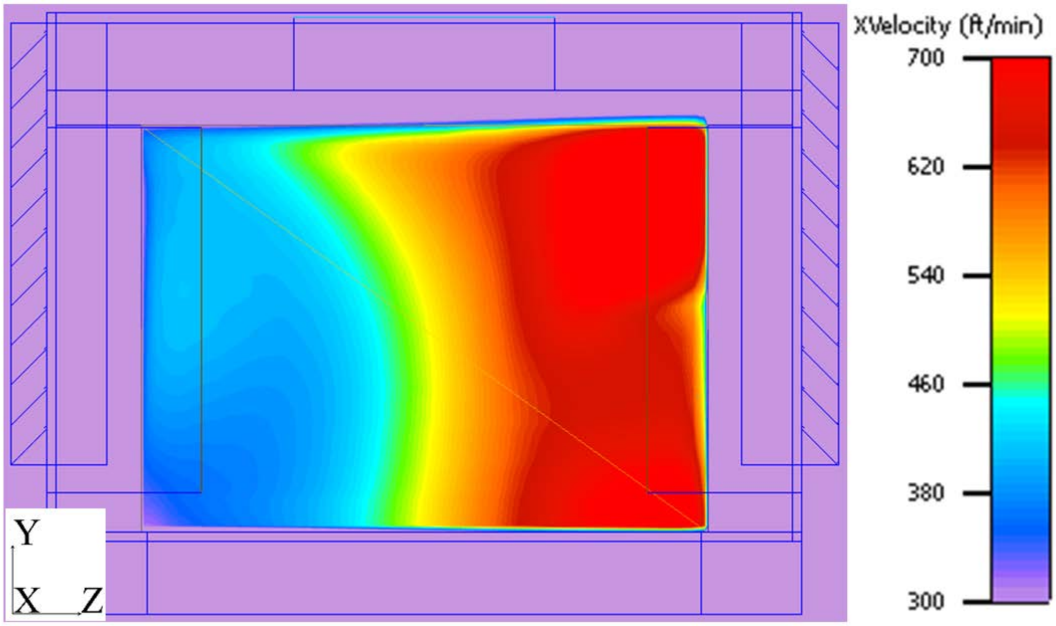

Figure 16b Case 2 X-Velocity Profile

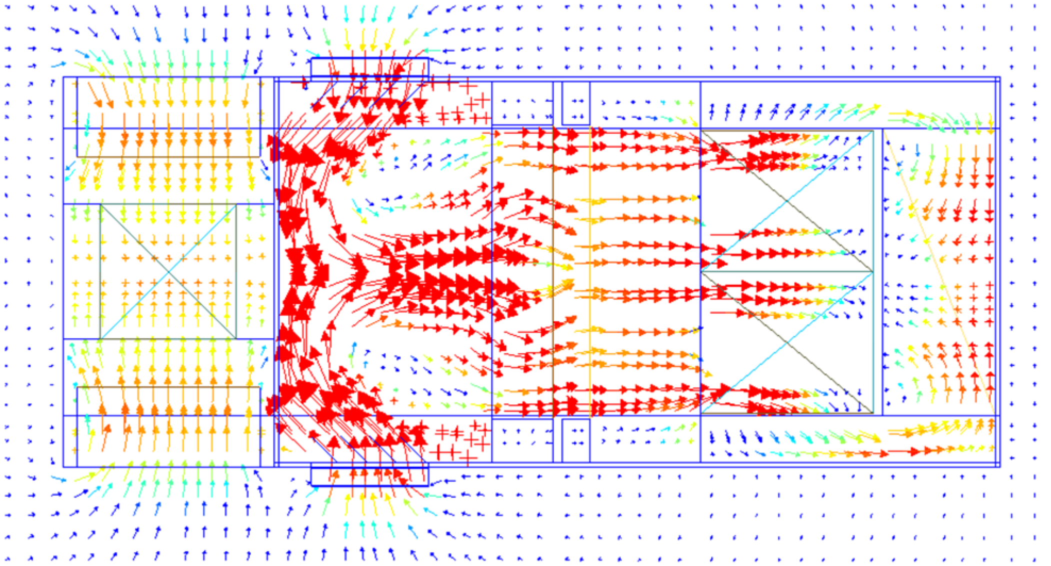

Figure 17a Case 3 Velocity Profile Top View

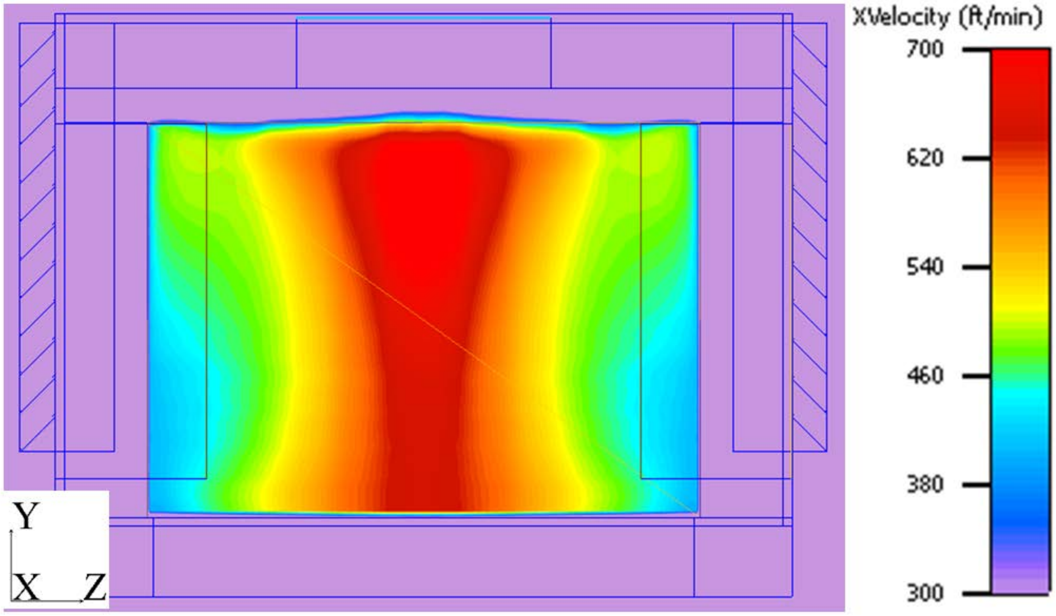

Figure 17b Case 3 X-Velocity Profile

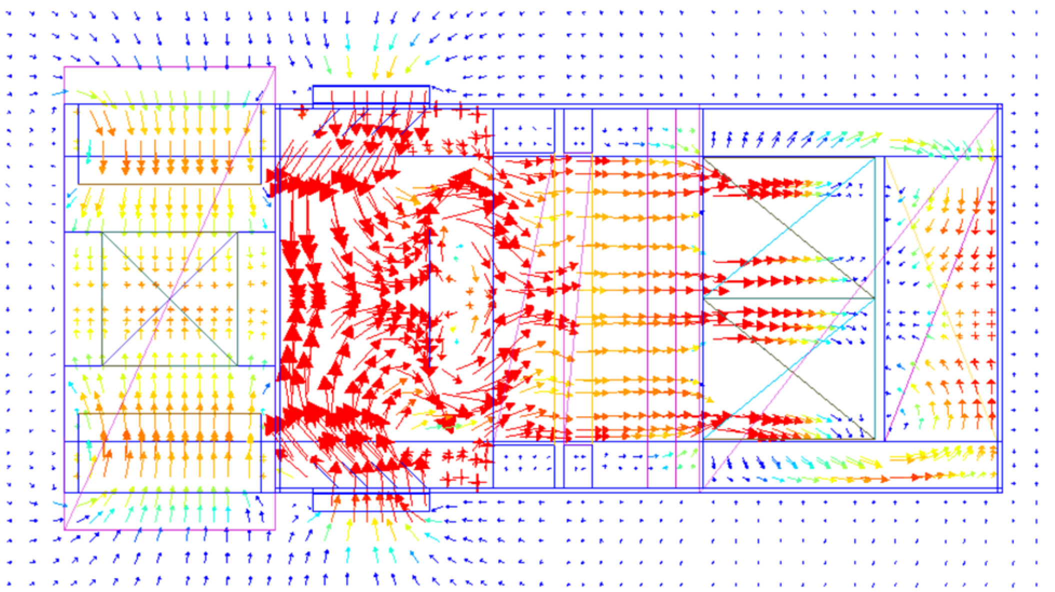

Figure 18a Case 3.1 Velocity Profile Top View

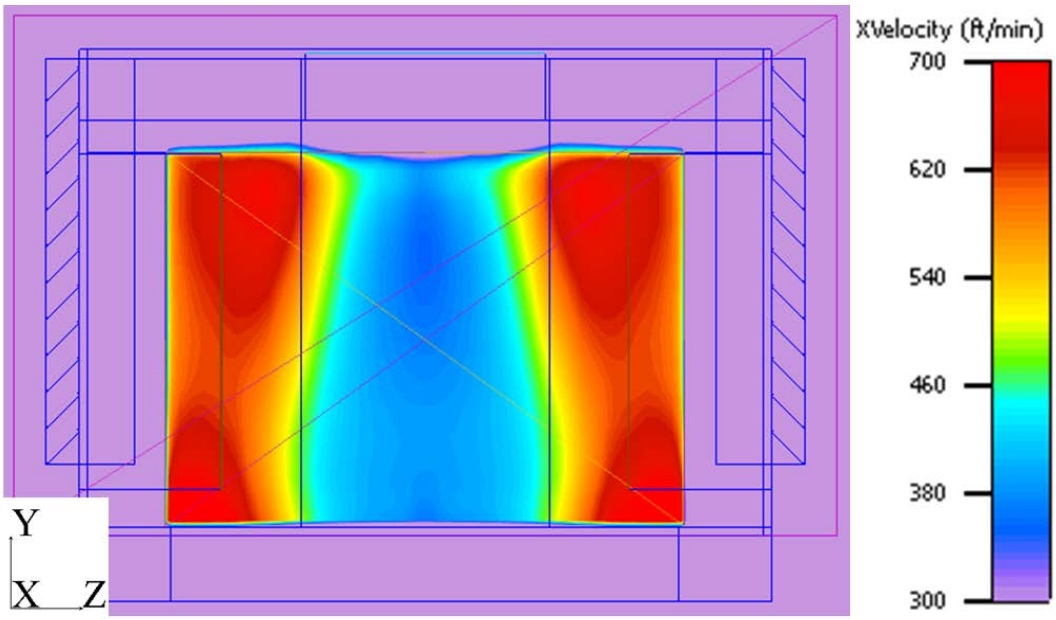

Figure 18b Case 3.1 X-Velocity Profile

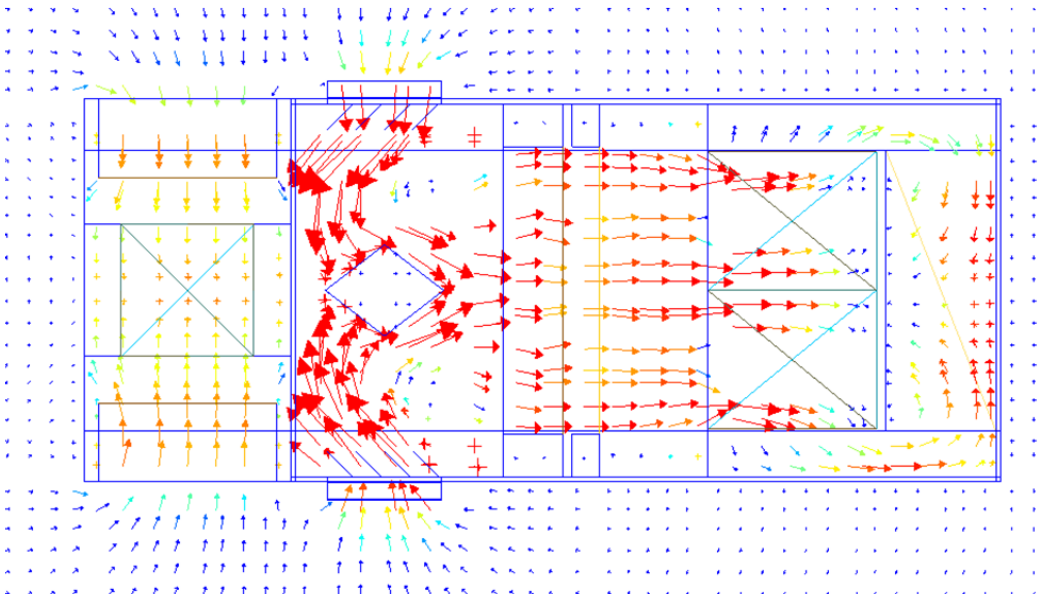

Figure 19a Case 3.2 Velocity Profile Top View

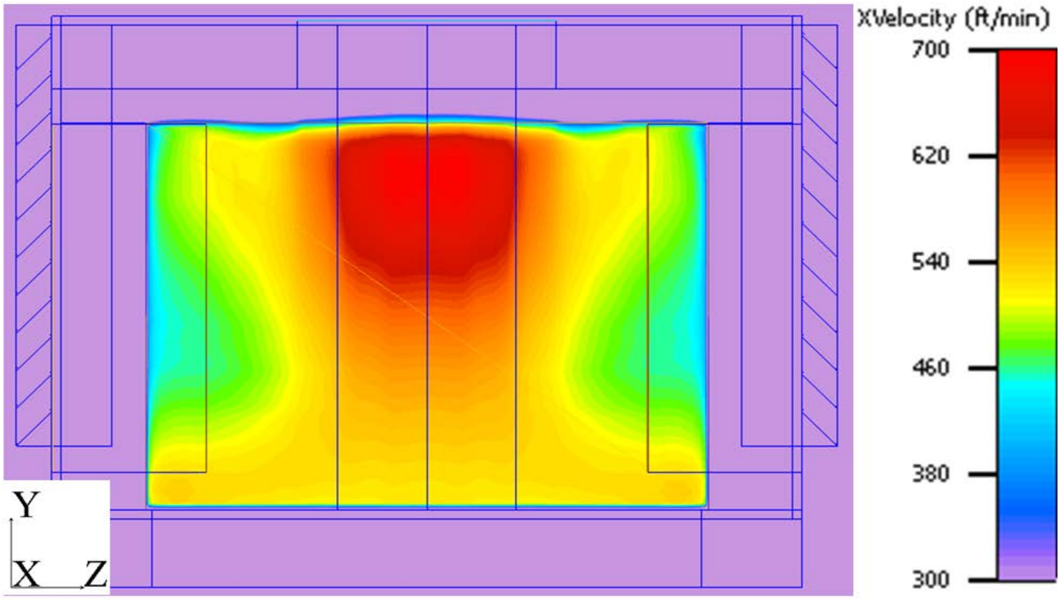

Figure 19b Case 3.2 X-Velocity Profile

Discussion

In table 2, the maximum difference in static pressure between CFD results and calculated values is 5.3%. This is a small difference and the CFD model could be considered to provide good system resistance representation of the actual components. Further, table 3 shows that the difference in, both, temperature and specific humidity between the CFD results and the theoretical values at all four points is negligible.

Note that the supply air temperature, 56.1°F (13.4°C), and relative humidity, 88% (i.e. RH at 56.1°F and 0.0085 lb/lb), in table 3 are colder and more humid than what is recommended for a Class 1 data centers [2]. This is because the CFD model is setup so that DEC and IEC units are assumed to be at 88% and 80% saturation efficiencies, respectively. However, in practical situations, the supply air temperature and humidity can be controlled by such methods as introducing hot data center return air into the mixing chamber, reducing the amount of volume flow rate delivered to the data center, etc.

Figures 13 and 14 show how air temperature and specific humidity change as air flows through ASC-20. Since hot air return dampers are completely closed in this model, both, figures show that the mixing chamber has same color as the ambient, indicating that no change in air property occurs in this section. Dry-bulb temperature sharply decreases in the IEC- DEC section to that of the supply air condition. Specific humidity sharply increases as air flows over the DEC section. Although air leaving the CT is about 20°F lower in dry-bulb temperature than the ambient, it should not be introduced into the mixing chamber since it has high moisture content (0.0123 lb/lb specific humidity).

Table 4 shows that there is negligible difference (less than 1%) between the total power consumptions calculations for the Baseline Case and Case 1. This indicates that placing the cooling unit on top of an IT container or adjacent to it may not have any effect on the amount of energy consumption by the blowers and CT fan.

Figure 15a shows air flow pattern and figure 15b shows the x-component of velocity for the Baseline Case. The red areas on figure 15b indicate that x-component of velocity is around 700 FPM which is higher than commonly suggested 500 FPM maximum velocity. Since six Z-Line Series HV 2" filters will be used to cover a 20 ft2 area, those filters located in the red region may degrade in performance faster than the other filters.

Air flow distribution over the face of air filters may be improved by placing blanking panels inside the mixing chamber and changing orientation of inlet dampers. Changing orientation of only one set of inlet dampers as in figure 16 (Case 2), both sets of inlet dampers as in figure 17 (Case 3), or placing a rectangular blanking panel inside the mixing chamber as in figure 18a (Case 3.1) worsen the maldistribution of air flow through the filters. Figure 19 (Case 3.2) shows that the red color is concentrated in one region which covers approximately equal red area as the Baseline Case.

Although uniform distribution has not been achieved in the above cases, a different configuration of blanking panels and orientation of dampers could provide a more uniform air flow distribution over the face of air filters. Air filter face area larger than 20 ft2 may provide a more uniform air flow distribution. Further, the current volume flow rate through the filters, 10,704 CFM, could be reduced to 10,000 CFM by utilizing a fan curve for the blowers associated with lower speed of rotation.

Conclusion

An actual cooling system, ASC-20, has been modeled in a CFD tool and the model was verified by comparing simulation results with specifications of ASC-20 and its components. Simulation results showed that there is negligible difference between supplying air in as downdraft or horizontally to an IT container. Orientation of inlet dampers and placement of blanking panels inside the mixing chamber affect how air flow is distributed over the face of air filters. Uniform distribution of air flow over the face of air filters may be achieved with proper placement of blanking panels and orientation of inlet dampers.

Acknowledgments

This work is supported by NSF I/UCRC in Energy-Smart Electronic Systems (ES2).

References

[1] "Technical Guide for: ASC," 2010. [Online]. Available: http://mesteksa.com/fileuploads/Literature/Applied%20Air/Evaporative%20Cooling%20Units/TGASC-1.pdf.

[2] "ASHRAE TC 9.9: 2011 Thermal Guidelines for Data Processing Environments – Expanded Data Center Classes and Usage Guidance," 2011.

[3] “Glasfloss® Industries: Z-LINE® SERIES SB, ZL, HV and MR-11.” Product Bulletin 6ZLINE. Section 6. 10-12-12. www.glasfloss.com

[4] “MUNTERS HUMI-KOOL: CELdek, GLASdek Performance (6560/15 at various depths).”

[5] “All Standard Products: EZ Kleen® Air Filters.” Research Products Corporation. 1998.

[6] 2009 ASHRAE Handbook - Fundamentals

CFD Analysis of Free Cooling of Modular Data Centers

Abstract

Air-side economizers use outside air for cooling information technology (IT) equipment completely or part of the time (coupled with traditional computer room air conditioning (CRAC) units). This system is often used in colder climates and requires less energy since it doesn't use compressors for cooling incoming air. In this paper, thermal performance of an air side economizer for a modular data center is studied using computational fluid dynamics (CFD). The modular data center is comprised of two 12 ft x 40 ft (3.66 m x 12.19 m) IT containers, one 12 ft x 40 ft (3.66 m x 12.19 m) power/cooling module, and a 12 ft x 36 ft (3.66 m x 10.97 m) plenum. Blowers in the power/cooling module draw outside air, pass it through filters, and distribute the air between the two IT modules. The IT modules are arranged in a hot/cold aisle arrangement with a total heat load of 1.2 MW. The two IT modules contain more than 5000 servers, actuator controlled louvers, and sensors needed for cooling system control. CFD analysis of the modular data center showed the importance of louver angles at the inlet of the IT containers. Based on the simulation results improvements have been made to the modular data center by adjusting the angle of the louvers to improve airflow distribution in the servers. This change resulted in significant improvement in the mean exhaust temperature at the servers.

Keywords

Computational Fluid Dynamics (CFD), FloVENT, Modular Data Center, Containerized Data Center, Cold/Hot Aisle

Nomenclature

Primitives: Basic building blocks from which all FloVENT geometry is built, either specifically or inherently using assemblies or SmartParts. [1]

SmartParts: FloVENTs geometric tools that are designed to represent actual parts such as fans, filters, hollow boxes, etc. They are “complicated assemblages of primitives2 which can be quickly generated parametrically, with different levels of modeling to choose the level of detail required.” [1]

1. Introduction

Data centers comprised of racks and corresponding servers form the backbone of today’s cloud computing. Continuous operation of large numbers of servers can generate large amounts of heat which in turn requires high capacity cooling systems. These cooling systems can consume a significant portion of the energy required to run a data center and can negatively impact data center efficiency.

Significant research has been conducted into alternative methods that reduce cooling system energy consumption and improve overall efficiency. Free cooling is one of these alternative methods; in this paper, it is studied for a particular configuration of power/cooling and IT modules in a modular data center.

Free cooling is the most efficient cooling alternative for data center cooling. In this method, ambient air is introduced into the data center through filters, and is then forced by fans that provide the required flow rate to directly cool the server equipment. The heated server exhaust air is then vented back out to the ambient. This cooling method is highly effective at reducing energy consumption for data centers in cooler climates where it can be utilized for a significant portion of the year.

This paper discusses free cooling of a modular data center using CFD analysis. Compared to traditional data centers, modular data centers have the primary advantage in their potential for ease and speed of deployment, possible lower capital and operating costs [2]. The modular data center under study is comprised of one 12 ft x 40 ft (3.66 m x 12.19 m) power/cooling module, two 12 ft x 40 ft (3.66 m x 12.19 m) IT modules, and one 12 ft x 36 ft (3.66 m x 10.97 m) plenum. The power/cooling module contains all of the primary free cooling components (fans, intake filters, actuator-controlled louvers, and environmental controller), while the two IT modules contain actuator controlled louvers and house over 5000 servers along with sensors needed for cooling system control.

Figure 1 shows ambient air passing through the power/cooling module, dividing between the two IT modules and entering into the cold aisles of each IT containers. Each IT module contains two sets of 21 racks placed to the left and right hand side of the cold aisle. The two hot aisles in each IT container are located opposite the cold aisle across each set of 21 racks.

Figure 2 shows details of the power/cooling module. In addition to the cooling components, the power/cooling module contains input power panels, transformers, power distribution, and UPS backup components.

2. Modeling and Simulation

2.1. Assumptions

Steady state conditions are assumed for all simulations. Ambient air is assumed to be dry air at 27˚C. Radiation heat transfer is not considered in the simulation.

2.2. Modeling

Containers and louvers of the IT modules and the power/cooling module were first imported from a Pro/E model of the modular data center using FloMCAD into

FloVENT. The imported model is then simplified by removing parts and changing geometries that do not play significant role in thermal analysis. Doing so decreases the number of cell count needed to obtain successful CFD simulation thereby reducing computational time. Internal components of the power cooling and IT modules are then represented using the CFD tool's SmartParts. Parts that are small compared to the size of the modular data center were simplified to 2D models. These parts include walls of the containers, filters, blowers, and louvers. Sets of servers in a rack are represented using a Rack SmartPart which captures what happens only at the inlet and exhaust of a set of servers. This SmartPart does not contain any grid cell inside it which further reduces the number of cell count and the computational time.

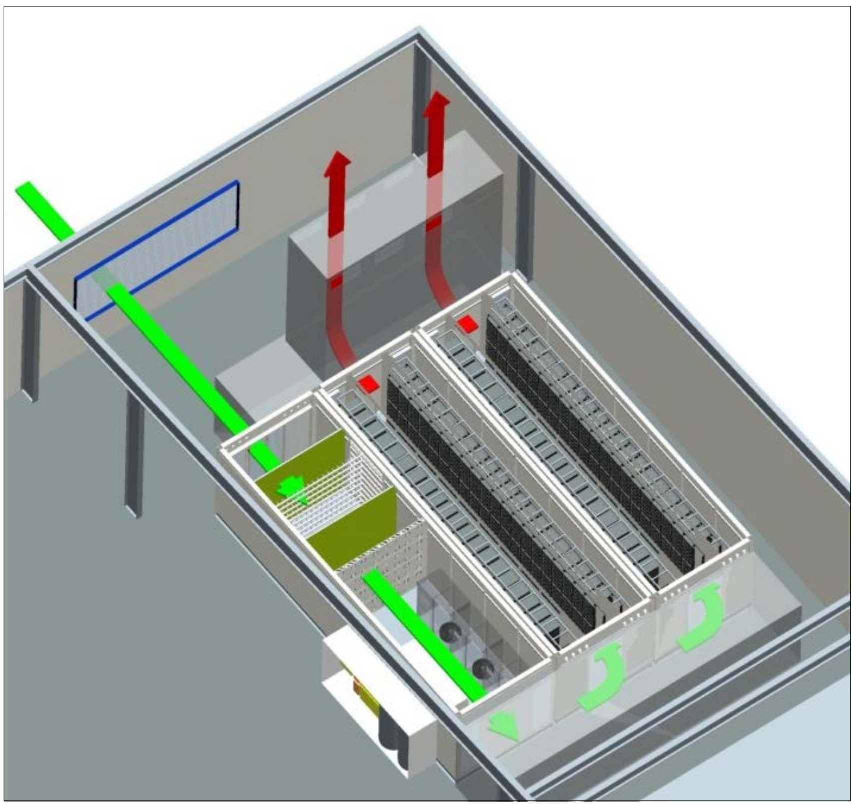

Figure 1 Schematics showing airflow path: Green arrow shows cold ambient air and red arrows show hot exhaust air

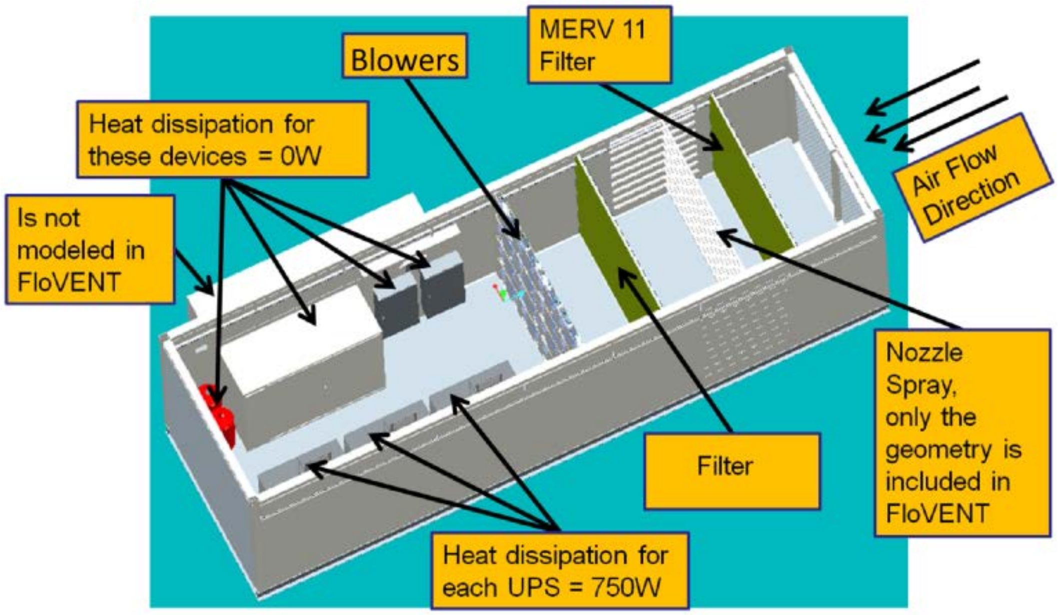

Figure 2 Description of the power/cooling module

Filters, intended to be used in the modular data center were tested in an airflow bench and the resulting system resistance curve is used to create resistance SmartParts which represented the filters.

Figure 3 shows a baseline model of the entire modular data center with roofs removed ready for thermal analysis. Summary of heat dissipation values in the data center is given in Table 1.

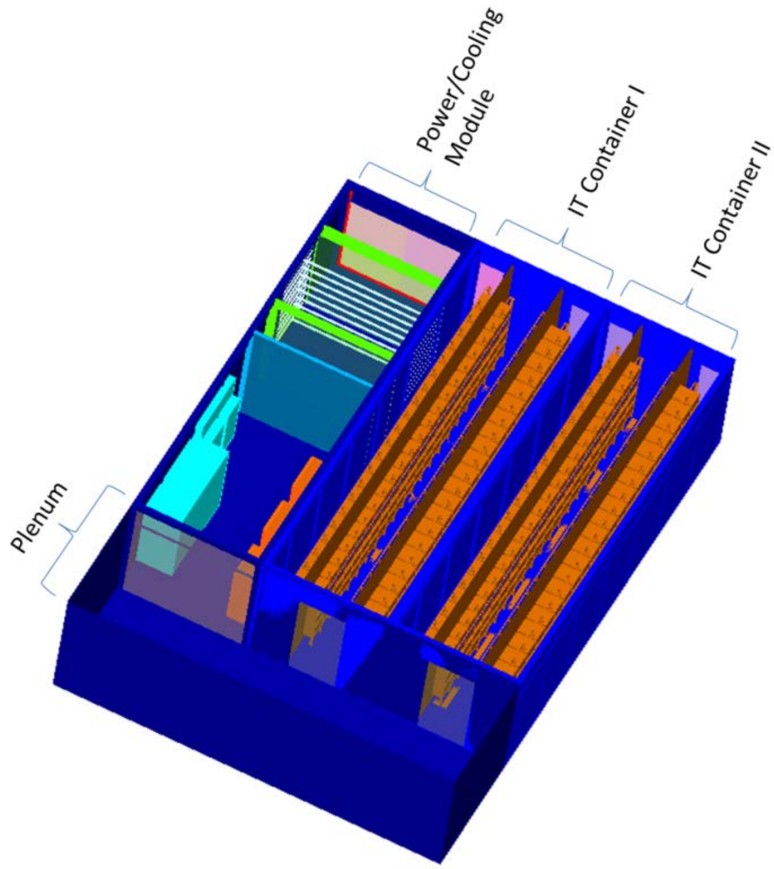

Figure 3 Isometric view of entire system with roofs removed, thermal model

Table 1 Heat load description

Number of Item(s)	Item	Heat Load (W)
1	Rack	14226 (at 40% load)
1	IT Container	597,475
2	IT Containers	1,194,950
1	Power Cooling Module	2250
The Entire System (i.e. 1 Power Cooling Module + 2 IT Containers)		1,197,200

In addition to the baseline case, other cases have been run to investigate effect of different components in the modular data center. Case 1 is the same as the baseline case except here all blowers in power/cooling module have been removed. In Case 2 effect of number of servers on the operating point of server fans is shown by running two different simulations on a single IT container. In Case 2a, Figure 4, simulation is run on one IT container with only one set of servers in it. In Case 2b, Figure 5, a total of 42 set of servers, 21 set of servers placed on each side of the cold aisle, are used in the simulation.

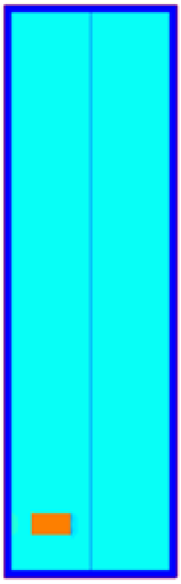

Figure 4 Case 2a: A single set of server mounted in one IT container

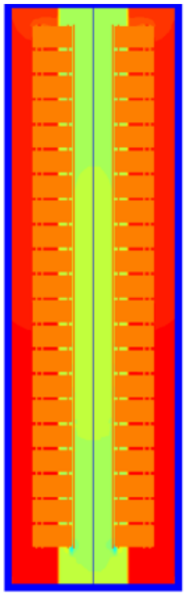

Figure 5 Case 2b: All sets of servers as in the baseline case mounted in one IT container

2.3. Meshing and Simulation

Structured Cartesian mesh is used to generate a total of 3.4 million grid cells. K-ε turbulence model is used in the CFD simulation since it is the preferred model for cases where turbulence is to be modeled over large empty volumes within an enclosure [1].

3. Results

The thermal profile on a horizontal cut plane passing through the modular data center is shown in Figure 6. The maximum temperature in the modular data center is 16°C above the inlet temperature, 27°C.

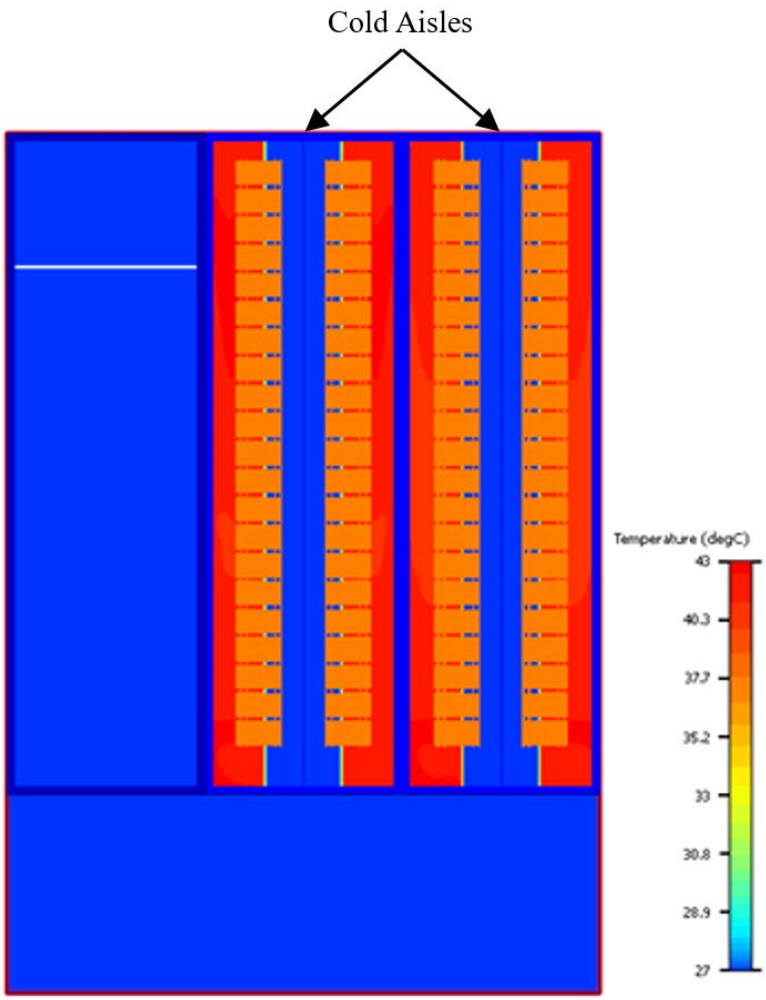

Figure 6 Baseline Case - Temperature Profile (Top View)

Figures 7 and 8 show airflow patterns in the cold aisle of IT module I with IT container inlet louvers inclined at 45° and 0°, respectively. Louvers at these two degrees of inclination are shown in Figures 9 and 10. Figure 7 shows strong air circulation around mid-length of the cold aisle whereas no circulation is visible at this location in Figure 8. Comparison of Figures 7 and 8 clearly show the effect of inlet louvers on airflow distribution in the cold aisle.

Air circulation forms a low pressure region at its center. Thus server fans which have to draw air from regions of strong circulation in the cold aisle will have to overcome higher differential pressure as long as the pressure in the hot aisle is relatively uniform. Overcoming higher pressure differential means less air flow passing through the fans which in turn results in high temperature at the servers. This observation is seen in Figure 11 which shows mean exhaust temperatures at the exhaust of sets of servers numbered in increasing order starting from the rack closest to the inlet louvers.

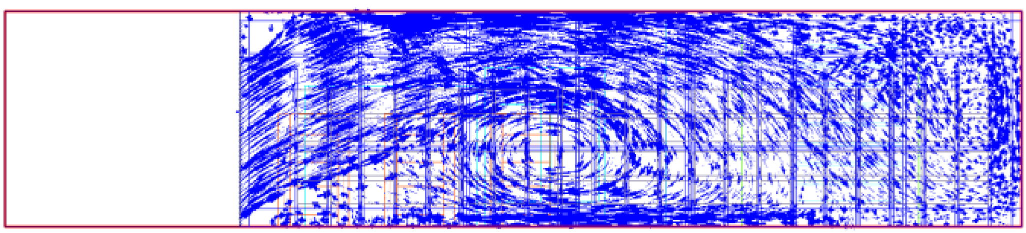

Figure 7 Louvers at 45°: Cold aisle of IT container I, side view

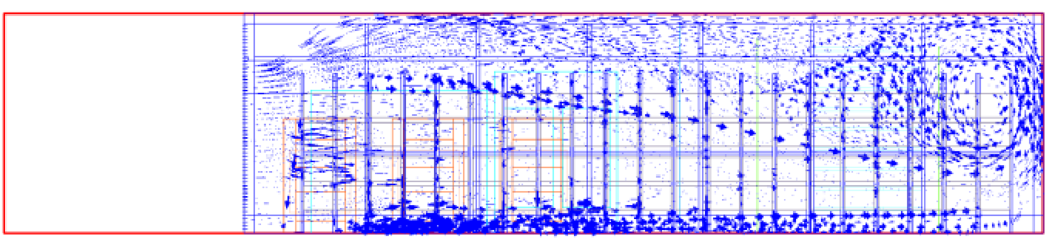

Figure 8 Louvers at 0°: Cold aisle of IT container I, side view

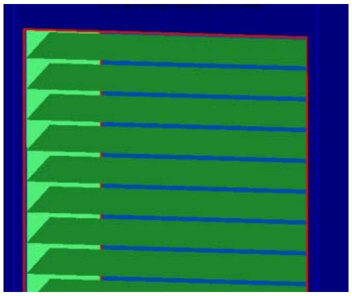

Figure 9 Louvers inclined at 45º

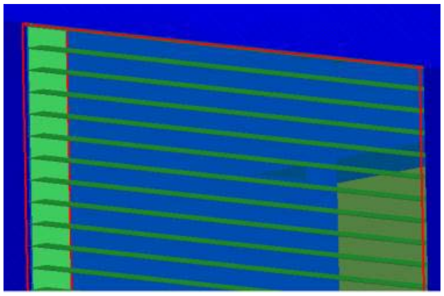

Figure 10 Louvers inclined at 0º

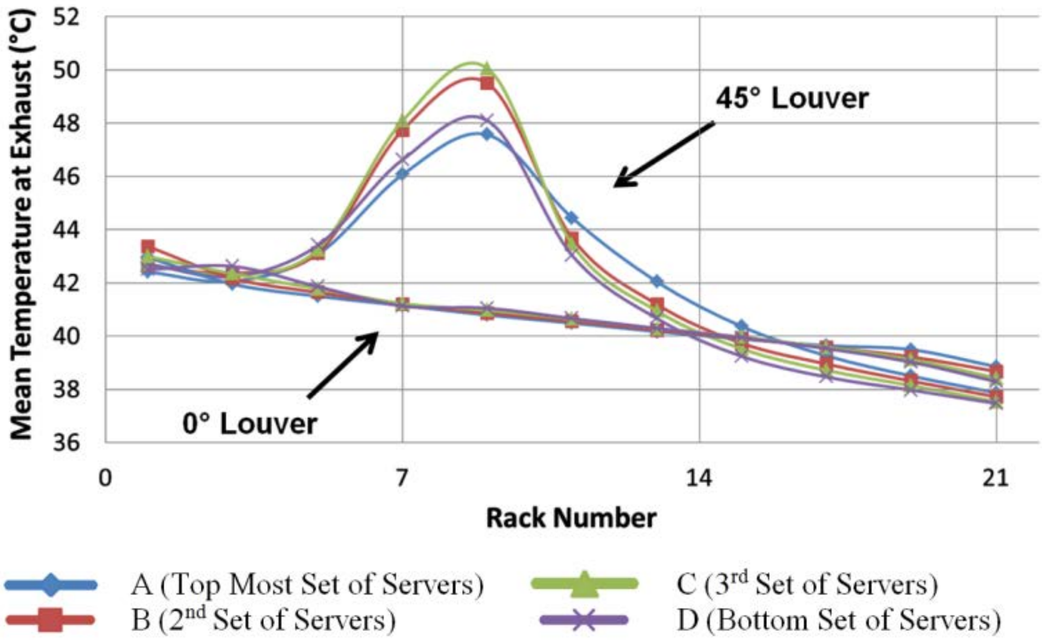

Figure 11 Comparison of effect of 0° and 45° inclined louvers on the mean exhaust temperature of the top set of servers in IT container I

Figure 12 and Figure 13 show a representative server fan operating point for the baseline case and Case 1, respectively. Although the operating point of server fans for Case 1 show the need for overcoming higher pressure differential when compared to the baseline case, the difference is small (less than 1 in H_2O (249 Pa)).

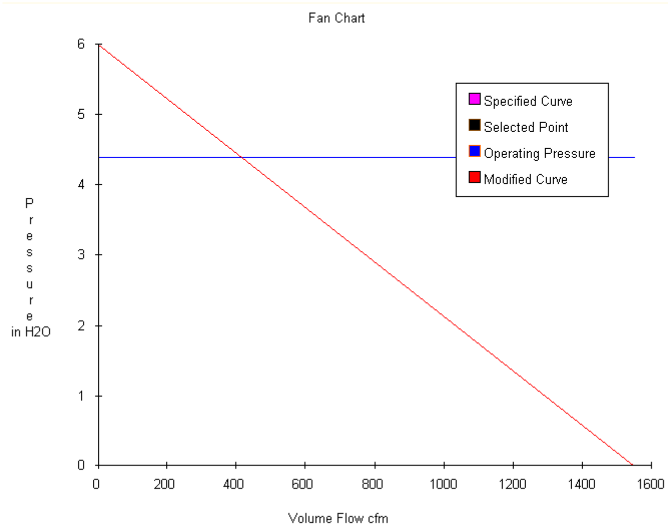

Figure 12 Baseline Case: Fan operating point for one of the top set of servers

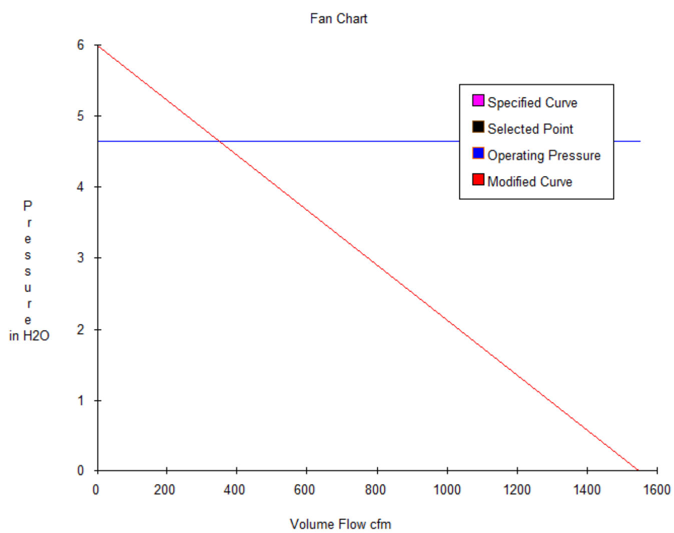

Figure 13 Case 1: A single set of server mounted in one IT container and it fan operating point

Simulation results for Case 2a and Case 2b are shown in Figures 14 and 15, respectively. For the case with only one set of servers in the IT container, the fan on the set of servers has to overcome small resistance when compared to the operating points of server fans in Case 2b. This is due to the additional resistance created at the inlet and exhaust of the IT container when large volume of air is required to pass in Case 2b.

4. Conclusion

Airflow pattern of modular data centers is important to understand why temperature and volume flow rate variations occur within rows of racks and sets of servers within a rack. For the particular configuration of power/cooling module, plenum, and two IT containers, CFD analysis has shown maldistribution of volume flow rate in racks and sets of servers caused by circulation of air in the cold aisle. It has been shown that to improve the airflow distribution in the sets of servers, setting the appropriate louver angle is important.

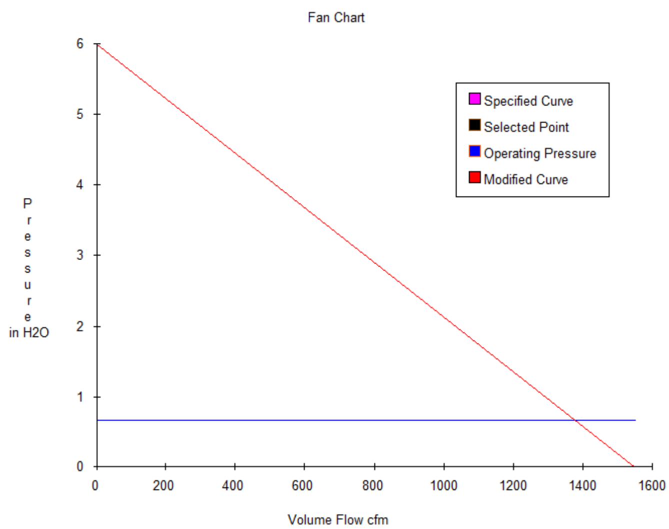

Figure 14 Case 2a: Fan operating point for a single set of server mounted in one IT container

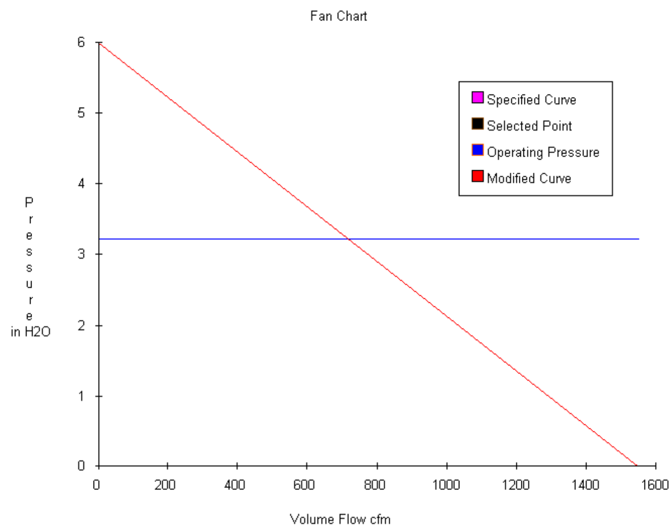

Figure 15 Case 2b: Fan operating point for a representative set of server mounted in one IT container

Results from Case 1 suggest that it could be possible to operate the data center without the need for blowers found in the power/cooling module as long as there are strong server fans in use.

Case 2 showed operating point of a set of server fans changes based on the number of servers in a given IT container. Thus in the design phase of IT containers it is important to consider the number of servers to be placed in a modular data center with respect to the desired server fan operating point.

Acknowledgments

This work is supported by the National Science Foundation.

References

1. FloVENT User Guide. Software Version 9.2.

2. Bramfitt, M., and H. Coles. Modular/Container Data Centers Procurement Guide: Optimizing for Energy Efficiency and Quick Deployment. Lawrence Berkeley National Laboratory. February 02, 2011

CFD Modeling of the Test Bed Modular Data Center

CFD model of the IT pod and its cooling unit, ASC-15, have been created in FloVENT 10.1. For the IT pod, each of the 120 servers are represented as a compact model using the Rack SmartPart. The system resistance curve obtained from lab test (see Figure 3-15) is used to build a model for the flow resistance of the server. The server has four SUNON PMD1204PJB1-A fans and one other fan for the power supply unit (see Figure 3-7). All five fans are represented with a single equivalent fan performance curve assuming that all fans are in parallel and the power supply fan also has same performance curve as the other four server fans. The fan performance curve for the SUNON PMD1204PJB1-A fans is shown in Figure 3-25 [60]. The fan curve identified as 4048 is used in the model. The equivalent fan performance curve for all five fans is shown in Figure 3-26.

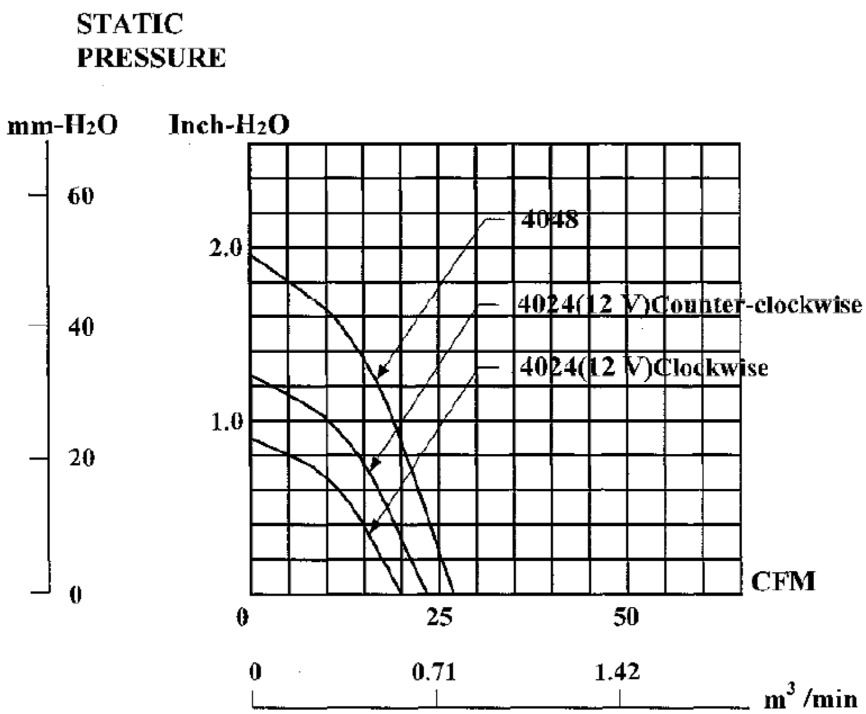

Figure 3-25 SUNON PMD1204PJB1-A fan performance curve [60]

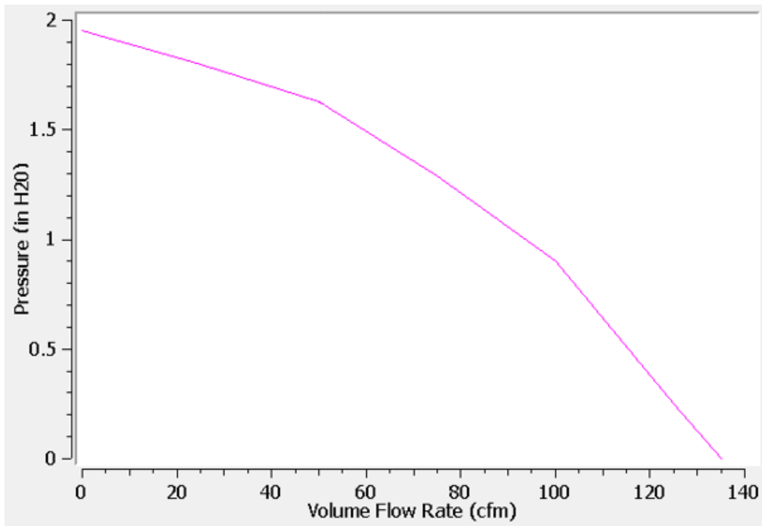

Figure 3-26 Equivalent fan performance curve representing performance of all server fans in parallel

Modeling methodology for the ASC-15 is similar to that of ASC-20 which is discussed in section CFD Modeling of Indirect/Direct Evaporative Cooling Unit for Modular Data Center Applications. Thus discussion of the ASC-15 unit is limited to clarifying the modeling technique used for the DEC and the IEC sections of ASC-15 or ASC-20.

FloVENT 10.1 does not allow creating a saturation curve for the DEC and the IEC models. To work around the issue, the flow and heat transfer equations are decoupled and the model is run twice -- the first to compute the flow solution and the second to compute the thermal distribution. Decupling the equations is possible since the flow in the cooling unit and the IT pod is dominated by forced convection. The first run allows determination of the volume flow rate through the DEC and IEC units. Which is then used to find the face velocity of these units by dividing the volume flow rates by their respective surface areas. The saturation effectiveness at the calculated face velocity is obtained from Figure 3-21. Using the saturation effectiveness value, the volume flow rate, the density, the specific heat capacity of air, and the specific process (i.e. constant wet-bulb or constant dew-point temperature) air has under goan, the amount of heat removed from and the amount of water added to the air can be calculated for, both, DEC and IEC units. These values are then applied to the CFD tool's Source SmartPart. Then the model is run a second time to find the for flow and heat distribution.

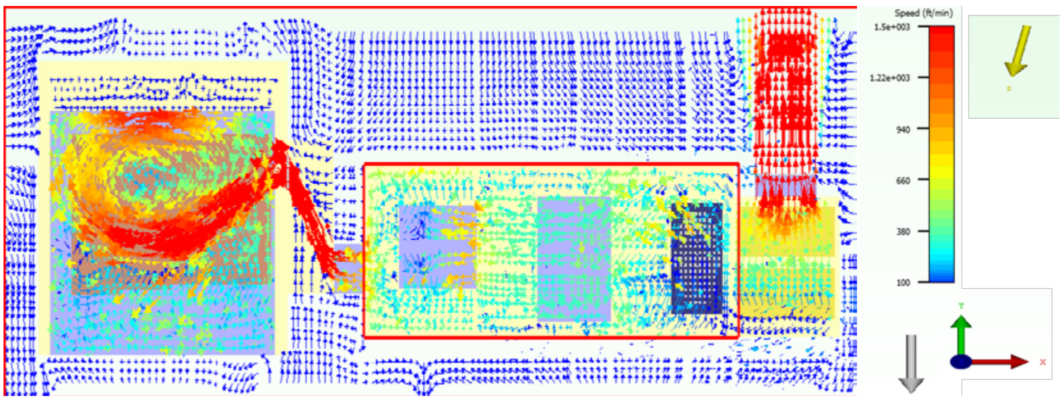

Figure 3-27 shows velocity profile of a vertical plane that cuts through the cold aisle, air supply duct, and the cooling unit

Figure 3-27 shows velocity profile of the data center with a cut plane going through the cold aisle, the supply duct, and the cooling unit. Top figure of Figure 3-28 shows temperature profile on same cut plane as shown in Figure 3-27. Ambient air is considered to be at 40ºC (104ºF) and there is no mixing of hot data center air with the ambient in the mixing chamber. Air temperature can be seen to decrease as it passes through the the IEC coils and DEC media. Although the temperature leaving the cooling tower is at lower temperature than supply air to the IT pod, the humidity level of air leaving the cooling tower is close to saturation point and thus cannot be introduced in to the cold aisle. Another cut plane is shown in the bottom figure of Figure 3-28 that cuts the IT pod and the cooling unit horizontally. Here also, the change in temperature of the ambient air can be seen as is flows across the IEC section and the DEC.

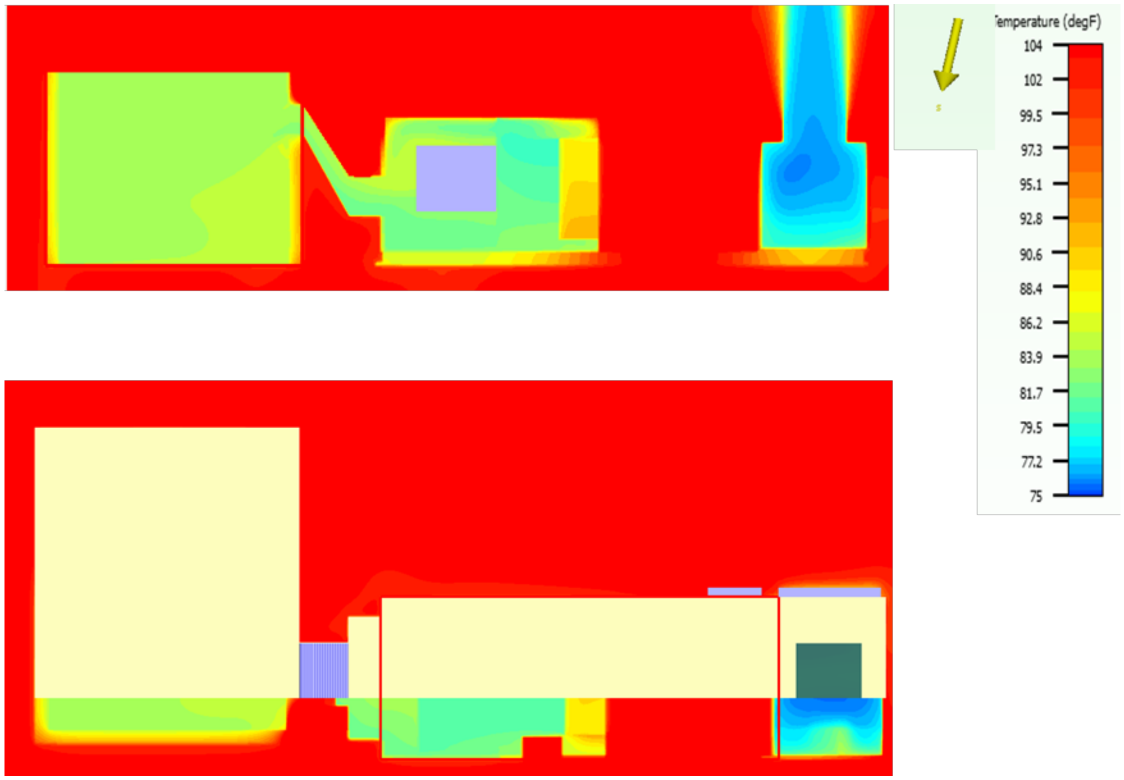

Figure 3-28 Top figure: vertical cut plane through the cooling unit and the cold aisle showing temperature profile. Bottom figure: Top view showing horizontal cut plane through the IT pod and the cooling unit.

Weather bin data analysis

To estimate number of hours a given data center could use ASE, DEC, and IEC, weather data of the data center's location needs to be analyzed. A MATLAB code is written to calculate the number of hours in a year outside air conditions fall within specified regions on a psychrometric chart. Two sets of regions are prepared based on the recommended and Class A1 allowable envelopes as defined in 2011 ASHRAE Thermal Guidelines [9]. A psychrometric chart divided into regions based on the recommended envelope will be referred to as Chart I while a psychrometric chart which is divided based on Class A1 allowable envelope will be referred to as Chart II. Chart I and Chart II at sea level conditions are shown in Figure 3-29 and Figure 3-30.

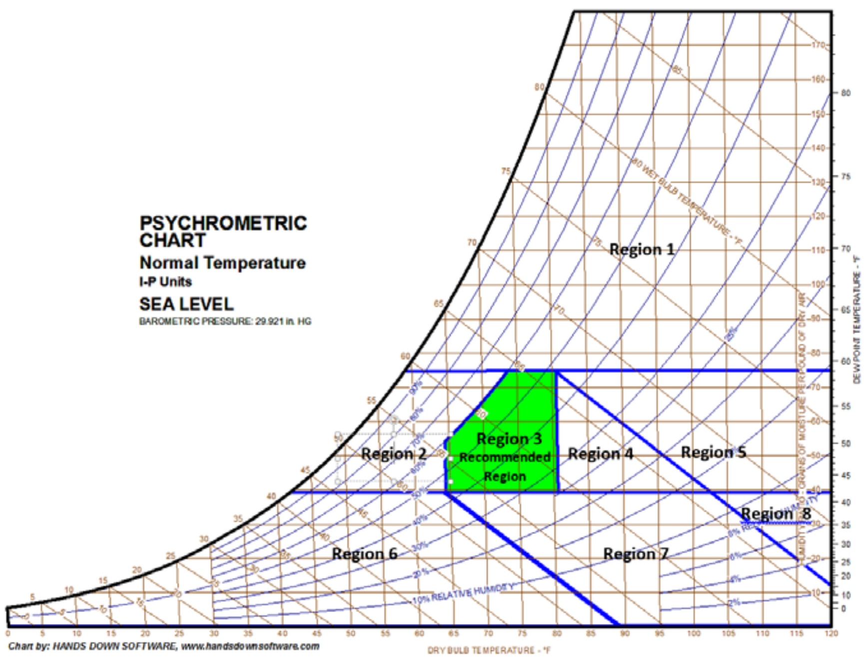

Figure 3-29 Chart I: Psychrometric chart regions based on the recommended envelope

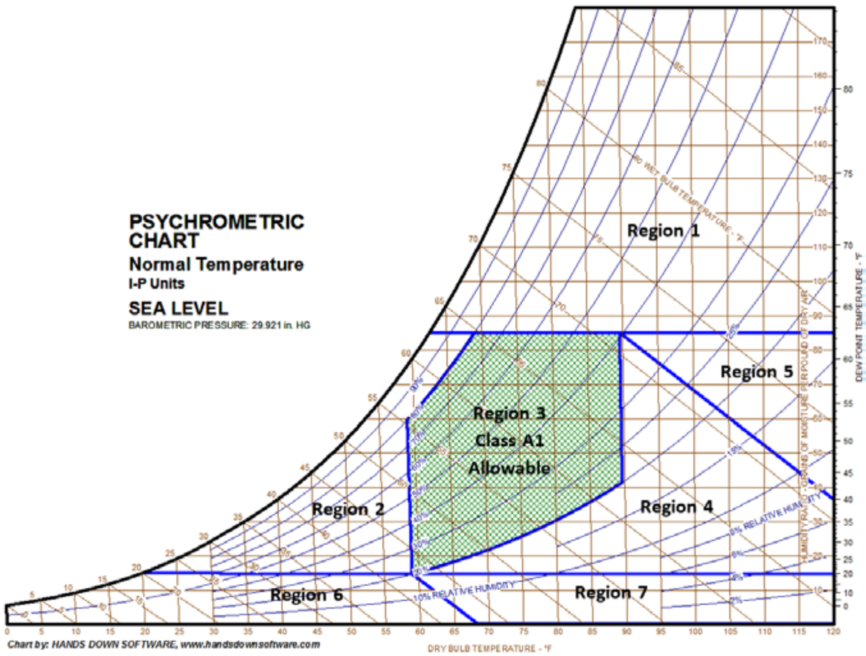

Figure 3-30 Chart II: Psychrometric chart regions based on Class A1 allowable region

The regions in both charts are divided based on the cooling capability of ASC-15-2A11 unit to bring outside air into the target regions: recommended or Class A1 allowable. For both charts, if outside air falls in Region 1, this cooling unit cannot be used to bring outside air into the target regions since outside air contains too much moisture. Dehumidifiers, DX cooling units, or multi-stage IEC units may need to be used. For all regions other than Region 1, the ASC-15-2A11 can be used to bring outside air into the target regions. Below is a summary of how this may be achieved if outside air falls in:

- Region 2: mix hot return air with outside air
- Region 3: outside air directly
- Region 4: either DEC or IEC can be used for the chart based on the recommended envelope but only DEC is guaranteed to work for the chart based

on the Class A1 allowable envelope. It may be more efficient to use the I/DEC mode.

- Region 5: IEC needs to be used. It may be more efficient to use the I/DEC mode.
- Region 6: mix hot return air with outside air. It may be necessary to run the DEC section to add moisture.
- Region 7: DEC needs to be used. It may be more efficient to use the I/DEC mode.
- Region 8: Both IEC and DEC need to be used.

In the discussion above the return air conditions are disregarded since the focus is mainly on determining whether it's possible to use ASC-15-2A11 to bring outside air to the target regions. However, if conditions of return air are better than that of outside air, it would be more energy and water efficient to minimize outside air and cool the return air. For example, at sea level, if outside air has dry-bulb temperature of 110°F and dew-point temperature of 50°F (Region 5 in Chart I), and the return air has dry-bulb temperature of 90°F and dew-point temperature of 50°F (Region 4), it's better to minimize outside air and use IEC to cool the return air.

To estimate the number of hours the test bed modular data center, which is located in Dallas, TX, could use ASE, DEC, or IEC, hourly weather data from a nearby weather station is analyzed. Figure 3-31 and Figure 3-32 show Typical Meteorological Year 3 (TMY3) data for Dallas/Fort Worth International Airport (DFW AP) plotted on Chart I and Chart II, respectively. Percentage of hours TMY3 data from [61] fell in the regions of Figure 3-29 and Figure 3-30 is shown in the pie charts Figure 3-33 and Figure 3-34.

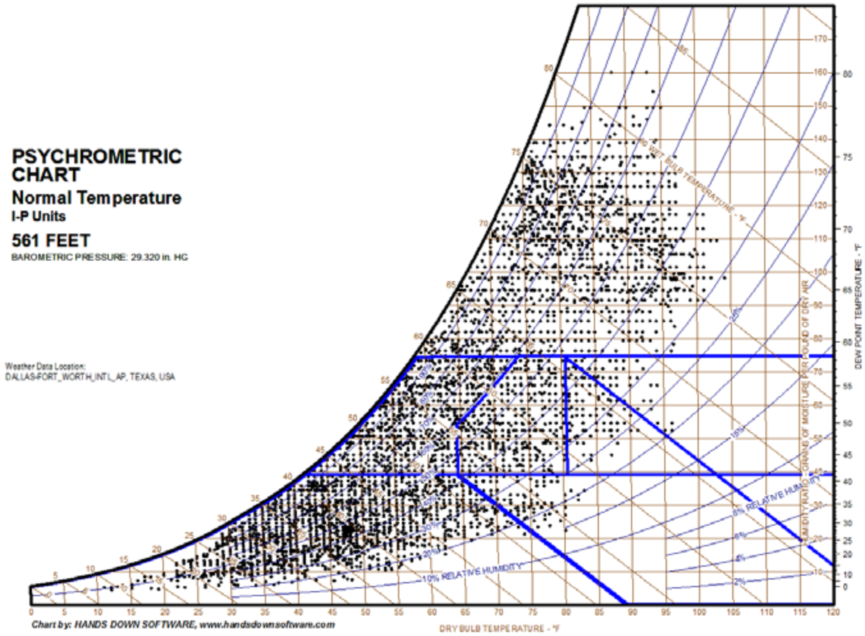

Figure 3-31 TMY3 hourly weather data for DFW AP on Chart I

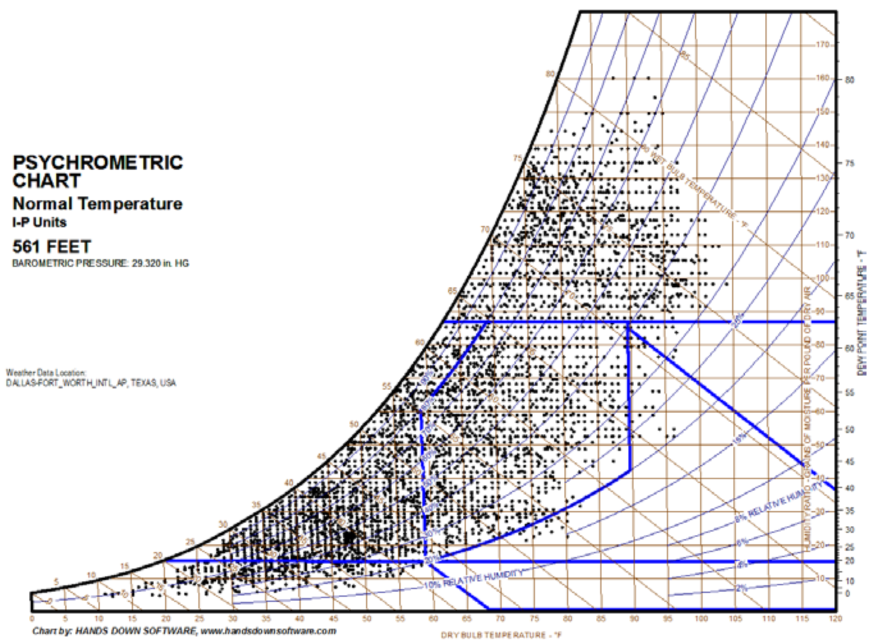

Figure 3-32 TMY3 hourly weather data for DFW AP on Chart II

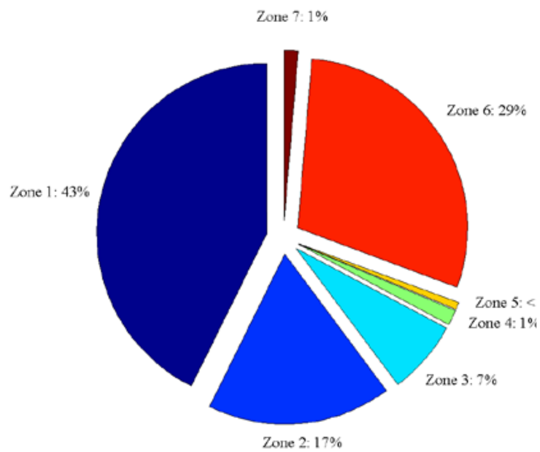

Figure 3-33 Percentage of hours in a year outside air conditions fell in Chart I

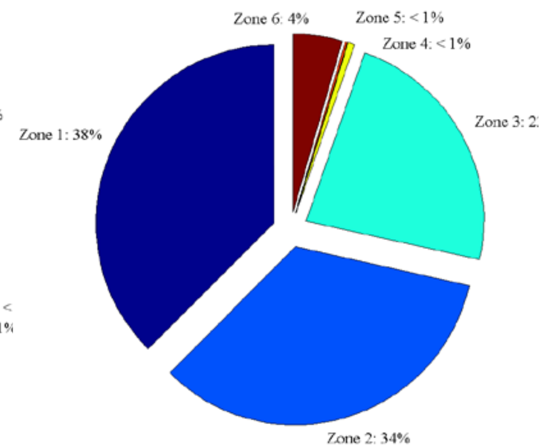

Figure 3-34 Percentage of hours in a year outside air conditions fell in Chart II

Figure 3-35 shows a map of the largest American data centers. TMY3 weather data from weather stations near most of the data centers on the map is analyzed. The results are shown in Table 3-6 and Table 3-7.

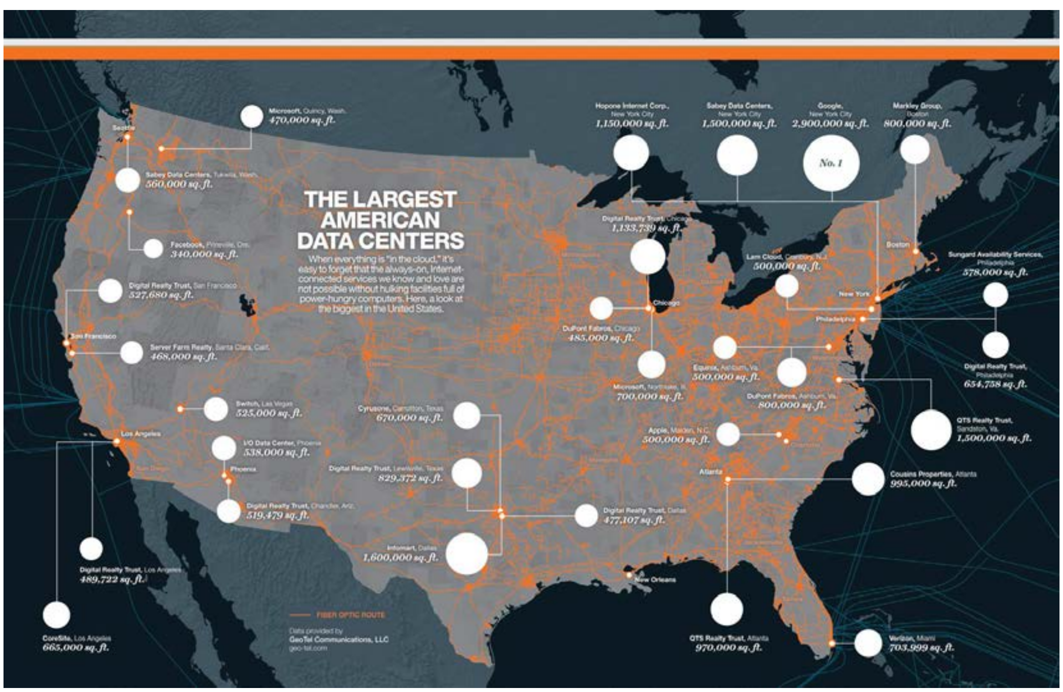

Figure 3-35 The largest American data centers [62]

Table 3-6 TMY3 data analysis: regions based on Chart I

	Zones based according to Chart I							
	Zone 1	Zone 2	Zone 3	Zone 4	Zone 5	Zone 6	Zone 7	Zone 8
Dallas-Fort Worth, TX	43	17	7	2	< 1	29	1	
Atlanta, GA	36	22	7	1	< 1	32	1	0
Chicago, IL	20	22	6	1	< 1	51	< 1	0
New York City, NY	25	22	7	< 1	< 1	45	< 1	0
Richmond, VA	32	22	6	2	< 1	38	< 1	0
Philadelphia, PA	24	21	7	1	< 1	45	< 1	0
San Francisco, CA	< 1	78	7	< 1	< 1	14	< 1	0
Los Angeles, CA	22	62	5	< 1	0	10	1	0
Phoenix, AZ	10	8	8	9	9	34	21	< 1
Seattle, WA	< 1	50	9	< 1	< 1	40	< 1	0
Ephrata, WA	0	9	11	6	< 1	66	6	0
Miami, FL	81	9	6	< 1	< 1	2	1	0

Table 3-7 TMY3 data analysis: regions based on Chart II

	Zones based according to Chart II							
	Zone 1	Zone 2	Zone 3	Zone 4	Zone 5	Zone 6	Zone 7	Zone 8
Dallas-Fort Worth, TX	38	34	23	< 1	< 1	4	0	0
Atlanta, GA	29	39	24	< 1	< 1	7	< 1	0
Chicago, IL	13	51	20	< 1	0	15	0	0
New York City, NY	20	51	18	< 1	< 1	10	0	0
Richmond, VA	25	45	20	< 1	< 1	9	< 1	0
Philadelphia, PA	19	46	21	< 1	< 1	14	0	0
San Francisco, CA	0	70	30	< 1	0	0	0	0
Los Angeles, CA	6	50	44	< 1	0	< 1	< 1	0
Phoenix, AZ	5	21	38	28	4	2	2	0
Seattle, WA	0	75	24	< 1	0	1	0	0
Ephrata, WA	0	58	34	4	< 1	4	< 1	0
Miami, FL	76	7	17	< 1	0	0	0	0

Chapter 4

Summary and Discussion

Data centers have become an important segment of modern infrastructure. They house IT equipment which is used for digital data storage, processing, and transmission. IT equipment in data centers need to be properly cooled to maintain its reliable operation. Energy consumption of the cooling system in data centers, however, contribute a significant portion of the overall data center energy consumption. Since energy consumed by the cooling unit does not serve the main reason why data centers are built (i.e. store, process, and transmit digital data), reducing energy consumption of the cooling unit can significantly improve energy efficiency of data centers. To this goal, research at companies, research institutions, et cetera has resulted in recommendations on various aspects of how data centers including type of cooling systems, airflow management, construction, site selection, et cetera. Various sources recommend using ASE when ambient air conditions are favorable.

In this dissertation, temperature, humidity, and contamination factors that limit use of ASE have been discussed. To use outside air for cooling data centers at wider temperature and humidity range than is possible with ASE systems, evaporative cooling technology can be used. Both ASE and evaporative cooling systems, specifically DEC, IEC, and I/DEC, are not mechanical cooling systems, which have been reported as contributing a large portion of cooling cost in data centers. A test bed modular data center that uses a cooling unit, ASE-15-2A11, which operates in ASE and I/DEC has been used for this study.

To estimate the power consumption of the IT pod in the test bed modular data center, a server has been tested using two server stress tools. Another test was performed on the server to determine its airflow requirement. Estimated power consumption of the IT pod and test results of the server airflow requirement are used to guide selection of blowers for the cooling unit that uses ASE and I/DEC.

The DEC media of the cooling unit is tested in lab to find its system resistance curve and saturation effectiveness curves. The test results are then used to create model of a DEC media in the CFD model of the test bed modular data center. From test results, it's observed that to wet the DEC media close to saturation, it takes 15 min to 20 min and to dry the media close to dry state, it takes about 20 min at 500 FPM, 40% RH, and 90ºF upstream air.

Using staging reduces scale build up on DEC media. It was shown that using unequal sections allows for more number of stages which provide precise control of humidity and temperature than equally sectioned media. A 100 in wide media is used as an example to demonstrate how unequally divided sections can improve total number of stages available compared to equally divided sections.

Detailed description and modeling of ASC-20-2A11 has been included. Simulation results of the ASC-20-2A11 unit show that, in some areas of its filter wall, air speed is in excess of 700 FPM which is much higher than is typically recommended by filter manufacturers – 500 FPM. Placing baffles in the mixing chamber could create a more uniform air speed distribution on the filter.

Although the IT pod, which is modeled with ASC-15-2A11 unit, has hot/cold aisle containment in place, not all servers have equal air flow. The ASC-15-2A11 CFD model shows air circulation in the cold aisle. This kind of airflow creates low pressure area at the center of the circulation and makes it harder for server fans, which are close to the center of circulation, to draw in air. Another reason for maldistribution of air flow though the servers is that air enters the cold aisle at high speed and at 90º from the direction of air intake to the servers. This also makes it difficult for severs which are close to the air inlet to draw in air.

Air circulation in the cold aisle and its effect on server fans is also discussed in the CFD Analysis of Free Cooling of Modular Data Centers section. Here, changing the angle of air inlet louvers to the IT containers from 45º to 0º improved the air flow distribution in the servers. In addition, this model showed that as the number of servers increased in a single IT container, the operating point of the server fans change. This is mainly because of increased back pressure in the hot aisle due to increase in amount of volume flow rate that needs to leave the hot aisle. In this model and in the test bed modular data center IT pod models, high back pressure is observed. In data centers that use CRAC units, the blower of the CRAC unit draws in hot air exhausted from IT equipment because it creates negative pressure in the hot aisle side. In ASE systems, the blower in the cooling units cannot assist hot air removal from the hot aisle if the return air dampers are closed. Thus exhaust fans need to be provided in ASE systems.

A psychrometric chart was divided into regions based on the recommended and the allowable Class A1 envelopes to show in what outside air temperature and humidity one or more of the ASE, DEC, IEC, or I/DEC can be used to bring outside air into the recommended or allowable Class A1 envelopes. Using these charts, weather bin data analysis was performed using Dallas / Fort Worth International Airport TMY3 data.

Future works

The IT pod in the test bed modular data center needs to have an exhaust fan installed. CFD modeling can help in the selection process by finding the IT pod’s inlet and exhaust system resistance.

For vertically split distribution configuration with unequal sections, scale formation may need to be investigated since with increased number of stages, some of the sections may cycle through wet / dry states more often than others. In addition, sequence of operation in going from one stage to the next may need further analysis. For example, for a media that's divided into four unequal sections as in Table 3-4, two options are available to go from 30% (stage 3) wet to 40% (stages 4 and 6) wet states.

Instead of having a fixed set point for supply air temperature and humidity, a flexible set point which falls within the target envelope may be used to improve water and energy consumption of the ASE and I/DEC systems.

Appendix A

MATLAB Code to Calculate Width of Unequal Sections for Vertically Split DEC Media Distribution

```matlab
% This code calculates width of direct evaporative cooling media sections
% that will maximize the number of stages for a given number of sections.

clear; clc; close all;
%% Inputs
Ns = 4; % number of sections
L = 100; % total width of the DEC media (length unit can be m, in, ...)
%%
L1 = L/sum(1:Ns); % smallest section width
Ln = L1*[1:Ns]; % all sections
%% Initialize
C = cell(1,Ns);
a=[];
q = 0;
Tb = zeros(100,Ns+1);
%% Loop
for i = 1:Ns
   C{i} = nchoosek(Ln,i); %Find possible combinations
   [row,col] =  size(C{i});
   if i == 1;
      disp('Width of each DEC section (same unit as input total length) ')
      Width = C{1}
   else
   end
   for k = 1:row
```

```
        m = sum(C{i}(k,:));
        a = [a;m];
        q = q+1;
        %% 1 & 0 indicate which pump is on. (4 pumps considered)
        for ij = 1:col
            if C{i}(k,ij)==Width(1);
                Tb(q,1) = 1;
            elseif C{i}(k,ij)==Width(2);
                Tb(q,2) = 1;
            elseif C{i}(k,ij)==Width(3);
                Tb(q,3) = 1;
            elseif C{i}(k,ij)==Width(4);
                Tb(q,4) = 1;
            end
        end
    end
end
b = round(a./L*100*10)./10;
Lb = length(b);
%% Results
% column 1 is the stage number
% columns 2 through 5 indicate which pump section needs to be on
% column 6 is percentage of wetted media
Tb = [ [1:Lb]' Tb(1:Lb,1:Ns) b];
[Stages, ia, ic] = unique(Tb(:,Ns+2));
```

```
Number_of_Unique_Stages = length(Stages)

figure('Color',[1 1 1]);

set(gca,'Color',[1 1 1]);

plot(a,b,'.')

xlabel('Width of DEC Media')

ylabel('Wet DEC Width (%)')

axis([0 L 0 100])

%% Print

formatSpec = '%5.0f %5.0f %5.0f %5.0f %5.0f %5.1f \n'; %

fprintf(formatSpec,Tb')

SortedTb = sortrows(Tb,Ns+2)
```

References

[1] EPA. *ENERGY STAR Rating for Data Centers: Frequently Asked Questions* [Online]. Available: https://www.energystar.gov/ia/partners/prod_development/downloads/DataCenterFAQs.pdf?acac-cbed.

[2] J. Gantz and D. Reinsel, "Extracting Value from Chaos," June 2011.

[3] M. Chen, S. Mao and Y. Liu. Big data: A survey. *Mobile Networks and Applications 19(2),* pp. 171-209. 2014. Available: http://dx.doi.org/10.1007/s11036-013-0489-0. DOI: 10.1007/s11036-013-0489-0.

[4] J. Koomey. Growth in data center electricity use 2005 to 2010. Analytics Press. Oakland, CA. 2011[Online]. Available: http://www.analyticspress.com/datacenters.html.

[5] P. Delforge. (2015, February 6). *America's Data Centers Consuming and Wasting Growing Amounts of Energy* [Online]. Available: http://www.nrdc.org/energy/data-center-efficiency-assessment.asp.

[6] Cisco. Data center power and cooling. Cisco. 2011 [Online]. Available: http://www.cisco.com/c/en/us/solutions/collateral/data-center-virtualization/unified-computing/white_paper_c11-680202.pdf.

[7] N. Rasmussen. Calculating total cooling requirements for data centers. 2011 [Online]. Available: http://www.apcmedia.com/salestools/NRAN-5TE6HE/NRAN-5TE6HE_R3_EN.pdf?sdirect=true.

[8] Data center best practices guide: Energy efficiency solutions for high-performance data centers. Pacific Gas and Electric Company. 2012 [Online]. Available: http://www.pge.com/includes/docs/pdfs/mybusiness/energysavingsrebates/incentivesbyindustry/DataCenters_BestPractices.pdf.

[9] ASHRAE TC 9.9. 2011 thermal guidelines for data processing environments – expanded data center classes and usage guidance. *2012(2/27),* 2011.

[10] "Harmonizing global metrics for data center energy efficiency," The Green Grid, Mar. 2014.

[11] PUE™: A comprehensive examination of the metric. The Green Grid. 2012 [Online]. Available: http://www.thegreengrid.org/~/media/WhitePapers/WP49-PUE%20A%20Comprehensive%20Examination%20of%20the%20Metric_v6.pdf?lang=en.

[12] Water usage effectiveness (WUE™): A green grid data center sustainability metric. The Green Grid. 2011[Online]. Available: http://www.thegreengrid.org/~/media/WhitePapers/WUE.

[13] Carbon usage effectiveness (CUE): A green grid data center sustainability metric. The Green Grid. 2010 [Online]. Available: http://www.thegreengrid.org/~/media/WhitePapers/CarbonUsageEffectivenessWhitePaper20101202.ashx.

[14] Focused cooling using cold aisle containment. Emerson Network Power. [Online]. Available: http://www.emersonnetworkpower.com/documentation/en-us/brands/liebert/documents/white%20papers/focused%20cooling%20using%20cold%20aisle%20containment.pdf.

[15] J. Whitney and P. Delforge, "Data center efficiency assessment - scaling up energy efficiency across the data center industry: Evaluating key drivers and barriers," Natural Resources Defense Council, August 2014.

[16] D. Beaty and T. Davidson. Data centers: Datacom airflow patterns. *Ashrae J. 47(4),* pp. 50-54. 2005.

[17] V. K. Arghode and Y. Joshi. Experimental investigation of air flow through a perforated tile in a raised floor data center. *Journal of Electronic Packaging 137(1),* pp. 011011-011011. 2015. DOI: 10.1115/1.4028835.

[18] ASHRAE Technical Committee 9.9. Datacom series. Available: https://ashrae.org/resources--publications/bookstore/datacom-series.

[19] "ANSI/ASHRAE/IES Standard 90.1-2013: Energy Standard for Buildings Except Low-Rise Residential Buildings (I-P Edition)," 2013.

[20] ASHRAE, "Psychrometrics," in *2001 ASHRAE Handbook: Fundamentals*, Inch-pound ed. Atlanta, GA: American Society of Heating, Refrigerating, and Air-Conditioning Engineers, 2001, pp. 6.1-6.21.

[21] L. Theodore, F. Ricci and T. Vanvliet. *Thermodynamics for the Practicing Engineer* (1st ed.) 2009.

[22] R. W. Koca, W. C. Hughes and L. L. Christianson. Evaporative cooling pads: Test procedure and evaluation. *Appl. Eng. Agric. 7(4),* pp. 485-490. 1991.

[23] Big Dutchman. *RainMaker*. Available: http://bigdutchmanusa.com/swine-production/environmental-technology/cooling/rainmaker/.

[24] R. Miller. (2012, July 16). *Facebook Revises its Data Center Cooling System* [Online]. Available: http://www.datacenterknowledge.com/archives/2012/07/16/facebook-revises-data-center-cooling-system/.

[25] "ANSI/ASHRAE Standard 133-2008: Method of Testing Direct Evaporative Air Coolers," 2008.

[26] Munters. *CELdek® by Munters*. Available: https://www.munters.com/en/campaigns/aghort-campaigns/celdek-by-munters/.

[27] Munters. *GLASdek®*. Available: https://www.munters.com/en/munters/products/coolers--humidifiers/glasdek/.

[28] *Aspen Pad Roll*. Available: http://www.indoorcomfortsupply.com/cgi-bin/commerce.exe?preadd=action&key=2838.

[29] *Big Dutchman (R) Plastic Evaporative Cooling Pads*. Available: http://www.qcsupply.com/big-dutchman-plastic-evaporative-cooling-pads.html.

[30] OXYCOM. *OXYVAP®*. Available: http://www.oxy-com.com/C4140-Products.html.

[31] C. Batchelor. (2014, February 6). *Condair humidifies & cools Facebook* [Online]. Available: http://www.condair.com/condair-humidifies-facebook.

[32] (2012, August 9). *Water Efficiency at Facebook's Prineville Data Center* [Online]. Available: http://www.opencompute.org/blog/water-efficiency-at-facebooks-prineville-data-center/.

[33] J. D. Palmer. Evaporative cooling design guidelines manual for New Mexico schools and commercial buildings. New Mexico Energy Conservation and Management Division. 2002 [Online]. Available: http://www.emnrd.state.nm.us/ECMD/Multimedia/documents/EvapCoolingDesignManual.pdf.

[34] N. H. D. Champs. Myths and realities of indirect evaporative cooling thermodynamic performance. *ASHRAE Trans 117(1),* pp. 119-130. 2011. Available: http://search.ebscohost.com/login.aspx?direct=true&db=a9h&AN=67359302&site=ehost-live.

[35] (2012, May). *NSIDC Data Center: Energy Reduction Strategies - Airside Economization and Unique Indirect Evaporative Cooling*. Available: http://energy.gov/sites/prod/files/2013/10/f3/nsidc_dcstrategies.pdf.

[36] K. Wicker. (2003, November/December). *Life below the wet bulb: The Maisotsenko cycle* [Online]. Available: http://www.coolerado.com/pdfs/PowerMagMCTCfiguresCooleradoTIC.pdf.

[37] I. Metzger, O. VanGeet, C. Rockenbaugh, J. Dean and C. Kurnik. Psychrometric bin analysis for alternative cooling strategies in data centers. *ASHRAE Trans 117(2),* pp. 254-261. 2011. Available: http://search.ebscohost.com/login.aspx?direct=true&db=a9h&AN=67217579&site=ehost-live.

[38] *Conductivity/Total Dissolved Solids: A measure of the impurities in water supplies for domestic and industrial use.* [Online]. Available: http://www.lennox.ie/files/7513/7933/3763/Eutech_Conductivity_TDS_and_Salinity.pdf.

[39] Munters. Water treatment advice for industrial applications with CELdek and GLASdek equipped evaporative coolers. *(EB-WTM-0408),* 2004.

[40] Energy Labs Inc. *Evaporative Cooling Systems*. Available: http://www.energylabs.com/web2/brochures/ELI_Evaporative.pdf.

[41] ASHRAE TC 9.9 Mission Critical Facilities, Technology Spaces, and Electronic Equipment. *2011 Gaseous and Particulate Contamination Guidelines For Data Centers*. Available: http://tc0909.ashraetcs.org/documents/ASHRAE%202011%20Gaseous%20and%20Particulate%20Contamination%20Guidelines%20For%20Data%20Centers.pdf.

[42] J. C. Tannehill, D. A. Anderson and R. H. Pletcher, "Governing equations of fluid mechanics and heat transfer," in *Computational Fluid Mechanics and Heat Transfer*, 2nd ed., W. J. Minkowycz and E. M. Sparrow, Eds. Washington, DC: Taylor & Francis, 1997, pp. 249-350.

[43] V. K. Arghode and Y. Joshi. Modeling strategies for air flow through perforated tiles in a data center. *IEEE Transactions on Components, Packaging and Manufacturing Technology 3(5),* pp. 800-810. 2013. DOI: 10.1109/TCPMT.2013.2251058.

[44] W. A. Abdelmaksoud, T. Q. Dang, H. E. Khalifa, R. R. Schmidt and M. Iyengar. Perforated tile models for improving data center CFD simulation. Presented at Thermal and Thermomechanical Phenomena in Electronic Systems (ITherm), 2012 13th IEEE Intersociety Conference On. 2012. DOI: 10.1109/ITHERM.2012.6231414.

[45] S. V. Patankar. Airflow and cooling in a data center. *Journal of Heat Transfer 132(7),* pp. 073001-073001. 2010. DOI: 10.1115/1.4000703.

[46] N. Ahuja. Datacenter power savings through high ambient datacenter operation: CFD modeling study. Presented at Semiconductor Thermal Measurement and Management Symposium (SEMI-THERM), 2012 28th Annual IEEE. 2012. DOI: 10.1109/STHERM.2012.6188833.

[47] D. Seger and A. Solberg. (2008, April 25). *Economizer performance: Applying CFD modeling to the data center's exterior*. Available:

http://searchdatacenter.techtarget.com/tip/Economizer-performance-Applying-CFD-modeling-to-the-data-centers-exterior?vgnextfmt=print.

[48] Aztec Sensible Cooling. Indirect and indirect/direct evaporative units. *(TGASC-1),* 2010. Available: http://www.appliedair.com/modules/news/upload/%7BBC036927-4E95-47BD-A79B-F6B55467BD7A%7D_TGASC-1.pdf.

[49] S. Sathyanarayan, B. Gebrehiwot, V. Sreeram, D. Sawant, D. Agonafer, N. Kannan, J. Hoverson and M. Kaler. Steady state CFD modeling of an IT pod and its cooling system. Presented at Thermal Measurement, Modeling & Management Symposium (SEMI-THERM), 2015 31st. 2015. DOI: 10.1109/SEMI-THERM.2015.7100159.

[50] *lookbusy -- a synthetic load generator*.

[51] G. Woltman. *GIMPS: Mersenne Prime Search*. Available: http://mersenne.org.

[52] S. Sathyanarayan. Experimental and computational analysis of an IT pod and its cooling system. *ProQuest Dissertations and Theses* 2014. Available: http://search.proquest.com.ezproxy.uta.edu/docview/1650627401?accountid=7117.

[53] *Instruction Manual for AMCA 210-99 Airflow Test Chamber*. Available: http://www.fantester.com/.

[54] V. Sreeram. Factors affecting the performance characteristics of wet cooling pads for data center applications. *ProQuest Dissertations and Theses* 2014. Available: http://search.proquest.com.ezproxy.uta.edu/docview/1650627292?accountid=7117.

[55] "CELdek Evaporative Media," 2003.

[56] B. Gebrehiwot, N. Dhiman, K. Rajagopalan, D. Agonafer, N. Kannan, J. Hoverson and K. Mike. CFD modeling of indirect/direct evaporative cooling unit for modular data center applications. Presented at ASME 2013 International Technical Conference and Exhibition on Packaging and Integration of Electronic and Photonic Microsystems, InterPACK 2013. 2013. DOI: 10.1115/IPACK2013-73302.

[57] B. Gebrehiwot, K. Aurangabadkar, N. Kannan, D. Agonafer, D. Sivanandan and M. Hendrix. CFD analysis of free cooling of modular data centers. Presented at Semiconductor Thermal Measurement and Management Symposium (SEMI-THERM), 2012 28th Annual IEEE. 2012. DOI: 10.1109/STHERM.2012.6188834. (c) 2012 IEEE.

[58] © 2013 ASME. Reprinted, with permission, from Gebrehiwot, B., N. Dhiman, K. Rajagopalan, D. Agonafer, N. Kannan, J. Hoverson and Mike, K., CFD Modeling of Indirect/Direct Evaporative Cooling Unit for Modular Data Center Applications, ASME 2013 International Technical Conference and Exhibition on Packaging and Integration of Electronic and Photonic Microsystems, InterPACK 2013, July 2013.

[59] © 2012 IEEE. Reprinted, with permission, from Gebrehiwot, B., K. Aurangabadkar, N. Kannan, D. Agonafer, D. Sivanandan and Hendrix, M., CFD analysis of free cooling of modular data centers, Semiconductor Thermal Measurement and Management Symposium (SEMI-THERM), 2012 28th Annual IEEE, March 2012.

[60] Sunonwealth Electric Machine Industry Co., Ltd. *SUNON Specification for Approval: DC Brushless Fan, Model PMD1204PJB1-A, P/N (2)*. Available: http://datasheet.octopart.com/PMD1204PJB1-A-Sunon-Fans-datasheet-126742.pdf.

[61] *National Solar Radiation Data Base: 1991- 2005 Update: Typical Meteorological Year 3*. Available: http://rredc.nrel.gov/solar/old_data/nsrdb/1991-2005/tmy3/by_state_and_city.html.

[62] M. Lev-Ram. (2014, June 2). *What's the next big thing in big data? Bigger data.* Available: http://fortune.com/2014/06/02/fortune-500-big-data/.

Biographical Information

Betsegaw Gebrehiwot graduated with a Bachelor of Science in mechanical engineering in December 2010 from The University of Texas at Arlington (UT-Arlington). He worked on an electronic cooling project in summer 2010 as an LSAMP undergraduate scholar under Prof. Dereje Agonafer and was interested to further study thermal management of electronic cooling systems in graduate school. After his bachelor's degree, he joined graduate school at UT-Arlington as a B.S. to Ph.D. student.

In graduate school he worked on many projects involving thermal management of electronic systems which include a modular data center that has many blade servers, a Cisco Nexus 7010 switch cabinet, a modular data center which uses fogging type direct evaporative cooling, remote radio head units under natural convection and solar radiation, small telecommunication enclosures, a telecommunication shelter at 10,000 ft elevation which uses wet cell batteries for storing solar energy, and a test bed modular data center which uses a cooling unit that operates in air-side economization and two-stage indirect/direct evaporative cooling modes. In addition, he worked on designing of next generation antenna mounting structure.

Betsegaw enjoys working with others and solving electronic system thermal management problems. He is a member of the American Society of Mechanical Engineers (ASME) and the American Society of Heating, Refrigerating and Air-Conditioning Engineers (ASHRAE).